Calcium regulation in chloroplasts and the role of calcium-dependent phosphorylation of transketolase in carbon metabolism

Agostinho Manuel Gomes Rocha

Dissertation
der Fakultät für Biologie
der Ludwig-Maximilians-Universität München

vorgelegt von
Agostinho Manuel Gomes Rocha
aus
Ovar, Portugal

München, den 26.06.2012

Erstgutachter: Prof. Dr. Ute C. Vothknecht
Zweitgutachter: Prof. Dr. Jörg Nickelsen
Tag der mündlichen Prüfung: 17.07.2012

Table of contents

1 Introduction

As sessile organisms, plants are continuously exposed to biotic and abiotic stimuli. In order to enable acclimation, they have successfully developed a vast number of specific and regulated signalling processes. This allows plants to coordinate their cellular metabolism in response to these environmental changes. In order to (co-)regulate all metabolic pathways plants use elaborated mechanisms of communication that relay signals received by different receptors via intracellular secondary messengers. Thereby, secondary messengers provide a solution to amplify the strength of the signal in a specific manner.

1.1 Calcium as a secondary messenger

The divalent ion of calcium (Ca^{2+}) is a ubiquitous and well-known secondary messenger in all eukaryotic organisms (Berridge et al. 2000; Clapham 2007). It mediates stimulus-response in diverse cellular processes. Such processes include metabolism, ion transport, transcription, protein folding, protein phosphorylation, and many more (Yang and Poovaiah 2003; Dolmetsch et al. 1998; Trewavas 1999; Li et al. 1998). Intracellular Ca^{2+}concentration is maintained at a low resting level by pumps that transport this cation across membranes into intracellular calcium stores or out to the extracellular space. In response to biotic or abiotic stimuli, temporary and spatially controlled changes on calcium concentration are produced. They are subsequently perceived and decoded by specific sensor-transducers resulting in the selective activation of targeting effectors that regulate specific processes. There are structural motifs such as the EF-hand domains that are able to bind calcium with high affinity (Nakayama and Kretsinger 1994). The EF-hand domain is formed by two helices separated by a loop which is composed of negatively charged residues responsible for the binding of calcium. The most well studied EF-hand protein family that is found in all eukaryotes are the calmodulins (CaMs). CaM is not an enzyme but an allosteric activator of target proteins either by a calcium-regulated interaction or as a permanent component of an enzyme complex (Stefan et al. 2008). Calcium regulation is best investigated in the cytosol and the nucleus (for recent reviews: DeFalco et al. 2010; Dodd et al. 2010; Kudla et al. 2010), while the role of calcium for chloroplast function needs to be further studied.

1.2 Calcium regulated processes in chloroplasts

Chloroplasts are characteristic organelles of photosynthetic eukaryotes originated from an ancient symbiosis in which a supposedly already nucleated cell engulfed an ancestral photosynthetic cyanobacterium (Cavalier-Smith 2000; Margulis 1970). Further evolution has resulted in the transfer of genes from the symbiont to the nuclear genome (Martin and Herrmann 1998), resulting in a tight coordination and communication between the organelle and the nucleus. In addition to photosynthesis, plastids perform many essential biochemical functions such as fatty acid biosynthesis, nitrite and sulphate reduction and amino acid biosynthesis (Lopez-Juez and Pyke 2005; Nelson and Ben-Shem 2004; Neuhaus and Emes 2000). To ensure that chloroplast development and function is closely coordinated with the requirement of the surrounding cell, environmental and developmental signals have to be transduced into the organelle.

Early studies suggested that chloroplasts contribute to the homeostasis of cellular calcium as well as other ions (Portis and Heldt 1976). Studies on calcium content showed the calcium concentration in the chloroplast to be between 15 to 25 mM (Neish 1939; Larkum 1968; O'Keefe and Dilley 1977; Nobel 1969; Yamagishi et al. 1981). Considering that calcium forms insoluble precipitates with phosphate, this concentration is quite high. Therefore it is believed that Calcium is associated with membranes and macromolecules, otherwise complexed and/or sequestered within the thylakoid lumen (Brand and Becker 1984). The free stromal calcium concentration of non-illuminated chloroplasts was estimated to be about 2–6 µM (Kreimer et al. 1988) whereas the resting calcium concentrations in the cytosol is in the nanomolar range (Johnson et al. 1995). Several studies indicate the presence of a calcium transporter/pump between the chloroplast envelope and cytosol (Kreimer et al. 1985; Muto et al. 1982; Ferro et al. 2003) and a cation channel in the thylakoid (Enz et al. 1993). Still, their molecular identity has not been identified so far. A diurnal rhythm of calcium flux into the stroma has been shown by using the calcium indicator aequorin (Johnson et al. 1995; Sai and Johnson 2002). The stromal free calcium concentration was about 150 nM in the light. Within 20-25 minutes after transition of chloroplasts from light to dark, a transient calcium increase was observed to about 5-10 µM (Johnson et al. 1995). In addition to this feauture, very little is still known about the calcium fluxes within this organelle.

Most of the studies on calcium-dependent chloroplast processes focus on photosynthesis and CO_2-fixation. Ferredoxin, the electron transfer mediator protein of the photosystem I PSI) has been identified as a specific calcium-binding protein. It exhibits a higher capacity for binding calcium in its reduced state (Surek et al. 1987). Calcium is also required as a co-factor in photosystem II (PSII) for the oxygen evolution system (Miqyass et al. 2007). PSII contains a set of intrinsic membrane proteins (PsbA, B, C, D, E, and F) and three tightly-bound extrinsic proteins. In eukaryotes, these are PsbO, PsbP and PsbQ. Of these, PsbO has been reported as a Calcium -binding protein (Heredia and De Las Rivas 2003; Kruk et al. 2003). Shutova and collaborators (2005) showed that calcium might be involved in proton-dependent activation/deactivation of PsbO by testing the binding of calcium under different pH conditions. Using a basic pH, similar to the stromal pH under light conditions, PsbO undergoes conformational changes and the amino acid residues required for binding become exposed to the medium allowing the binding of Ca^{2+}or Mn^{2+}. However, at pH 7, estimated stromal pH upon dark conditions, the binding does not occur (Shutova et al. 2005). Calcium has also been shown to be essential for photo-assembly of PSII manganese clusters by preventing photoinactivation (Chen et al. 1995). The role of calcium is clearly important for oxygen evolution within PSII, however, the mechanism for delivery of the cation into the complex is still an open question.

The Calvin-Benson-Bassham cycle (CBB) is responsible for CO_2 fixation within the context of photosynthesis and calcium was shown to modulate activation and catalysis of the enzymes fructose 1,6-bisphosphatase (FBP) and sedoheptulose l,7-biphosphatase (SBP). Hertig and Wolosiuk demonstrated that calcium had a positive effect on FBP activation by pre-incubating the enzyme together with fructose-bisphosphate (1980; 1983). This calcium activation was furthermore shown to be linked to the redox status of the enzyme. The reduced FBP, was shown to behave in the same activity range as oxidized FBP pre-incubated with calcium and fructose 1,6-bisphosphate (Chardot and Meunier 1990). In similar way, SBP becomes activated when reduced by thioredoxin upon dark-light transitions (Cadet and Meunier 1988). Nevertheless, high calcium concentrations inhibit the catalytic efficiency of FBP and SBP (Charles and Halliwell 1980; Portis and Heldt 1976; Wolosiuk et al. 1982).

Other chloroplast processes are also regulated by calcium. The thylakoid calcium sensing protein CAS binds calcium with low affinity but high capacity (Han et al. 2003). CAS is

believed to be a key regulator of the stomatal closure process (Han et al. 2003; Nomura et al. 2008; Tang et al. 2007; Weinl et al. 2008) and to be involved in photosynthesis regulation (Vainonen et al. 2008). The calcium-regulated network was further extended with the identification of several CaM-regulated proteins in plastids. NAD Kinase, which catalyzes the phosphorylation of NAD in the presence of ATP, was the first CaM-regulated enzyme identified in plants (Anderson et al. 1980). TIC32, a component of the protein import machinery, represents the predominant calmodulin-binding protein of the inner envelope affecting protein import in a calcium-CaM dependent manner (Chigri et al. 2006). Several other CaM-binding proteins have been identified in the chloroplast, including PsaN, a subunit of PSI (Reddy et al. 2002), the chaperonine CPN10 (Yang and Poovaiah 2000), as well as the AAA^{+}-ATPases, CIP111 and AFG1L1 (Buaboocha et al. 2001; Bussemer et al. 2009). However, no CaM was so far identified in plastids and very little is known on EF-hand containing proteins in this organelle. So far, only the (p)ppGpp synthase-degradase (Kasai et al. 2004; Kasai et al. 2002; Tozawa et al. 2007) and a chloroplast envelope localized member of the calcium-dependent mitochondrial carrier family SAMTL (Stael et al. 2011; Ferro et al. 2003) were shown to bind calcium via their EF-hands.

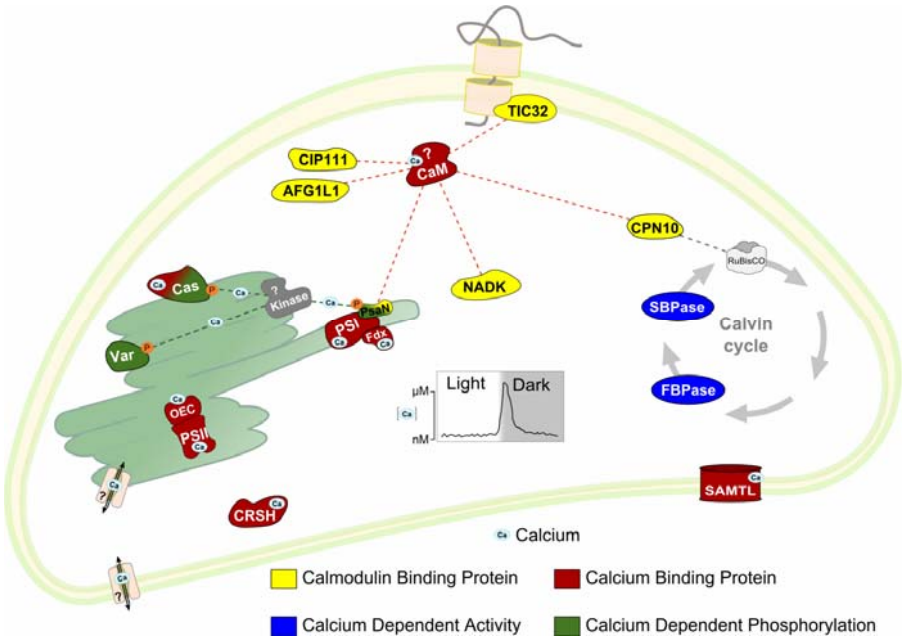

Fig. 1 - Overview of the calcium-regulation network in chloroplasts - Depicted are proteins/processes in chloroplasts that have been correlated to calcium, including direct calcium-binding (yellow), calmodulin-binding (red), calcium-dependent phosphorylation (green) or effects of calcium on enzyme activity (blue) (adapted from Rocha and Vothknecht 2012).

An overview of the known calcium-regulated processes in chloroplasts is given in figure 1. Nevertheless, the current knowledge on regulation of chloroplast calcium-dependent processes is still limited and merits further investigation.

1.3 The chloroplast phosphoproteome

The first event regulated by protein phosphorylation within the chloroplasts was identified in 1977 when Bennett demonstrated phosphorylation of light-harvesting complex (LHC) proteins (Bennett 1977). Phosphorylation was shown to be used for the adjustments of the photosynthetic machinery to light and changes in redox status (Schwacke et al. 2003; Durek et al. 2010). However, three decades later, several thylakoid proteins have been shown to undergo phosphorylation but very few protein kinases involved in this regulation have been identified. The best described are the thylakoid-associated "state transition" kinases Stt7 and Stl1 from Chlamydomonas and their Arabidopsis orthologs STN7 and STN8. They reversibly phosphorylate diverse components of the PSII and its light-harvesting antenna (LHCII) (Bonardi et al. 2005; Bellafiore et al. 2005; Heazlewood et al. 2008). They are involved in optimizing the photosynthetic acclimation to fluctuating light conditions and repair of photodamaged PSII (Rochaix 2007; Tikkanen and Aro 2012). In higher plants, the STN8 kinase was also found to be involved on the phosphorylation of CAS in a light-dependent manner, with the phosphorylation site on the stromal domain (Vainonen et al. 2008). It was further suggested that phosphorylation cascades initiated at the thylakoid membrane may regulate chloroplast processes via soluble stromal kinases such as casein kinase II (Larkin et al. 2007; Goujon et al. 2010; Wittekind et al. 1989). Nevertheless, no direct evidence for the phosphorylation of chloroplast kinases by other kinases has so far been presented. Further steps in the understanding of this process were recently provided by advances in phosphopeptide enrichment methods combined with improvements of mass spectrometric analysis instruments. These techniques have unravelled new phosphorylation sites in the chloroplast proteome (Preisinger et al. 2008; Baginsky 2009; Reiland et al. 2009) and a wide range of phosphoproteins in chloroplasts (Reiland et al. 2009). Nevertheless, the overall knowledge about chloroplast phosphoproteome remains very scarce (Bayer et al. 2012).

While phosphorylation/dephosphorylation represents a widespread form of regulation of enzyme activity, the phosphorylation reaction in turn can be regulated in different manners. One well-described form is the control by calcium and CaM via calcium-dependent protein kinases (CDPK) or calcium-CaM-dependent kinases (Harper and Harmon 2005; Kudla et al. 2010). CDPKs are bifunctional proteins which contain a kinase domain and a CaM-like domain. The calcium-induced conformational change of the CDPK directly stimulates the kinase activity resulting in the phosphorylation of the kinase substrate. In contrast, calcium-CaM-dependent kinases are regulated by calcium that induces the binding of CaM to the kinase. While calcium-dependent regulation of phosphorylation is well described for the cytosol, calcium-dependent phosphorylation of chloroplast proteins has only been detected recently for several thylakoid proteins (Stael et al. 2011).

1.4 Primary carbon metabolism

In photo-autotrophic organisms, photosynthesis converts light energy into ATP and NADPH which acts as the reducing power source for several cellular processes. The Calvin-Benson-Bassham cycle (CBB), also called reductive pentose phosphate cycle, fixes atmospheric CO_2 into carbon backbones that are used for starch and sucrose biosynthesis (Bassham et al. 1950). The reduction of carbon from CO_2 to hexose ($C_6H_{12}O_6$) requires ATP for free energy and NADPH as a reducing agent. These reactions take place in the stroma of the chloroplasts and comprise three stages: fixation of CO_2 by ribulose 1,5-bisphosphate carboxylase/oxygenase (RuBisCO) to form 3-phosphoglycerate; reduction of 3-phosphoglycerate to produce hexose sugars; and re-generation of ribulose 1,5-bisphosphate by extensive carbon shuffling.

Plants can also carry out the Pentose Phosphate Pathway (PPP). This pathway is common to all living organisms where glucose is oxidized and decarboxylated to generate NADPH needed for the biosynthesis of many biomolecules (Kruger and von Schaewen 2003). The PPP furthermore provides pentose sugars used in the synthesis of nucleic acids like RNA, DNA and nucleotide coenzymes as well as less common four- and seven-carbon sugars. This pathway is also known as the hexose monophosphate pathway, the phosphogluconate pathway, or the pentose shunt (Berg JM 2002). Generally, the PPP breaks down glucose into pentose to generate NADPH, whereas the CBB uses NADPH to reduce carbon dioxide and generate hexoses. For that reason, the CBB is sometimes referred to as the reductive

pentose phosphate pathway (Sillero et al. 2006). The PPP and the CBB share several enzymes such as ribose 5-phosphate isomerase, ribulose 5-phosphate 3-epimerase, transaldolase and transketolase.

1.4.1 Transketolase as a key enzyme

Transketolase (TKL; EC 2.2.1.1) is a ubiquitous key enzyme of carbon metabolism, especially in plants due to its amphibolic role in both the CBB and the PPP. TKL was first isolated from yeast in 1953 (Racker et al. 1953) and since then, has been characterized from a number of sources. It belongs to the group of a thiamine diphosphate-dependent enzymes, and requires Mg^{2+} ions for catalytic activity. The ability of TKL to transfer two-carbon dihydroxyethyl moieties from different ketose-phosphate sugars (donor substrate) onto divers aldose-phosphate sugars (acceptor substrate) (Murphy and Walker 1982; Villafra.Jj and Axelrod 1971; Schenk et al. 1997) is an important part of several metabolic pathways. The biocatalyst ability of transferring two carbons for the formation of new sugars makes TKL also a very important enzyme for industrial organic synthesis (Schenk et al. 1998; Turner 2000; Fessner 1998).

TKL catalyzes two reactions within the regenerative part of the CBB:

F6P + G3P → E4P + X5P
S7P + G3P → R6P + X5P

In the PPP pathway, the enzyme catalyzes the same reactions in a reverse direction within the non-oxidative branch of the pathway (Stitt and Aprees 1979):

E4P + X5P → F6P + G3P
R6P + X5P → S7P + G3P

Thereby, TKL plays an important role in the production of several precursors of different metabolic pathways (Fig. 2). For example, E4P is required for the shikimate pathway that produces aromatic amino acids as well as precursors for secondary metabolites involved in plants defense and signalling (Dixon and Paiva 1995). The pentose sugars R5P and X5P are important for synthesis of ribose 5-phosphate, a precursor of nucleotide and nucleic acids synthesis (Pilz et al. 1984). F6P and G3P are involved in glycolysis, gluconeogenesis and starch biosynthesis (Hers and Hue 1983; Dennis and Greyson 1987).

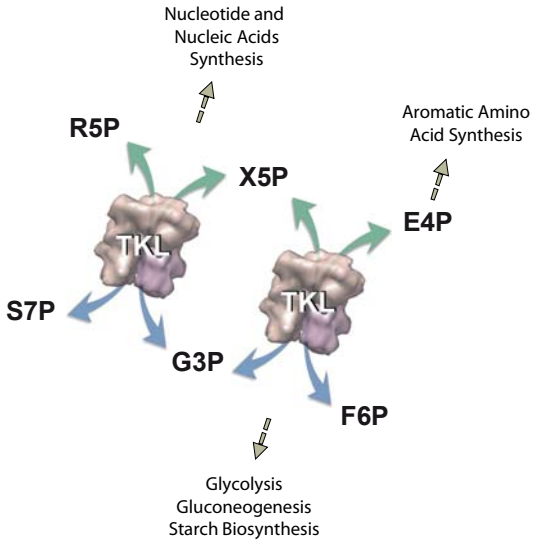

Fig. 2 - Transketolase catalyzes reversible reactions - Reactions catalyzed by tansketolase are showed by thick arrows, and dashed lines indicate some destination of the TKL products. The abbreviated substrates are as follows: F6P, fructose 6-phosphate; G3P, glyceraldehyde 3-phosphate; R5P, ribulose 5-phosphate; X5P, xylulose 5-phosphate; S7P, sedoheptulose 7-phosphate; E4P, erythrose 4-phosphate.

In plants, TKL was first isolated and characterized from spinach chloroplasts (Teige et al. 1998). The Arabidopsis genome contains two paralogues of TKL (AtTKL1 and AtTKL2). AtTKL1 is generally expressed with highest expression levels in leaves and other green tissue. AtTKL2 is mainly present in late seeds (Schmid et al. 2005) (Fig. 3).

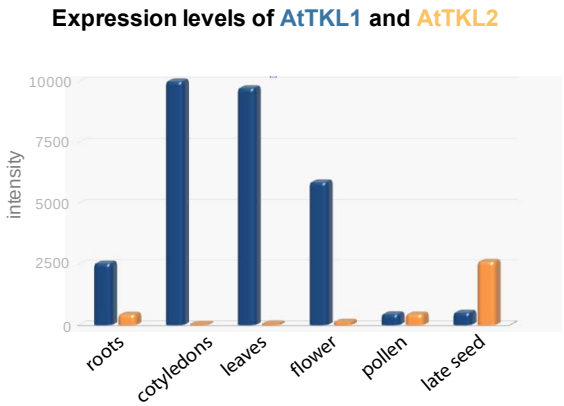

Fig. 3 - Expression levels of both TKL homologues in Arabidopsis - AtTKL1 is the most expressed protein with high intensity in leaves and other green tissues and AtTKL2 is mainly expressed in non photossynthetic tissues.

1.5 Aim of this study

The aim of this research was to investigate the calcium-dependent regulation in chloroplasts with a special focus on calcium-dependent protein phosphorylation.

Specific goals of this study were:

1) To identify new targets of calcium-dependent protein phosphorylation involved in the regulation of chloroplasts processes as well as the kinases and phosphatases conveying this regulation;

2) To elucidate the role of these calcium-dependent phosphoproteins and to understand the environmental and developmental signals that are transduced in this manner;

3) To identify new calcium-binding proteins in the chloroplast and to characterise their regulation mechanisms;

4) In general, to better understand the role of protein phosphorylation in the network of calcium regulatory events.

2 Materials

2.1 Chemicals

Table 1 - Materials used in this study

Name	Company
Chlamydomonas reinhardtii TKL (CrTKL; CL54b03) clone	Kazuza DNA Research Institute (Japan)
X5P	Sigma-Aldrich (Germany)
F6P	
G3P	
R5P	
TPP	
ß-NAD	
ß-NADH	
G3PDH	
Oligonucleotides	Eurofins MWG Operon (Germany)
Complete protease inhibitor cocktail	Roche (Germany)
Phosphatase inhibitor Phospho-Stop (EDTA Free)	
Immobilon PVDF membrane	Milipore (Germany)
Ni-NTA agarose	Quiagen (Germany)
Protein A sepharose	Thermo (Germany)
Chitin beads	New England Biolabs (USA)

2.2 Enzymes and kits

Table 2 - Enzymes and kits used in this study

Name	Company
Restriction enzymes	Fermentas (Germany), New England Biolabs (USA), GeneCraft (Germany)
DNA-polymerase	
Nucleobond AX	Macherey-Nagel (Germany)
Nucleospin Extract II	
NucleoSpin RNA II	
RNase H Minus, Point Mutant	Promega (Germany)

2.3 Molecular weight and size markers

For SDS PAGE, the following protein weight standards were used: "Low Molecular Weight Marker" consisting of α-lactalbumin, soybean trypsin inhibitor, trypsinogen, carbonic anhydrase, glyceraldehydes 3-phosphate dehydrogenase, egg albumin, and bovine albumin (14.2, 20.1, 24.0, 29.0, 36.0, 45.0, and 66.0 kDa, respectively) (Sigma-Aldrich, Germany) or PageRuler^{TM} Prestained Protein Ladder Plus (Fermentas, Germany). The DNA marker GeneRuler™ 1kb DNA Ladder Plus (Fermentas, Germany) was used for agarose gels.

2.4 Oliogonucleotides

Table 3 - Oligonucleotides used in this study

Name	Sequence (5'-3')
AtTKL1-fw	ATAAGCGGCCGCGCTGTTGAGACTGTTGAGCCAACCA
AtTKL1-rv	ATAAGGATCCTTAGAAGAATGACTTGGCCG
AtTKL1 Ser$_{428}$Asp-fw	CACCAGAGGACCCAGGTGATG
AtTKL1 Ser$_{428}$Asp-rv	ACCTGGGTCCTCTGGTGTGTA
AtTKL1 Ser$_{428}$Ala-fw	CACCAGAGGCTCCAGGTGATG
AtTKL1 Ser$_{428}$Ala-rv	ACCTGGAGCCTCTGGTGTGTA
AtTKL1-YFP-fw	ATAGGGCCCATGGCTTCTACTTCTTCCCTCGCTCTC
AtTKL1-YFP-rv	ATAGCGGCCGCAGAAGAATGACTTGGCCGCA
AtTKL2-fw	ATAAGCGGCCGCGCCGCCGTAGAGGCAATCGTGACA
AtTKL2-rv	TATTGGATCCTTAAATAAGTGACTTGGCTG
AtTKL2-YFP-fw	ATAGGGCCCATGGCTTCTACTTCTTCTCTAGCG
AtTKL2-YFP-rv	ATAGCGGCCGCAAATAAGTGACTTGGCTGCT
AtCP12-1-fw	ATACCATGGCTACATCGGAAGGAGAGAT
AtCP12-1-rv	TTAGCGGCCGCAATTATCATAAGTACGACAC
AtPsaN-fw	TTATTATCCATGGCTGCTTCTGCTAATGCTGGCGTCAT
AtPsaN-rv	AATATAGCGGCCGCATATAAGAATAGATGAAAAC
CrTKL-fw	ATACATATGCAGACCATGCTGAAGCAGCGCTGCC
CrTKL-rv	ATACTCGAGGTGCTGCAGGGTGGCCTTGG
E4PDH-fw	ATACATATGACCGTACGCGTAGCGATAAA
E4PDH-rv	ATACTCGAGCCTGAAAGCAACAGTAGCCA

Table 4 - Accession numbers of proteins used in this study

	Organism	Genebank Accession /AGI
AtTKL1	*Arabidopsis thaliana*	NP_567103.1 / At3g60750
AtTKL2	*Arabidopsis thaliana*	NP_566041.2 / At2g45290
AtCP12-1	*Arabidopsis thaliana*	NP_566100.2 / At2g47400
PsaN	*Arabidopsis thaliana*	NP_201209.1 / At5g64040
CAS	*Arabidopsis thaliana*	NP_197697.1 / At5g23060
VAR1	*Arabidopsis thaliana*	NP_568604.1 / At5g42270
VAR2	*Arabidopsis thaliana*	NP_850156.1 / At2g30950
SAMTL	*Arabidopsis thaliana*	NP_850252.1 / At2g35800
CrTKL	*Chlamydomonas reinhardtii*	XP_001701881
E4PDH	*Escherichia coli*	NP_289494.1

2.5 Plasmid DNA vectors

Table 5 - List of vectors used in this study

Vector	Purpose	Company
pTwin1	Protein expression	New England Biolabs (USA)
pET21b	Protein expression	Novagen (Germany)
pBIN19	Plant transformation	(Bevan 1984)

2.6 Bacteria strains

Table 6 - List of bacteria strains used in this study

Organism	Strain name	Company
E. coli	DH5α	(Hanahan 1985)
E. coli	ER2566	NEB (USA)
E. coli	BL21(DE3)	Novagen (USA)
A. tumefaciens	AGL1	(Lazo et al. 1991)

2.7 Isotopes

Radioactive nucleotides [γ–^{32}P] ATP (3000 Ci/mmol) and $^{45}CaCl_2$ ((13.90 mCi/mg) were provided from Perkin Elmer (USA).

2.8 Antibodies

Primary polyclonal antibody (α-AtTKL1) was generated in rabbit raised against purified recombinant mature AtTKL1 protein (Biogenes, Germany).

2.9 Plant material and growth conditions

Arabidopsis thaliana (cultivar Columbia Col-0) and *Nicotiana benthaminana* were grown on soil and *Pisum sativum* (cultivar Arvika) was grown on vermiculite, both at 22°C under a 16h/8h photoperiod at 150 μmol·m^{-2} · s^{-1}. *Chlamydomonas reinhardtii* (cw15 cell wall-less strain) were grown as described previously by Rochaix (1988) under illumination at 20 μmol·m^{-2} ·s^{-1} at 25°C.

3 Methods

3.1 Nucleic acid methods

3.1.1 General nucleic acid methods

Standard molecular biological methods were performed according to Sambrook J (1989). This includes: amplification of DNA by the polymerase chain reaction, agarose gel electrophoresis, detection of DNA, determination of DNA concentration, growing conditions of bacteria and bacterial transformation (Sambrook J 1989). RNA isolation, restrictions and ligation of DNA fragments were performed according to the manufacturers of the enzymes or kits. The plasmids were generated by alkaline lysis with SDS (Sambrook, 1989) or kit according to the manufacturer. Purification of PCR products and purification of DNA fragments from agarose gels were carried out also according to the manufacturer's instructions.

3.1.2 Plasmid DNA mini preparation from *E. coli*

An over-night-culture of 2 ml was centrifuged for 2 min at 16,000 g and the supernatant was removed. The pellet was resuspended in 200 µl of resuspension buffer P1 (50 mM Tris/HCl pH 8.0, 10 mM Na_2EDTA (including 100 µg/ml RNase) followed by addition of lysis buffer P2 (200 mM NaOH, 1% SDS) to lyse the cells. To mix the suspension, the tubes were inverted three times and incubated for 5 min at RT. The *E. coli* lysate was neutralized by the addition of 200 µl of neutralisation buffer P3 (3 M potassium acetate pH 5.5) and mixed by inverting three times. After 20 min incubation at 4°C the suspension was centrifuged for 10 min at 16,000 g. To precipitate the DNA the supernatant was mixed with 0.7 times isopropanol and incubated at -20°C for 20 min followed by centrifugation at 16,000 g at 4°C. The supernatant was removed and the pellet was washed with 500 µl 70% EtOH. The pellet was dried at RT and resolved in 50 µl H_2O.

3.1.3 Reverse transcription RT-PCR

Reverse transcription was carried out using the Promega M-MLV reverse Transcriptase, RNase H Minus, Point Mutant, according to the manufacturer's instructions. In a final

volume of 14 µl 1 µg total RNA and 0.5 µg oligo (dT)15 were mixed and heated to 70°C for 5 min, then cooled quickly on ice for 5 min followed by the addition of 5 µl MMLV RT 5x Reaction Buffer, 1.25 µl 10 mM dNTP mix and 1µl M-MLV RT (H-). The reaction was mixed and incubated at 40°C for 60 min. 1-2 µl reverse transcripted cDNA was used for PCR amplification using the Taq from GeneCraft (Germany).

3.2 Protein methods

3.2.1 General protein methods

Proteins were separated by SDS-PAGE according to Laemmli (1970). Polyacrylamide gels were stained by coomassie brilliant blue R250 (Sambrook J 1989). Chlorophyll concentration was determined as described by Arnon (1949). Protein concentration was determined either according to Lowry et al. (1951) or by using the coomassie Bradford protein assay kit (Thermo, Germany) according to manufacture instructions. Transfer of proteins onto PVDF membranes was done according the semi-Dry-Blot method (Khyse-Andersen 1984). Radiolabeled proteins were detected by exposure to phosphoimager screens analysed on a Typhoon Trio (GE Healthcare) or by exposure to X-ray film at -80°C (FUJI).

3.2.2 Purification of stromal extracts from Arabidopsis and Pisum

Chloroplasts were purified from 6-7 weeks old Arabidopsis leafs as described by Seigneurin-Berny et al. (2008) and from 7-9 days old pea leafs as described by Waegemann and Soil (1991). Chloroplasts were disrupted by suspension in lysis buffer (20 mM Tricine/NaOH pH 7.6, 10% (v/v) glycerol, 1 mM DTT) supplemented with 5 mM EGTA, protease and phosphatase inhibitors. After incubation on ice for 15 min, membranes and soluble components were separated by centrifugation at 60,000 g for 10 min. To extract membrane associated proteins, the membrane pellet was subsequently resuspended with lysis buffer containing 0.8 M NaCl and centrifuged again at 60,000 g for 10 min. Supernatants of the first and second centrifugation were combined, concentrated and desalted into lysis buffer using Vivaspin^{TM} 500 columns (3 kDa cutoff, GE Healthcare) and is referred to as stromal protein fraction. The remaining pellet contained the membrane protein fraction. All procedures were carried out on ice or at 4°C.

3.2.3 Preparation of Chlamydomonas total cell extract

Total cell extract out of *Chlamydomonas reinhardtii* (cw15 cell wall-less strain) was prepared as described above for chloroplasts.

3.2.4 Expression and protein purification using the pTWIN system

The isolation of recombinant proteins without tag was done using the IMPACT™-pTWIN protein purification system from NEB, according to the manufacturer's instructions. All TKLs, AtPsaN and AtCP12-1 lacking the N-terminal amino acids were cloned into pTWIN1 in frame with the N-terminal intein tag. Point mutations at position Ser_{428} in the $AtTKL1_{(S/A)}$ and $AtTKL1_{(S/D)}$ variants were generated by site-directed mutagenesis on the pTWIN-AtTKL1 plasmid. An overnight culture of *E. coli* (ER2566) carrying the pTWIN expression plasmid was inoculated in 500 ml LB with 100 µg/ml ampicillin. The culture was incubated at 37°C under vigorous shaking until OD_{600} of 0.6 was reached and expression was induced by 1 mM IPTG. The culture was incubated at 16°C over night under vigorous shaking and *E. coli* were harvested by centrifugation for 10 min at 2,900 g. Bacterial pellets were resuspended in 20 ml pre-cooled pTWIN buffer B1 (20 mM HEPES/NaOH pH 8.5; 1000 mM NaCl; 1 mM EDTA; 1 mM DTT). To break the cells, the French press was used and lysate was clarified by centrifugation at 16,000 g at for 20 min. The supernatant was applied to a column packed with 2 ml (bed volume) of chitin beads which were washed in precooled pTWIN buffer B1. The column was washed with 100 ml of pre-cooled pTWIN buffer B1 and fast flushed with 4 ml pre-cooled pTWIN buffer B2 (20 mM HEPES/NaOH pH 7.0; 500 mM NaCl; 1 mM EDTA; 1 mM DTT). To induce protein cleavage the column was incubated at RT over night. After the elution with pTWIN buffer B2, the buffer was exchanged to 20 mM Tricine/NaOH pH 7.6, 1 mM DTT and the protein was concentrated by ultrafiltration in Vivaspin™ 500 columns (3 kDa cutoff, GE Healthcare). Unless otherwise stated, all purification steps were performed on ice or at 4°C.

3.2.5 Expression and protein purification using the 6x-His tag system

The CrTKL and E4PDH were purified under native conditions by using pET21b with a C-terminal 6x-Histidine tag. An overnight culture of *E. coli* (ER2566 or BL21) carrying the

respective expression plasmid was inoculated in 500 ml LB with 50 µg/ml ampicillin. The culture was incubated at 37°C under vigorous shaking until OD_{600} of 0.6 was reached and expression was induced by 1 mM IPTG. The culture was incubated at 37°C for 4 hours under vigorous shaking and *E. coli* were harvested by centrifugation for 10 min at 2,900 g. Bacterial pellets were resuspended in 20 ml 50 mM HEPES/NaOH pH 8.5; 300 mM NaCl; 10 mM imidazole; 1 mM DTT and cells disrupted by French press. The cellular extract was centrifuged for 20 min at 16,000g and supernatant incubated 1h30 and under agitation with 500 µl of Ni-NTA superflow. The incubated solution was then poured in a column and beads were washed with 200 ml of 50 mM HEPES/NaOH pH 8.5; 300 mM NaCl; 20 mM imidazole; 1 mM DTT. Proteins were eluted with 50 mM HEPES pH 8.5; 300 mM NaCl; 250 mM imidazole; 1 mM DTT. The buffer was exchanged to 20 mM Tricine/NaOH pH 7.6, 1 mM DTT and the protein was concentrated by ultrafiltration in Vivaspin^{TM} 500 columns (3 kDa cutoff, GE Healthcare). Unless otherwise stated, all purification steps were performed on ice or at 4°C.

3.2.6 Standard protein phosphorylation assays of endogenous proteins

Phosphorylation assays for the detection of endogenous phosphoproteins were conducted using 10 - 20 µg soluble stromal proteins from either Arabidopsis or Pisum. Assays were carried out in a total volume of 50 µl in kinase buffer (20 mM Tricine/NaOH pH 7.6, 10 mM $MgCl_2$, 10% (v/v) glycerol, 1 mM DTT, 5 µM ATP and 2–5 µCi [γ–^{32}P] ATP) supplemented with either 5 mM $CaCl_2$, 5 mM CdOAc, 5 mM ZnOAc, 5 mM $CuCl_2$, 5 mM $MnCl_2$, 5 mM $NiSO_4$, or 2 mM EGTA. Reactions were carried out for 25 min at RT and stopped by the addition of 12 µl of 4xSDS-sample buffer. Proteins were separated by SDS-gel electrophoresis and stained with coomassie brilliant blue R-250. Radiolabeled proteins were detected by exposure to phosphoimager screens analysed on a Typhoon Trio (GE Healthcare) or by exposure to X-ray film at -80°C (FUJI).

3.2.7 Phosphorylation assays of recombinant proteins

100 - 200 ng recombinant of AtTKL1, AtTKL1$_{(S/D)}$ AtTKL2, CrTKL, PsaN, CAS, VAR1, VAR2 or GST were used as substrate. Reactions were carried out using catalytically amounts (50–100 ng) of Arabidopsis stromal and extrinsic proteins, chloroplast membrane

proteins or Chlamydomonas total cell extract. Assays were carried out in a total volume of 50 µl in kinase buffer supplemented with either 5 mM $CaCl_2$ or 2 mM EGTA. Reactions were carried out for 25 min at RT and stopped by the addition of 12 µl of 4xSDS-sample buffer. Proteins were separated by SDS-gel electrophoresis and stained with coomassie brilliant blue R-250. Radiolabeled proteins were detected by exposure to phosphoimager screens analysed on a Typhoon Trio (GE Healthcare) or by exposure to X-ray film at -80°C (FUJI).

3.2.8 Kinase assay of immunoprecipitated proteins

By using stromal extracts out of Arabidopsis or Pisum purified chloroplasts, phosphorylation assays were conducted with about 100 µg total proteins in a total volume of 200 µl in kinase buffer supplemented with 5 mM $CaCl_2$. For LC-MS/MS proposes, the same assay was conducted in parallel but without radiolabeled [γ–^{32}P] ATP. Reactions were carried out for 25 min at RT and after incubated for 1 hour with 10 µl protein A-Sepharose and 6 µl of α-AtTKL1 antibody. The beads were washed three times with 800 µl of 20 mM Tricine/NaOH pH 7.6 and 1 mM DTT by centrifugation at 1,000 g for 2 minutes. The proteins were eluted with 50 µl SDS solubilization buffer, heated at 96°C and centrifugated at 14,000 g for 2 minutes. The samples were analyzed by SDS-PAGE separation and protein staining with coomassie brilliant blue R-250. The incorporation of radioactivity was measured by exposing the dry gel to X-ray film at -80°C (FUJI).

3.2.9 Protein separation by 2D-PAGE

For the calcium-dependent phosphorylation assays, phosphorylation reactions were conducted with 150 - 250 µg soluble stromal and extrinsic proteins. Assays were carried out in a total volume of 120 µl in kinase buffer supplemented with either 5 mM $CaCl_2$, or 2 mM EGTA. Reactions were carried out for 25 min and stopped by 480 µl of methanol and 120 µl chlorophorm. Samples were vigorously vortexed in between and centrifuged for 3 minutes at 14,000 g. After discarding the top aqueous layer, 480 µl methanol was added, samples vortexed and centrifuged for 6 min. Without disturbing the pellet, the methanol and chlorophorm was removed, pellets were washed with 300 µl 80 % acetone, and dried. All operations were carried at RT. For LC-MS/MS proposes, the same assay was

conducted in parallel but without radiolabeled [γ–^{32}P] ATP. Chloroform/methanol precipitated protein pellets from phosphorylation reactions were resuspended in 40 µl H_2O and solubilized in 200 µl rehydration buffer 1 (7 M urea, 2 M thiourea, 2% (w/v) CHAPS, 0.5% (v/v) IPG buffer, 0.002% (w/v) bromophenol blue and 1 mM DTT) for 30 minutes at RT. Proteins were applied to 11 cm immobilized Dry-Strips™ (pH 3-11, NL, GE Healthcare) and separated using the BioRad Protean IEF Cell Isoelectric Focusing System according to the following programme: Passive rehydratation a 20 °C for 16 hours; rapid – 0.5 kVh (0.5 kV); linear – 0.8 kVh (0.1 kV); linear – 7.0 kVh (6 kV); linear 3.7 kVh (6 kV); hold (0.5 kV) in a total of 12 kVh. Afterwards, the strips were equilibrated consecutively in equilibration buffer (75 mM Tris/HCl pH 8.8, 6 M urea, 30% (v/v) glycerol, 2% (w/v) SDS and 0.002% (w/v) bromophenol blue) containing 10 mg/ml DTT and in equilibration buffer containing 25 mg/ml iodacetamide for 20 min each. Proteins were separated in the second dimension by SDS-PAGE stained with coomassie brilliant blue R-250.

For the calcium-binding assays, 80 µl of soluble stromal and extrinsic proteins (150 - 250 µg) were resuspended in 400 µl rehydration buffer 2 (7 M urea, 2 M thiourea, 4% (w/v) CHAPS, 0.7% (v/v) IPG buffer, 0.002% (w/v) bromophenol blue and 40 mM DTT) for 30 minutes at RT. Proteins were applied to 24 cm immobilized Dry-Strips™ (pH 3-11, NL, GE Healthcare) and separated using the BioRad Protean IEF Cell Isoelectric Focusing System according to the following programme: Passive rehydratation a 20 °C for 20 hours; rapid – 1 h (0.15 kV); rapid – 1 h (0.3 kV); rapid – 1 h (0.6 kV); rapid – 1 h (1 kV); linear (ramp) – 1 h (10 kV); rapid – 45 kV/h (10 kV); hold (1 kV). Afterwards, the strips were equilibrated consecutively in equilibration buffer containing 10 mg/ml DTT and in equilibration buffer containing 25 mg/ml iodacetamide for 20 min each. Proteins were separated in the second dimension by SDS-PAGE and blotted on PVDF membrane.

3.2.10 Calcium overlaying assays

Assays were performed as described earlier by Maruyama et al. (1984) with minor modifications. When using recombinant proteins expressed in *E. coli,* proteins were directly spotted on activated PVDF membranes or when 2D analysis were required, proteins were blotted onto PVDF activated membrane. The membrane was washed three times for 15 min with 100 µl Ca^{2+} washing buffer (60 mM KCl, 5 mM $MgCl_2$,

60 mM imidazole/HCl pH 6.8). The membrane was incubated for 10 min at RT with 100 ml calcium washing buffer containing 30 µl $^{45}CaCl_2$. Subsequently, the membrane was washed for five minutes with 50% ethanol. Radioactivity signals were detected by exposure on phospho-imaging screens and analysed on a FUJI FLA-3000 (FUJIFILM, Germany). The membrane was subsequently stained with coomassie brilliant blue R-250. For LC-MS/MS proposes, the same assay was conducted in parallel but without blotting or performing the radiolabelling. This way, SDS-PAGE was stained with coomassie brilliant blue R-250 after the second dimension, and spots of interest were excised.

3.2.11 Analysis of peptides by LC-MS/MS

Coomassie brilliant blue stained gel bands or spots were processed as previously described by Spirek et al. (2010) and Bayer et al. (2011). Alternatively, samples were enriched for phosphopeptides by the use of TiO_2 following the procedure described by Mazanek et al. (2007). LC-MS/MS analysis was done in cooperation with the mass spectrometry facilities of the Max F. Perutz Laboratories (Austria). Peptides were separated on an UltiMate 3000 HPLC system (Dionex). Digests were loaded on a trapping column (PepMap C18, 5µm particle size, 300 µm i.d. x 5mm) equilibrated with 0.1% TFA (trifluoric acetc acid) and separated on an analytical column (PepMap C18, 3 µm, 75 µm i.d. x 150mm) applying a 90 minutes linear gradient from 2.5% up to 40% ACN with 0.1% formic acid. The HPLC was directly coupled to a LTQ-Orbitrap Velos mass spectrometer (Thermo Fisher Scientific) equipped with a nanoelectrospray ionization source (Proxeon, Denmark). The electrospray voltage was set to 1500 V. The mass spectrometer was operated in the data-dependent mode: 1 full scan (m/z: 300-1800, resolution 60,000) with lock mass enabled was followed by maximal 20 MS/MS scans. The lock mass was set at the signal of polydimethylcyclosiloxane at m/z 445.120025. Screening of the charge state was on, singly charged signals and ions with no charge state assigned were excluded from fragmentation. The collision energy was set at 35%, Q-value at 0.25 and the activation time at 10 msec. Fragmented ions were set onto an exclusion list for 90 s.

Raw spectra were interpreted by Mascot 2.2.04 (Matrix Science) using Mascot Daemon 2.2.2. The peptide tolerance was set to 2 ppm, MS/MS tolerance was set to 0.8 Da. Proteins were identified from the full genome sequence of TAIR9. Carbamidomethylcysteine was set as static modification, oxidation of methionine and phosphorylation of serine,

threonine, tyrosine were set as the variable modifications. Trypsin was selected as protease and two missed cleavages were allowed. MASCOT results were loaded into Scaffold (Ver. 3.00.02; Proteome Software) for an X! Tandem Search. Peptide identifications were accepted at a probability greater than 95% and protein identifications at a probability greater than 99%, as assigned by the Protein Prophet algorithm (Keller et al. 2002; Nesvizhskii et al. 2003). In case of phosphorylation studies spectra were reanalysed with Proteome Discoverer 1.2 (Thermo Scientific). Search parameters were set as described for the Mascot search. Results were pre-filtered using XCorr (+2, +3, +4) = 2, 2.5, 3 and identified phosphopeptides were subjected to stringent manual validation.

3.2.12 TKL activity assay using X5P and R5P as substrates

Conversion of X5P and R5P into G3P and S7P was measured as described previously by De La Haba et al. (1955) with minor changes. A 200 µl reaction mixture contained 20 mM glycylglycine/NaOH pH 7.2 or 8.0, 0.1 mM TPP, 0.14 mM ß-NADH, 15 mM $MgCl_2$, 5 mM $CaCl_2$, 20 units G3PDH (based on triosephosphate isomerase units) and 0.1 µg recombinant TKL. To measure kinetic parameters for X5P, 1.7 mM R5P was used and X5P content varied between 0.1 and 3.0 mM. To measure kinetic parameters for R5P, 1.5 mM X5P was used and R5P content varied between 0.125 and 3.0 mM. Conversion of NADH to NAD^+ was measured as change in Abs_{340} ($\varepsilon = 6220\ M^{-1} \bullet cm^{-1}$) using a Tecan Safire2 microplate reader at 30°C.

3.2.13 TKL activity assay using G3P and F6P as substrates

Conversion of F6P and G3P into E4P and X5P was measured as described by Naula et al. (2008) with minor changes. A 200 µl reaction mixture contained 50 mM Tris/HCl pH 7.2 or 8.0, 0.1 mM TPP, 2.5 mM ß-NAD, 15 mM $MgCl_2$, 5 mM $CaCl_2$, 20 - 30µg E4PDH and 2-3 µg recombinant TKL. To measure kinetic parameters for F6P, 2.0 mM G3P was used and F6P content varied between 0.1 and 20.0 mM. To measure kinetic parameters for G3P, 5.0 mM F6P was used and G3P content varied between 0.125 and 2.0 mM. A control reaction without TKL was carried out under the same conditions and with 2.0 mM G3P and 20.0 mM F6P. The solutions were quickly mixed for 30 sec and conversion of NAD^+

to NADH was measured as change in Abs_{340} (ε= 6220 M^{-1}•cm^{-1}) using a Tecan Safire2 microplate reader at 30°C.

3.2.14 Calculation of TKL specific activity and statistical analysis

Specific activity was expressed as µmol of oxidized/reduced NADH per minute per milligram of TKL. The kinetic parameters were obtained by fitting the experimental data to the Michaelis Menten equation (V = Vmax•[S]/(Km + [S]) using GraphPad Prism Software, Version 5.01, San Diego, CA, USA.

3.2.15 Sequence alignment and phylogenetic motif analysis

Sequence alignments were obtained by ClustalW software (Goujon et al. 2010; Larkin et al. 2007) and box-shading was performed by BOXSHADE 3.31 available at http://mobyle.pasteur.fr. The logo representing the residue probability around the phosphorylation site was generated using the Weblogo 3 program (Crooks et al. 2004) based on the sequence alignment. A complete list of accession numbers is given in Annex Table 1.

3.3 Plant methods

3.3.1 Agrobacterium mediated expression in *Nicotiana benthaminana* leafs

pBin19 35S: C-terminal YFP constructs were transformed via electroporation in *Agrobacterium* (AGL1) plated on LB media containing 50 µg/ml kanamycin. One clone was inoculated in LB media containing 50 µg/ml kanamycin and incubated over night at 30°C under shaking. On the next day 50 ml of LB media containing 50 µg/ml kanamycin was inoculated with the pre-culture and adjusted to an OD_{600} of 0.05. Then the culture was incubated at 30°C under vigorous shaking until an OD_{600} of 0.2 was reached. The bacteria suspension was harvested by centrifugation at 2,900 g at RT for 10 min and resuspended in 25 ml induction media (10 mM MES pH 6.0, 10 mM $MgCl_2$, 200 µM Acetosyringone). After 2 h incubation at 30°C the cells were again centrifuged at 2,900 g at RT for 10 min and resuspended in 10 ml of 5 % sucrose containing 200 µM acetosyringone. Leaves of 3-4

weeks old tobacco plants (*Nicotiana benthaminana*) were infiltrated with *Agrobacterium tumefaciens* (AGL1) carrying the different pBIN19 constructs. Infiltrated leaves were collected after 36 h and used for protoplast isolation as described previously by Koop et al. (1996). Fluorescence images were obtained using the confocal laser scanning microscope TCS-SP5 (Leica Microsystems, Germany) and the Leica LAS AF software.

3.4 Bacteria methods

3.4.1 Preparation of chemical-competent *E. coli*

Chemical-competent *E. coli* were prepared as previously described by Inoue et al. (1990) but with minor changes. A pre-culture of LB supplemented with 20 mM $MgSO_4$ was inoculated with 3-5 independent *E. coli* clones and incubated at RT under shaking over night. 600 ml of LB supplemented with 20 mM $MgSO_4$ was adjusted with the pre-culture to OD_{600} of 0.2 and incubated under shaking at RT until an OD_{600} of 0.5 was achieved. Cells were harvested by centrifugation at 700 g for 10 min at 4°C and resuspended in 50 ml ice cooled TB buffer (10 mM $CaCl_2$, 10 mM PIPES/NaOH pH 6.7, 15 mM KCl, 55 mM $MnCl_2$). After incubation on ice for 30 min the cells were again harvested by centrifugation at 400 g for 10 min at 4°C and resuspended in ice cooled TB buffer supplemented with 7% DMSO. The suspension was incubated on ice for additional 30 min, splited into 450 µl aliquots and frozen away at -80°C.

3.4.2 Preparation of electro-competent Agrobacteria

Over-night culture of Agrobacteria was inoculated in 600 ml LB and incubated at 30°C under vigorous shaking for 1.5 days until an OD_{600} of 1.5-2 was reached. The suspension was cooled down on ice for 10 min. The cells were precipitated by centrifugation for 15 min at 6,000 g at 4°C and resuspended in 50 ml of 1 mM HEPES/NaOH pH 7.0. Cells were again precipitated by centrifugation at 4,000 g at 4°C for 15 min and resuspended in 1 mM HEPES/NaOH pH 7.0. This washing step was additionally repeated twice and then the 1 mM HEPES pH 7.0 was replaced by 10 % glycerol. The cells were again precipitated by centrifugation at 4,000 g at 4°C for 15 min and resuspended in 4-6 ml 10 % glycerol. Aliquots of 400 µl per 1.5 ml vial tubes were frozen in liquid nitrogen and stored at -80°C.

4 Results

Plants are continuously exposed to different stimuli. In order to properly adapt to stresses and changes in their environment they evolved specific signalling transduction mechanisms to regulate various cellular processes in response to these stimuli. In many cases, these complex strategies involve cross-talk between different signalling networks and metabolic pathways, acting in a specific and orchestrated manner. In eukaryotic cells, calcium plays an important role in regulating a great variety of cellular processes by acting as a secondary messenger. However, very little is known about calcium-mediated regulation within endosymbiotic organelles, such as the chloroplast. The aim of this thesis was to investigate mechanisms of calcium-dependent regulation of chloroplast functions with a special focus on calcium-dependent protein phosphorylation.

4.1 Chloroplast targets of calcium-dependent protein phosphorylation

Protein phosphorylation/dephosphorylation is a well-established means to transfer signals and to regulate protein function or metabolic pathways (Cohen 2000). It represents a wide-spread form of regulation of enzyme activity and can by itself be regulated in different manners. One well described form is the control by calcium via CDPKs and calcium-CaM-dependent kinases (Cheng et al. 2002; Harmon et al. 2000). While phosphorylation/dephosphorylation is also a common regulatory mechanism in chloroplasts, no evidence for calcium-dependent phosphorylation of chloroplast proteins has so far been described.

To investigate potential calcium-dependent phosphorylation, intact chloroplasts were separated into soluble (stromal and extrinsic proteins) and membrane bound fractions. Phosphorylation assays were than performed using ^{32}P-labeled ATP in the presence or in the absence of calcium, using the calcium specific chelator ethylene glycol tetraacetic acid (EGTA) to remove any endogenous calcium. Following that, proteins were separated by 1D- (SDS) or 2D-PAGE (IEF-SDS) and phosphorylation patterns were analyzed by autoradiogram. Candidate proteins that undergo calcium-dependent changes in phosphorylation were subsequently identified by mass spectrometry.

4.1.1 Calcium-dependent protein phosphorylation assays using stromal extracts

Calcium-dependent phosphorylation was initially accessed within the soluble choroplastidic proteome of *Pisum sativum* and protein phosphorylation was analyzed by SDS-PAGE and autoradiography (Fig. 4, Pisum). A dominating 73 kDa protein was observed as being phosphorylated only in the presence of calcium and a protein of about 65 kDa was only phosphorylated in its absence. The same experiment was then performed with a stromal fraction from *Arabidopsis thaliana* (Fig. 4, Arabidopsis).

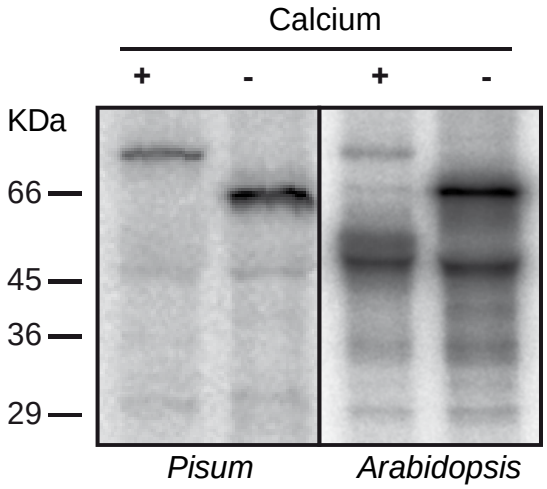

Fig. 4 - Calcium-dependent phosphorylation of stromal proteins - Autoradiograms of stromal proteins separated by SDS-PAGE after phosphorylation assays in the presence of calcium (+) or EGTA (-) in both Pisum and Arabidopsis.

In contrast to Pisum, more proteins were generally found to be phosphorylated, most of which showed no changes in correlation to the absence or presence of calcium. A clear difference in the phosphorylation pattern could again be observed for a few proteins, including the 65 kDa protein that is only phosphorylated in the absence of calcium. Two proteins of about 73 and 50 kDa showed phosphorylation only in the presence of calcium.

4.1.2 Specificity of phosphorylation to calcium

The 73 kDa phosphoprotein is especially intriguing due to the similar results obtained for Pisum and Arabidopsis. In order to ensure calcium specificity of the phosphorylation of the 73 kDa protein, phosphorylation reactions were performed in the presence of a number of different divalent cations such as nickel, manganese, cooper, zinc, cadmium and calcium as well as in the presence of EGTA (Fig. 5).

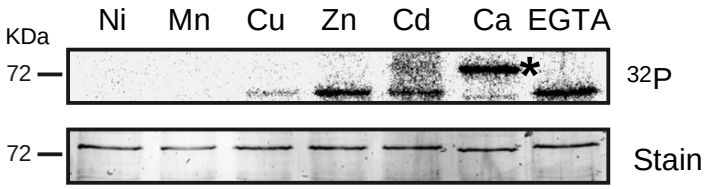

Fig. 5 - Calcium specific phosphorylation of the 73 kDa protein - Autoradiogram (upper panel) and coomassie brilliant blue stained gel (lower panel) of SDS-PAGE separated stromal proteins after phosphorylation assays in the presence of different cations or EGTA shows a strict calcium-dependency for the phosphorylation of the 73 kDa protein.

As can clearly be seen, the 73 kDa protein is only phosphorylated in the presence of calcium. None of the other divalent cations could replace calcium in the reaction confirming the specificity of the observation. Interestingly, the 65 kDa protein that is not phosphorylated in the presence of calcium is phosphorylated in the presence of several but not all divalent cations, indicating that the phosphorylation of this protein is not directly correlated to the presence or absence of calcium but might be influenced by other factors.

4.1.3 Identification of candidates by LC-MS/MS

To obtain a better resolution for the identification of the candidates, the proteins were separated on 2D-PAGE using isoelectric focusing in the first and SDS-PAGE in the second dimension (Fig. 6), resulting in a more detailed map of the phosphorylation pattern. As before, several proteins are clearly phosphorylated independently of calcium. However, some proteins are phosphorylated only in the presence of calcium (Fig. 6, spots A, C and D) and others only in the presence of EGTA (Fig. 6, spots F, G, H and I).

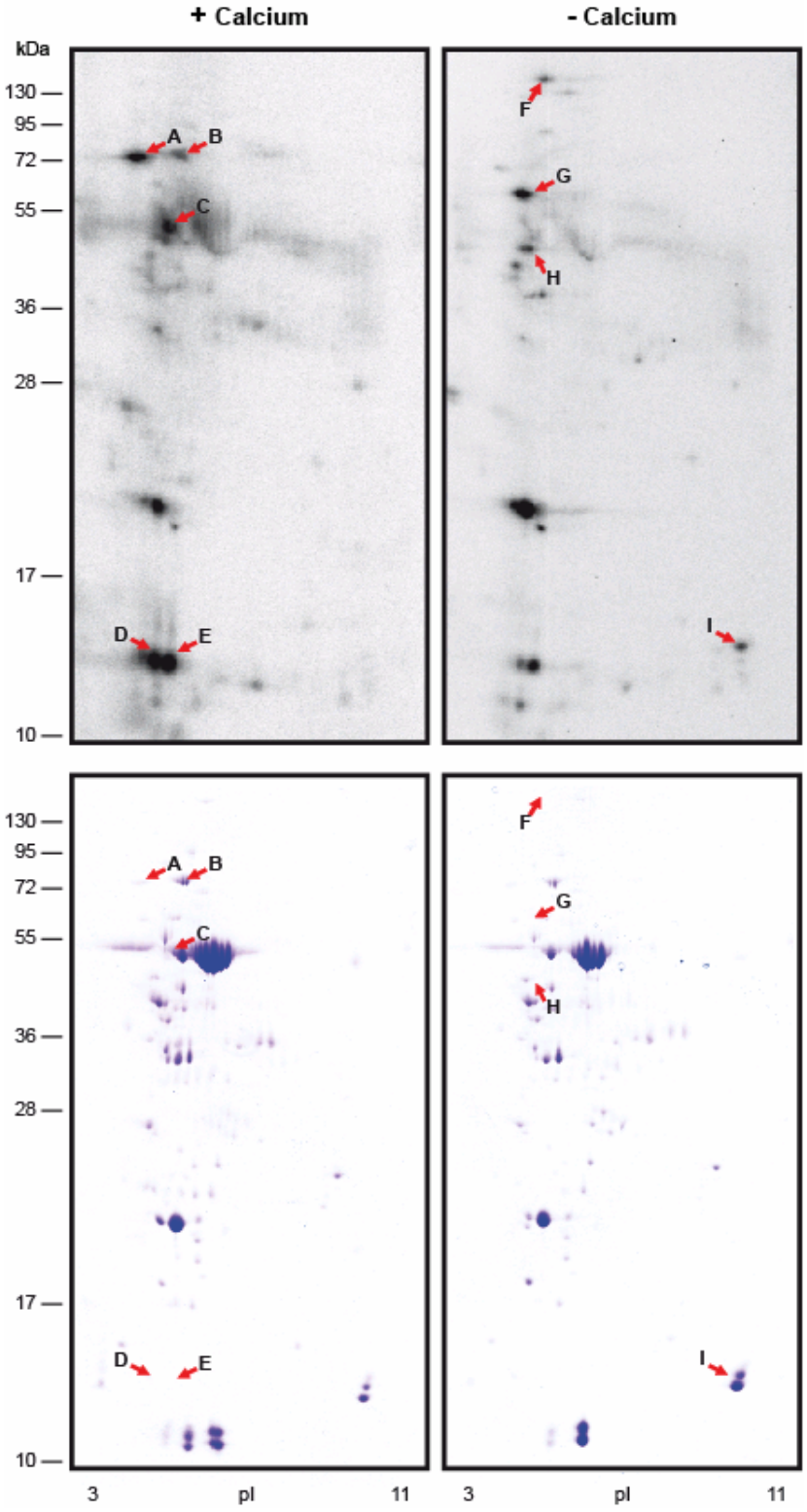

Fig. 6 - Identification of calcium-dependent stromal phosphoproteins - Autoradiograms (upper panel) and coomassie brilliant blue stained gels (lower panel) of stromal proteins from Arabidopsis. Proteins were separated by 2D-PAGE (IEF followed by SDS-PAGE), after phosphorylation assays in the presence of calcium (+) or EGTA (-). Proteins indicated by an arrow were excised and analyzed by LC-MS/MS.

From the coomassie stained gels it is also visible that some proteins in the region ~12 kDa undergoes a pI shift independently of phosphorylation but dependent on calcium.

In order to identify candidates, "cold" phosphorylation assays were performed with the same samples. Protein spots were excised out of the coomassie brilliant blue stained gel from the regions of interest and proteins were analyzed by mass spectrometry. As was to be expected from such a complex mixture of proteins, peptides were found that matched several different proteins, a list of which can be found as Annex Table 2. The candidate list was filtered based on the estimated molecular mass (excluding cleaved targeting peptides), the theoretical isoelectric point of the mature protein (Wilkins et al. 1999) and predicted chloroplastidic localization according to the Aramemnon database (Schwacke et al. 2003). Moreover, the list only displays proteins for which a phosphopeptide was previously identified in phosphoproteomic approaches (PhosPhAt database, Durek et al. 2010; Heazlewood et al. 2008).

4.2 Transketolase as a calcium-dependent phosphoprotein

LC-MS/MS analysis of the spots A and B (Fig. 6, coomassie brilliant blue stain) revealed several peptide masses that matched the predicted amino acid sequence of TKL from Arabidopsis (Fig. 7). The Arabidopsis genome encodes two isoforms of TKL, AtTKL1 (At3g60750) and AtTKL2 (At2g45290). Both proteins contain a predicted chloroplast targeting sequence and the triangle in Fig. 7 indicates the potential cleavage site for the transit peptide deduced by similarity to TKL from spinach (Teige et al. 1998). While AtTKL1 and 2 share 88.5% identity and 94.2% similarity on amino acid sequence level, the alignment in Fig. 7 shows that three peptides matched both isoforms, but the majority of peptides are specific for AtTKL1 (Fig. 7, grey boxes). None of the peptides was specific to AtTKL2, strongly indicating that the protein spots in position A and B represents AtTKL1.

Mature AtTKL1 after cleavage of the targeting peptide has a predicted protein mass of 73 kDa and a predicted IEP of 5.33, both of which correlates well with the features of the 73 kDa phosphoprotein upon 1D- and 2D-PAGE separation. Shifting of AtTKL1 to the acidic side of the gel is also in accordance with a post translational modification by phosphorylation.

Fig. 7 - Alignment of deduced amino acid sequences of AtTKL1 and AtTKL2 - Grey bars behind the sequence indicate the peptides found by tandem mass spectroscopy (Annex Table 3). A triangle indicates the potential cleavage site for the transit peptide as predicted by similarity to spinach transketolase (Teige et al. 1998). Lines under AtTKL2, represent the conserved amino acids between both proteins. Sequence alignment was performed using ClustalW 2.0 (Larkin et al. 2007; Goujon et al. 2010).

4.2.1 Calcium-dependent phosphorylation of recombinant AtTKL

To confirm calcium-dependent phosphorylation of AtTKL, phosphorylation assays were performed with recombinant proteins. Mature forms of both AtTKL1 and 2 without tag were produced using the pTWIN system and proteins were purified under native conditions. To be able to phosphorylate the recombinant proteins, "catalytic" amounts of stromal proteins were included in the reaction. As before, assays were performed in the presence of either Ca^{2+} or EGTA and the results were analysed by SDS-PAGE and autoradiogram (Fig. 8). To ensure that endogenous 73 kDa protein would not interfere with the results, control assays were performed without recombinant protein and no signal was detected at 73 kDa under these conditions (Fig. 8, Str).

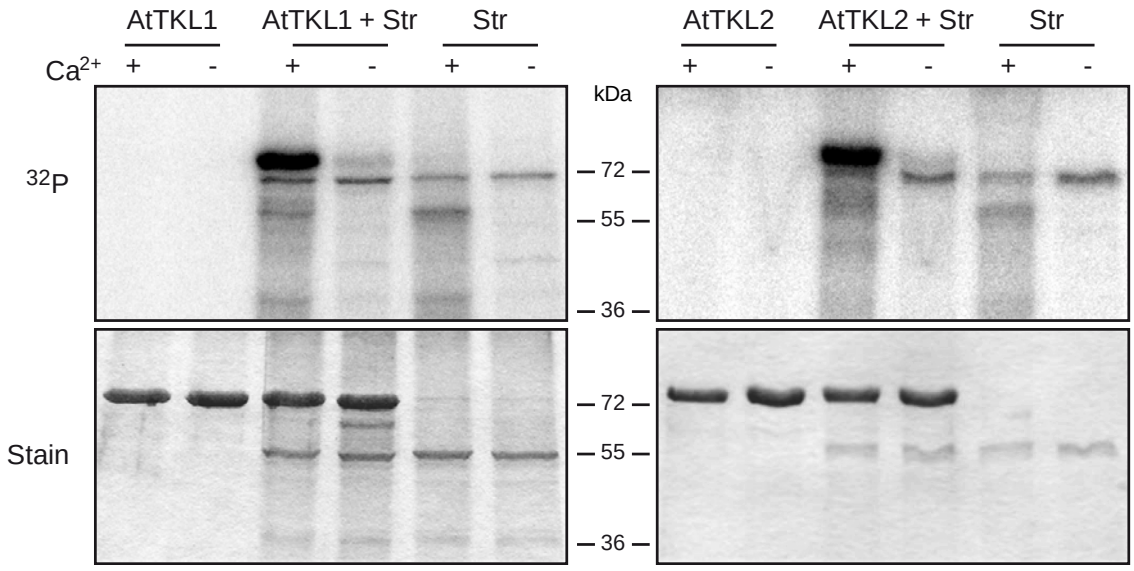

Fig. 8 -TKL is phosphorylated in a calcium-dependent manner - Recombinant AtTKL1 and AtTKL2 were expressed and purified in *E. coli*. Both proteins can be phosphorylation by 'catalytic' amounts of stromal and membrane extrinsic extract. Recombinant proteins and stromal extract alone were used as controls.

Assays with recombinant AtTKL without stroma also showed no phosphorylation indicating that no protein kinase from *E. coli* contaminated the purified protein (Fig. 8, AtTKL1 and 2). In the presence of stromal extract and recombinant protein, phosphorylation could be observed at the corresponding size of AtTKL1 and AtTKL2 only in the presence of calcium (Fig. 8, AtTKL1 and 2 + Str). This shows that recombinant AtTKL1 and AtTKL2 can both be phosphorylated by a stromal protein kinase in a

calcium-dependent manner, thereby confirming the identity of the 73 kDa phosphoprotein as chloroplast TKL.

Interestingly, a protein at about 68 kDa was phosphorylated in the stromal extract alone independent of calcium. This protein was not observed before, which might be due either to slight differences in the preparation of the stromal extract or inhibition of phosphorylation of this protein at higher stroma concentrations.

4.2.2 AtTKL is phosphorylated by a stromal kinase

To confirm the exclusive localization of the corresponding protein kinase in the chloroplast stroma, chloroplast proteins were separated into stromal (Str) and membrane proteins (Mem) and phosphorylation assays were performed with recombinant AtTKL1 and AtTKL2 (Fig. 9).

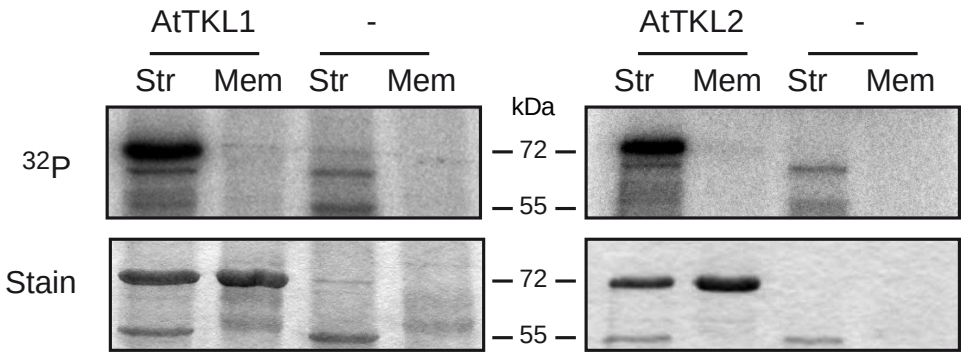

Fig. 9 - TKL is phosphorylated by a stromal kinase - Purified recombinant AtTKL1 and AtTKL2 can be phosphorylation by 'catalytic' amounts of stromal protein extracts (Str) but not by membrane proteins (Mem). Recombinant proteins, stromal and extrinsic extracts (Str) and membrane proteins (Mem) were used alone as controls. Upper panel shows the autoradiograms and lower panel the coomassie stained proteins.

It is clearly visible from the autoradiogram that both proteins can only be phosphorylated when stromal proteins are present in the assay but not in the presence of membrane proteins. Both chloroplast fractions were also tested individually without recombinant

proteins and no phosphorylation could be observed at 73 kDa. This confirms the phosphorylation of AtTKL by a soluble stroma-localized protein kinase.

4.2.3 Characterization of AtTKL1 phosphorylation

While the *in vitro* data indicate that both Arabidopsis TKLs can be phosphorylated in a calcium-dependent manner, the LC-MS/MS data suggested AtTKL1 as the target identified in the initial experiments. This is in good accordance with the fact that AtTKL1 seems to be the ubiquitous isoform with a high expression level especially in leafs (see Fig. 3), while AtTKL2 is only expressed in late seed. Therefore, subsequent experiments were preformed exclusively with AtTKL1.

To better understand the kinetics of the phosphorylation reaction, time-dependent and protein-concentration dependent phosphorylation assays were performed using recombinant AtTKL1 and "catalytic" amounts of stromal extract (Fig. 10). Results were not only visualized by SDS-PAGE and autoradiogram but also quantified with the software AIDA Version 3.52-046, according to the autoradiogram color intensity and expressed in Integral/Area - background intensity (PSL/mm^2).

Time-dependency of the reaction was measured by stopping the reaction at different time points between 0 to 25 minutes (Fig. 10, A). Phosphorylated AtTKL1 appears after about 30 seconds and the intensity of the phosphorylation signal increases until a saturation is reached after about 15 - 20 min. The phosphorylation dependency on AtTKL1 was also tested by using different amounts of recombinant protein (30 – 1000 ng) in the assay. Not surprisingly, the signal intensity increased in a linear manner with the increasing amount of AtTKL1 (Fig. 10, B) indicating that a wide range of substrate concentration can be used without affecting the kinase reaction.

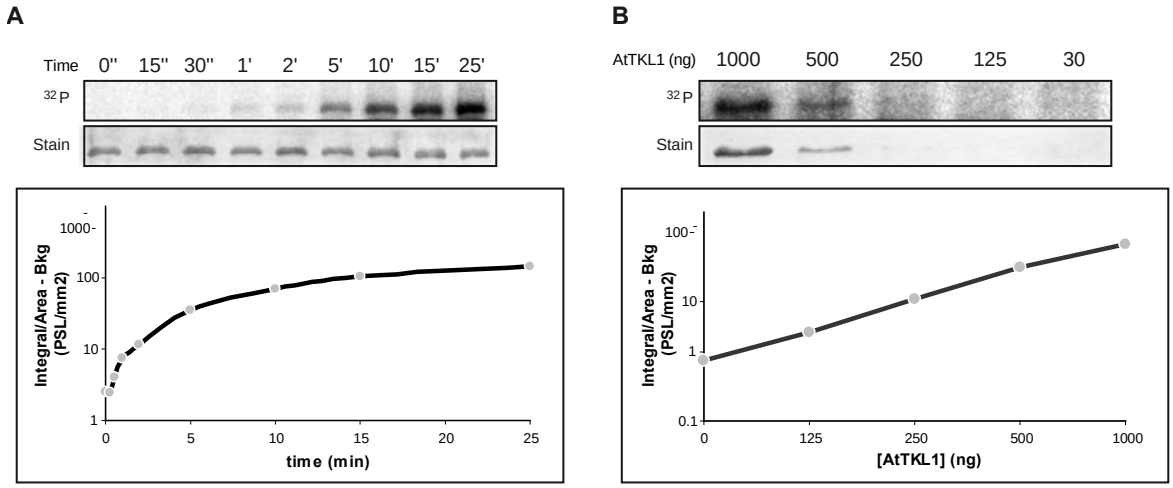

Fig. 10 - Characterization of AtTKL1 phosphorylation - A. Time course assay – Phosphorylation reactions were stopped at different time points (0 – 25 minutes) by addition of SDS-PAGE sample buffer and intensity of AtTKL1 phosphorylation was analyzed by autoradiogram after SDS-PAGE separation (upper panel). The lower panel represents a plot of time versus phosphorylation intensity. **B.** Protein concentration assay – Phosphorylation was performed with different amounts of recombinant AtTKL1. Upper panel shows the autoradiogram of reactions containing amounts of AtTKL1 ranging from 30 – 1000 ng protein). The chart in the lower panel represents the linear dependency of phosphorylation intensity on protein concentration. Intensity of phosphorylation was detected with the software AIDA Version 3.52-046, according to the autoradiogram color intensity and expressed in Integral/Area – background intensity (PSL/mm^2).

4.3 Topology and phylogeny of TKL

4.3.1 Identification of the phosphorylation site of AtTKL1

With the recent advances in mass spectrometry, it became the tool of choice for phosphopeptide identification. However, it is still challenging to investigate this post-translation modification in complex biological samples especially with phosphorylated proteins that are present only in low abundance.

To identify the exact position(s) at which AtTKL1 is phosphorylated, the endogenous Arabidopsis TKL was thus enriched by immuno-precipitation using stromal extract and an antibody raised against recombinant AtTKL1 (Fig. 11, A). Stromal extract (L) was incubated with protein A agarose and α-AtTKL1 and the flow-through containing unbound proteins was collected (FT). After thourough removal of unbound portein (W), proteins interaction with the antibody were removed from the beads by boiling the sample for 5 minutes with SDS solubilization buffer.

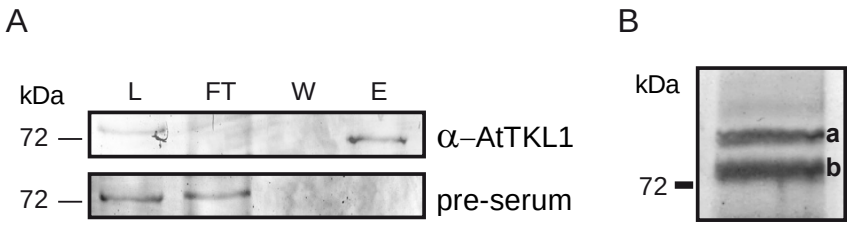

Fig. 11 - Enrichment of endogenous AtTKL by co-immuno-precipitation - **A.** Endogenous stromal AtTKL could be enriched by immune-precipitation with α-AtTKL1 (α-AtTKL1). Pre-immune serum was used as a control for the specificity of the antibody (pre-serum). Coomassie brilliant blue stain of: L - loading of stromal extracts; FT - flow through; W – washing; E – elution. **B.** Elution fraction of stromal AtTKL enriched by co-immuno precipitation after a "cold" phosphorylation assay. For a better resolution, proteins were separated by a 10% SDS-PAGE and stained with coomassie brilliant blue. Bands "a" and "b" were analyzed by LC-MS/MS (Table 7).

SDS-PAGE analysis shows that a protein band of the molecular mass of AtTKL could be eluted from the beads in the presence of α-AtTKL1. When pre-immunserum was used as a control, no protein bound to the beads indicating the specificity of the antibody to AtTKL (Fig. 12, A, pre-serum).

To determine the phosphorylation site of AtTKL1, a 'cold' calcium-dependent phosphorylation assay was performed with Arabidopsis stromal extract followed by immuno-precipitation using this antibody. This time, the elution fraction was separated on an SDS-PAGE with lower acrylamide concentration (10%) for a better separation of TKL from the heavy chains of the antibody (Fig. 11, B). Under these conditions, two protein bands can be observed in the elutate at 73 kDa and at 74 kDa. Both bands were independently excised out of the PAGE and analyzed by LC-MS/MS with a special focus on the identification of phosphopeptides. To increase the yield of phosphorylated peptides, a specific enrichment step with TiO_2 was performed.

Table 7 - Phosphopeptides identified in AtTKL1 - Arabidopsis proteins pulled down with the antiserum against AtTKL1 (see Fig. 11, B) were analysed by LC-MS/MS. A single phosphopeptide could be detected from the protein band at 74 kDa, which matches AtTKL1.

Band	Protein Identification	Phosphopeptide
a	AtTKL1 (At3g60750)	ALPTYTPES(p)PGDATR
b	AtTKL1 (At3g60750)	----

Only peptides belonging to AtTKL1 could be identified in both proteins confirming the specificity of the antibody. It also shows that both proteins represent AtTKL1. The analysis furthermore yielded a single phosphopeptide indicating a phosphorylation of serine in position 428 (Ser_{428}) in the AtTKL1 sequence (Annex Fig. 2). Interestingly, the phosphopeptide was only found in the protein with slightly higher molecular mass, indicating that the difference in separation behavior might be due to the phosphorylation (Figs. 11, B).

Since no further phosphopeptide was identified, a variant of AtTKL1 was constructed containing a serine to alanine exchange at this position. Purified recombinant AtTKL1 and $AtTKL1_{S/A}$ were then used for calcium-dependent phosphorylation assays with "catalytic" amounts of stromal proteins (Fig. 12).

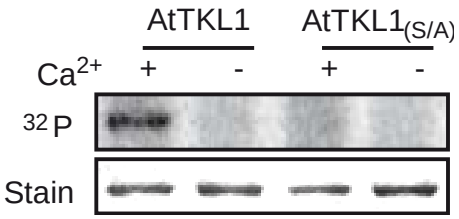

Fig. 12 - AtTKL1 is phosphorylated at a single serine residue - Recombinant $AtTKL1_{(S/A)}$ lacking Ser_{428} identified in the phosphopeptide analysis could no longer be phosphorylated by stromal extracts. Upper panel shows the autoradiogram and lower panel the commassie brilliant blue stain.

In contrast to the control assay with AtTKL1, no phosphorylation could be observed for recombinant $AtTKL1_{(S/A)}$ (Fig. 12) neither in the presence or absence of calcium, confirming that phosphorylation of AtTKL1 occurs solely at Ser_{428}.

4.3.2 Phylogenetic distribution of TKL phosphorylation

A sequence alignment of TKLs from a number of different photosynthetic organisms showed a conserved domain around the phosphorylated Ser_{428}. Based on the presence of an amino acid susceptible to undergo phosphorylation at this position, TKLs can be grouped in two classes. The first class includes vascular plants, where a serine or very rarely threonine residue (e.g. in *Pisum sativum*) are present (Fig. 13, upper panel). In contrast, the

second class includes TKLs from mosses, algae and cyanobacteria that exclusively possess aspartate in place of the serine (Fig. 13, lower panel).

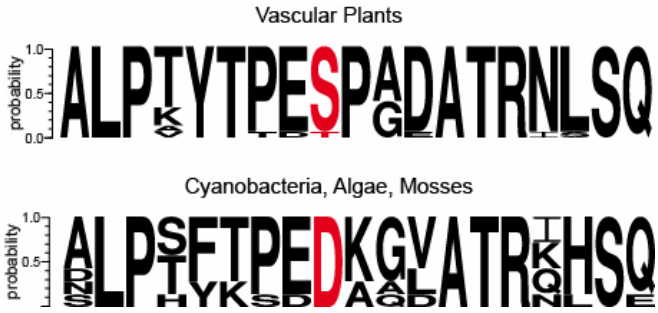

Fig. 13 - Phylogenetic conservation of TKL phosphorylation - Sequence alignment of the conserved region containing the phosphorilation site of AtTKL1 (red). Vascular plants contain a conserved serine (or with less occourence a threonine). TKLs from cyanobacteria, algae and mosses exclusively contain an aspartate in the same position. The probability analysis was based on the alignment included on Annex Fig. 3.

A serine residue is also found in TKL from Selaginella, a spike moss belonging to the lycophytes, which phylogentically are placed between the bryophytes and the euphyllophytes.

The presence of an aspartate makes it unlikely that non-vascular plant TKLs are phosphorylated at this position. Nevertheless, TKL phosphorylation of a non-vascular photosynthetic organism was also analysed. To that end, recombinant transketolase from *Chlamydomonas reinhardtii* (CrTKL) was expressed in *E. coli* and purified under native conditions. Using the recombinant protein and soluble extracts from this alga, phosphorylation assays with ^{32}P-ATP were performed in the presence or absence of calcium (Fig. 14).

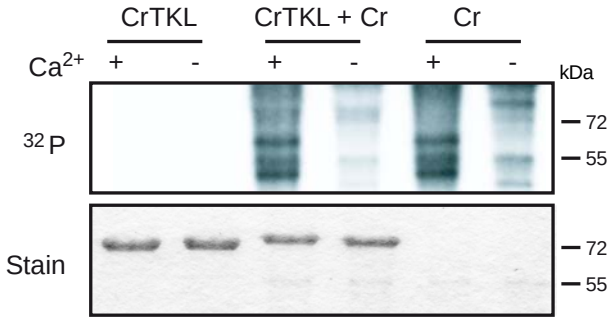

Fig. 14 - CrTKL is not phosphorylated - Phosphorylation assays with recombinant CrTKL and soluble extracts of *Chlamydomonas reinhardtii*. Reactions were performed in the presence of Ca^{2+} or EGTA and control reactions with recombinant protein or Chlamydomonas extracts alone were tested. Proteins were separated by SDS-PAGE, stained with coomassie brilliant blue (lower panel) and phosphorylation patterns analyzed by X-ray film (upper panel).

No phosphorylation of the recombinant protein could be observed at all in these assays including endogenous phosphorylation in the alga extracts around the 73 kDa region. However, other proteins in the extract undergo calcium-dependent phosphorylation showing that calcium-dependent kinases are present (~ 58 and 50 kDa). This data strongly suggests that CrTKL is not phosphorylated in the same manner as AtTKL1.

To confirm phosphorylation of TKL from other vascular plants, an immuno precipitation of the phosphorylated 73 kDa protein from Pisum was tested using the α-AtTKL antibody. A kinase assay in the presence of calcium was done with stroma isolated from purified chloroplasts from *Pisum sativum*. The phosphorylation reaction was subsequently incubated with the α-AtTKL1 antiserum and protein A agarose and endogenous PsTKL was pulled down. After SDS-PAGE separation and protein staining, phosphorylation of the pulled-down protein was evaluated by X-ray film. A protein of the correct size was pulled-down with the antibody and the autoradiogram showed that this protein is radiolabeled, thus strongly supporting that also PsTKL can be phosphorylated in the same calcium-dependent manner (Fig. 15).

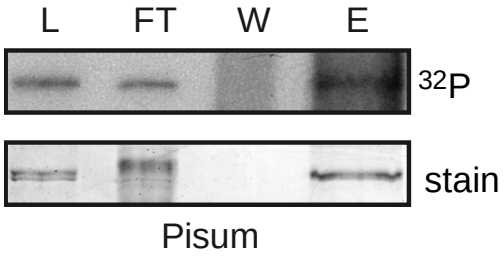

Fig. 15 - PsTKL is phosphorylated - The 73 kDa phosphorylated protein from Pisum stroma can be pulled-down with the antiserum against AtTKL1. Upper panel shows the autoradiogram and lower panel the correspondent gel stained with coomassie brilliant blue.

Together, these results suggest that calcium-dependent phosphorylation of TKLs might be evolutionary conserved in vascular plants but not present in algae or mosses.

In order to understand the role of phosphorylation for AtTKL1, the position of the Ser_{428} was assigned in a 3D model of the crystalized maize TKL (Gerhardt et al. 2003) (Fig. 16). The maize ZmTKL is highly similar to AtTKL1, including a strongly conserved domain around the phosphorylation site of Arabidopsis.

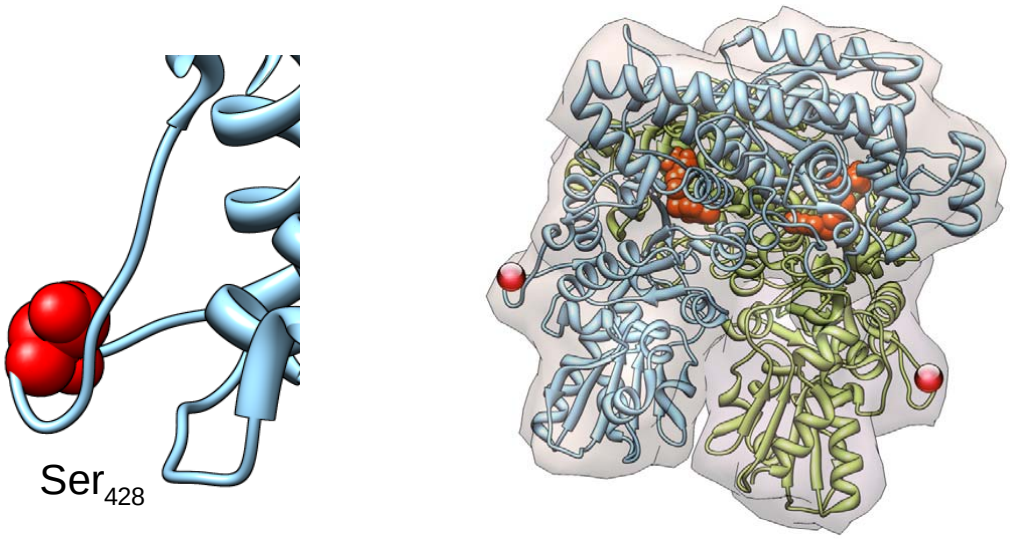

Fig. 16 - Modelling of the AtTKL1 phosphorylation site - The phosphorylation site (red sphere) was modelled onto the 3D-structure of the maize TKL (PDB 1ITZ), which contains a conserved serine in the same position as AtTKL1. The TPP cofactor is labelled in orange.

TKL forms a functional dimer with the active site located in a groove formed by the contact site of the two monomers The Ser_{428} is localized in a loop between α-helix 12 and

β-sheet 6 just at the beginning of the so-called central domain. While the central domain is involved in dimer interface formation as well as TPP cofactor binding, the phosphoserine is located in a loop that extents to both sides out of the compact center of the dimer (Fig. 16). It is far removed from the substrate entrance channel and the conserved residues that are required for binding of either the substrates or the TPP co-factor.

4.4 Influence of phosphorylation on TKL activity

TKL plays an important role in plant metabolism as an integral part of both the Calvin Benson cycle (CBB) and the pentose phosphate pathway (PPP). The enzyme is involved in the reversible conversion of the following phosphate sugars: ribose-5 phosphate (R5P), xylulose 5-phosphate (X5P), erytrose 4-phosphate (E4P), glyceraldehydes 3-phosphate (G3P), sedoheptulose 7-phosphate (S7P) and fructose 6-phosphate (F6P). This way, TKL is involved in several reactions that will yield different news phosphate-sugars. These sugars can serve as intermediates of important metabolic reactions including the regeneration of ribulose 1,5-bisphosphate as well as synthesis of nucleic acids, amino acids and other derivatives. The PPP also produces NAD(P)H for anabolic reactions in non-photosynthetic tissue and in the dark.

According to the 3D structure of TKL, the phosphorylation site is not in close proximity to the active center. Nevertheless, a post-translation modification by phosphorylation could affect protein structure and therefore the kinetics parameters of the enzyme. In order to study the influence of AtTKL1 phosphorylation on Ser_{428}, in vitro assays were setup to determine the kinetic parameters of TKL for several sugars. Recombinant AtTKL1 and a $AtTKL1_{(S/D)}$ variant, in which Ser_{428} was mutated to aspartic acid, were expressed in *E. coli* and purified under native conditions to apparent homogeneity (see Fig. 19). The $AtTKL1_{(S/D)}$ variant was included to mimic constant phosphorylation so that it could be compared to recombinant AtTKL1 which is present in a non-phosphorylated form under these conditions.

Diurnal studies have revealed an increase in stromal pH from 7 to 8 upon illumination (Heldt et al. 1973; Werdan et al. 1975). Furthermore, other stromal enzymes have been reported to change their activity in a light dependent manner (Woodrow et al. 1984;

Anderson 1973; Anderson 1974). Therefore, the experiment was extended by measuring the protein performance at pH 7.2 and 8.0 representing dark and light conditions. Kinetic parameters (Km, Vmax, and Kcat/Km) were than calculated for both TKL variants and for different substrates (X5P, R5P, F6P and G3P).

4.4.1 Kinetic parameters for X5P and R5P

The kinetic parameters of AtTKL1 for the reaction X5P + R5P → S7P + G3P were assessed by a well-established TKL assay (De La Haba et al. 1955) using a coupled reaction with triose phosphate isomerase (TPI) and glycerol 3-phosphate dehydrogenase (GDH) as shown in figure 17. The GDH reaction utilizes NADH and can therefore be measure photometrically. Special care was taken to ensure that neither GDH nor TPI where limiting under the chosen conditions.

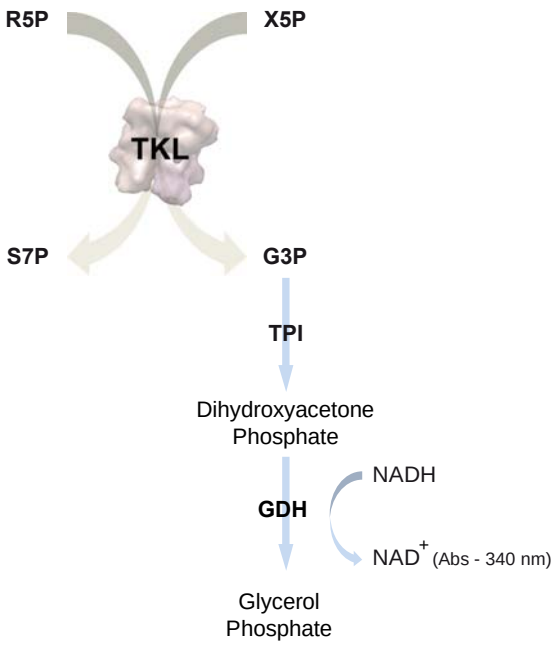

Fig. 17 - Standard coupled assay for measuring TKL activity using R5P and X5P as substrates - The conversion of X5P (ketol donor) and R5P (ketol acceptor) by TKL to S7P and G3P cannot be measured directly. The produced G3P will thus be converted in dihydroxyacetone phosphate (DHAP) by triose phosphate isomerase (TPI). The subsequent conversion of DHAP to D-glycerol 3-phosphate by glycerol 3-phosphate dehydrogenase (GDH) requires NADH. The output of measurement is the conversion of NADH to NAD^+ that can be detected by spectrophotometry at 340 nm.

To study the kinetic parameters for each sugar, the concentration of one substrate was varied between the range of 0.1 to 3.0 mM while the other sugar substrate was kept constant at a high concentration. All reactions followed Michaelis-Menten kinetics (Annex Fig. 1 shows the estimated fit and demonstrates the goodness-of-fit of the estimation routine) and maximum velocity of the reactions was calculated for a linear range of 5 minutes. Table 8 shows the mean values and standard deviation of Vmax, Km and Kcat/Km derived from these measurements.

Table 8 - Kinetic parameters of AtTKL1 for X5P - Purified AtTKL1 and AtTKL1$_{(S/D)}$ protein were used to determine the kinetic parameters by the method represented in Fig. 17. Each value represents the average of four independent determinations including standard deviation at different X5P concentrations (up to 3.0 mM) in the presence of 1.7 mM R5P.

		X5P		
	AtTKL1	**Vmax** (µmol/min•mg TKL)	**Km** (µM)	**Kcat/Km** (M^{-1}•s^{-1})
pH 7.2	**wt**	14.3 ± 0.3	164.3 ± 19.2	2.6•E+05
	S_{428}D	15.3 ± 0.3	260.6 ± 22.4	1.4•E+05
pH 8.0	**wt**	13.1 ± 0.3	115.9 ± 14.6	3.5•E+05
	S_{428}D	13.5 ± 0.3	102.5 ± 12.3	3.2•E+05

The analysis of the kinetic constant Vmax for X5P revealed no significant changes either depending on pH or between the two TKL variants. Nonetheless, at pH 7.2, the wild-type and S/D variant show different apparent Km_{X5P} values of 164.3 and 260.6 µM, respectively. This nearly two-fold increase of the Km_{X5P} is reflected by a two-fold decrease in catalytic activity. By contrast, at pH 8.0, both protein variants have comparable higher Km_{X5P} and Kcat/Km.

For R5P, no significant changes were observed between the two variants for both kinetic constants (Table 9). The pH has a large effect on the Michaelis constant and the catalytic efficiency. At pH 8.0 an increase in Km_{R5P} of about two to three fold is observed when compared to pH 7.2 and the catalytic efficiency decreased by about 40 % (Table 9).

Table 9 - Kinetic parameters of AtTKL1 for R5P - Purified AtTKL1 and AtTKL1$_{(S/D)}$ protein were used to determine the kinetic parameters by the method represented in Fig. 17. Each value represents the average of five independent determinations including standard deviation at different R5P concentrations (up to 3.0 mM) in the presence of 1.5 mM X5P.

		R5P		
pH	**AtTKL1**	**Vmax** (µmol/min•mg TKL)	**Km** (µM)	**Kcat/Km** (M^{-1}•s^{-1})
7.2	**wt**	18.4 ± 0.5	486.7 ± 42.5	9.2•E+04
	S_{428}D	17.9 ± 0.7	508.7 ± 58.3	9.3•E+04
8.0	**wt**	20.9 ± 0.8	1245.0 ± 104.8	4.1•E+04
	S_{428}D	20.6 ± 1.6	1399.0 ± 233.8	3.9•E+04

In summary, these results suggest that AtTKL1 activity is affected by pH, specifically for R5P. Furthermore, phosphorylation of TKL increases affinity for X5P at pH 7.2 but not at pH 8.0.

4.4.2 Kinetic parameters for F6P and G3P

The conventional and established substrates used for kinetic measurements of TKL are R5P and X5P. However, schematic in figure 18 represents an alternative method for measuring TKL activity as recently proposed by Naula et al. (2008).

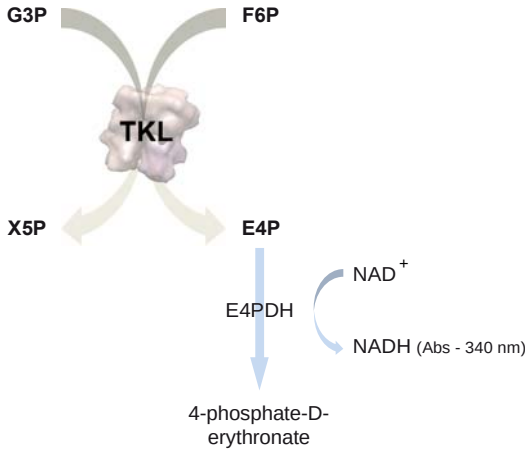

Fig. 18 - Coupled assay for measuring TKL activity using F6P and G3P as substrates - In a coupled reaction the conversion of F6P and G3P in X5P and E4P by TKL can be measured by a subsequent conversion of E4P into 4PE (4-phosphate-D-erythronate) by E4PDH that produces NADH. The output of measurement is the conversion of NAD^+ to NADH that can be detected by spectrophotometry at 340 nm.

This new method uses F6P (ketol donor) and G3P (ketol acceptor) as substrates. They will be converted in X5P and E4P and activity can be measured in a coupled reaction using erythrose 4-phosphate dehydrogenase (E4PDH) (E.C 1.2.1.72). This auxiliary enzyme converts E4P to 4-phosphate D-erythronate in a reaction that will reduce NAD^+ to NADH and can thus be measured photometrically.

The assay requires E4PDH as auxiliary enzyme and since it is not commercially available, recombinant enzyme was prepared in *E. coli*. The protein was purified under native conditions using a C-terminal 6xHis-tag and protein purity was confirmed by SDS-PAGE and staining with coomassie brilliant blue (Fig. 21, B). E4PDH was originally thought to be a G3P dehydrogenase (Alefounder and Perham 1989) but more recent studies revealed that G3P is not an efficient substrate (Zhao et al. 1995; Boschi-Muller et al. 1997). Figure 19, A depicts plots of NADH production *versus* time, when AtTKL1 or $AtTKL1_{(S/D)}$ are used together with E4PDH in this coupled reaction. Using 2.5 mM ß-NAD^+, 1.2 µg TKL, 20 µg E4PDH, 2.0 mM G3P and 5.0 mM F6P, the reaction reaches saturation at 2 relative units of absorbance in about 50 min. The affinity of E4PDH to G3P is reflected in a control assay without TKL (Fig. 19, A, blue line). Because it presents a very residual slope, control assays were run for all conditions analysed and in order to determine the final maximum slope of the TKL reaction, the slope value of the control reaction without TKL was deducted.

Since E4PDH was not previously characterized, several parameters were initial analysed to optimize the assay. The optimal concentration of G3P was accessed by varying concentrations of this phosphate sugar at a fixed concentration of E4PDH, AtTKL1 and F6P (Fig. 19, C). Maximum TKL activity occurs with 2.0 mM G3P and an inhibitory effect is observed with concentrations above this concentration. At 10.0 mM G3P, almost no AtTKL1 activity can be detected. To not limit the assay by the coupled reaction, optimal ratio of AtTKL1 and E4PDH to ensure excess of E4PDH activity was also elucidated (Fig. 19, D) and utilized in further assays. This way, the optimal conditions for this reaction were determined as: 2.0 mM G3P, $\geq$ 1.2 µg/200µl AtTKL1 and $\geq$ 10.0 µg/200µl E4PDH.

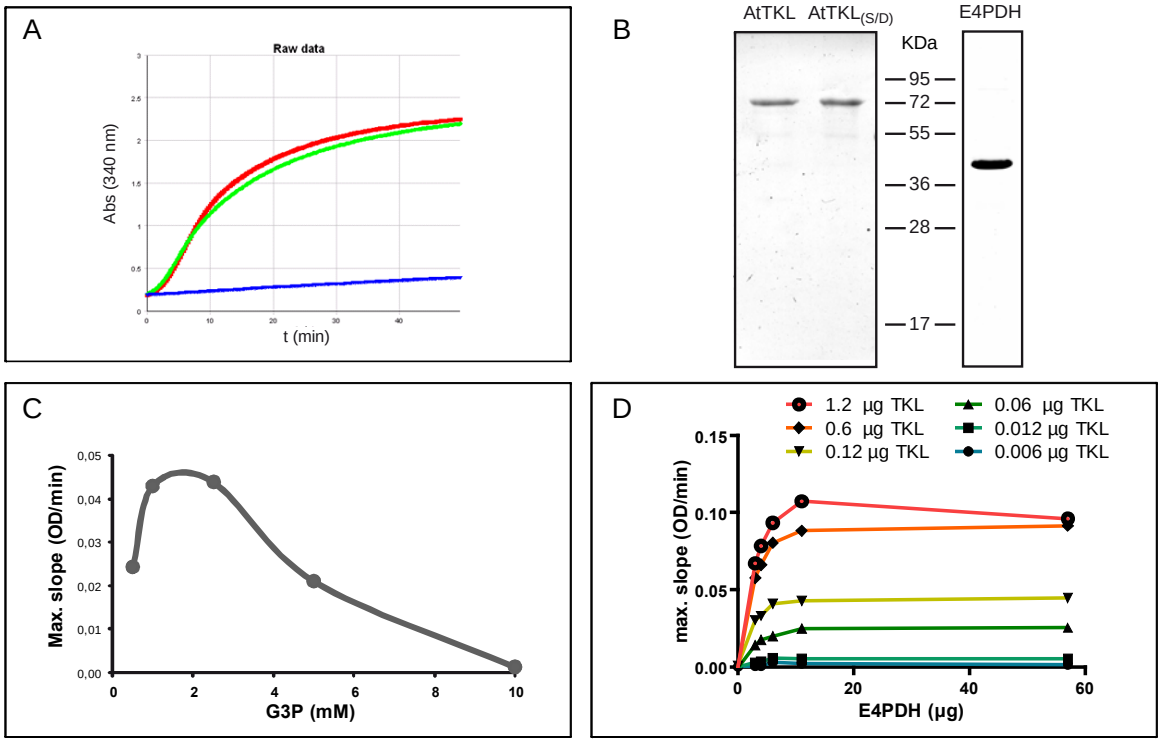

Fig. 19 - Characterization of the coupled reaction with E4PDH - A. Raw data of NADH production at 340 nm by using AtTKL1 (green), $AtTKL1_{(S/D)}$ (red) and a control reaction without TKL (blue). **B.** Recombinant AtTKL1, $AtTKL1_{(S/D)}$ and E4PDH used for kinetic assays. Protein was isolated and purity of the recombinant protein was confirmed by SDS-PAGE and coomassie brilliant blue staining. **C.** Inhibition of AtTKL1 activity by G3P. Different G3P concentrations were tested in the presence of 1.2 µg AtTKL1, 30.0 µg E4PDH and 10.0 mM F6P. The graph shows the maximum slope of reaction (OD_{340}/minute). **D.** Determination of the excess amount of E4PDH. The graphic represents the maximum slope of 200 µl reactions (OD_{340}/minute) by using different amounts of AtTKL1 (0.006, 0.012, 0.06, 0.12, 0.6, and 1.2 µg) and E4PDH (0.0, 1.5, 2.9, 5.7, 11.5 and 57.0 µg).

As before, the kinetic parameters of both TKL variants for F6P and G3P were determined at pH 7.2 and 8.0 (Annex Fig. 1 shows the estimated fit and demonstrates the goodness-of-fit of the estimation routine). All reactions followed Michaelis-Menten kinetics and maximum velocity of the reactions was calculated for a linear range of 5 minutes.

Table 10 shows the mean values and standard deviation of Vmax, Km and Kcat/Km of both enzymes for F6P. The analysis revealed a general increase of Km and Vmax for the wild type enzyme compared to the S/D mutant. Furthermore, both enzymes show a higher Km_{F6P} at pH 7.2 than at 8.0. The wild type Km_{F6P} increases four-fold to 23.1 mM and the mutant three-fold to 11.4 mM. However, these changes in Km_{F6P} are not reflected to the same extent in the catalytic efficiency. The Kcat/Km values are extremely low for both reactions and the differences in between the enzymes are about 20 to 25 %.

Table 10 - Kinetic parameters of AtTKL1 for F6P - Purified AtTKL1 and AtTKL1$_{(S/D)}$ protein were used to determine the kinetic parameters by the method represented in Fig. 18. Each value represents the average of four independent determinations including standard deviation at different F6P concentrations (up to 20.0 mM) in the presence of 2.0 mM G3P.

		F6P		
	AtTKL1	**Vmax** (µmol/min•mg TKL)	**Km** (mM)	**Kcat/Km** (M^{-1}•s^{-1})
pH 7.2	**wt**	4.0 ± 0.2	23.1 ± 1.7	1.4•E+01
	$S_{428}D$	2.4 ± 0.1	11.4 ± 0.6	1.7•E+01
pH 8.0	**wt**	5.5 ± 0.2	7.4 ± 0.8	6.1•E+01
	$S_{428}D$	4.1 ± 0.1	4.1 ± 0.3	8.0•E+01

The analysis of the kinetic parameters of AtTKL1 and AtTKL1$_{(S/D)}$ upon G3P is represented in Table 11 but differences between the two protein variants are relatively minor. Both enzyme variants have a higher Km_{G3P} (five-fold higher) and Vmax (two-to-three fold higher) at pH 8.0 compared to pH 7.2 that is reflected by a lower catalytic activity.

Table 11 - Kinetic parameters of AtTKL1 for G3P - Purified AtTKL1 and AtTKL1$_{(S/D)}$ protein were used to determine the kinetic parameters by the method represented in Fig. 18. Each value represents the average of five independent determinations including standard deviation at different G3P concentrations (up to 2.0 mM) in the presence of 6.0 mM F6P.

		G3P		
	AtTKL1	**Vmax** (µmol/min•mg TKL)	**Km** (µM)	**Kcat/Km** (M^{-1}•s^{-1})
pH 7.2	**wt**	0.7 ± 0.0	124.7 ± 19.2	7.3•E+02
	$S_{428}D$	0.8 ± 0.0	162.4 ± 21.2	6.1•E+02
pH 8.0	**wt**	1.5 ± 0.1	625.1 ± 118.7	2.9•E+02
	$S_{428}D$	1.8 ± 0.1	822.7 ± 83.6	2.7•E+02

4.5 TKL is localized exclusively in chloroplasts

The exact distribution of components of the PPP in plants is still a matter of debate. It was suggested that the two PPP enzymes TKL and aldolase are localized exclusively in chloroplasts, even though the PPP pathway is present in both chloroplasts and the cytosol.

This would require that chloroplast TKL not only provides enzymatic reactions for CBB and the chloroplast PPP but also for cytosolic PPP. So far, localization of TKL in plants was based on the presence of the targeting peptide as well as results from either LC-MS/MS analysis (Reiland et al. 2009; Joyard et al. 2010; Peltier et al. 2006; Kleffmann et al. 2004) or enzyme assays using different sub-cellular extract (Schnarrenberger et al. 1995; Teige M 1996). To assess these results, the subcellular localization of AtTKL1 and AtTKL2 was analysed by transient expression of YFP fusion proteins and confocal laser scanning microscopy. The full-length coding region of AtTKL1 and AtTKL2 was fused N-terminally to YFP in a vector suitable for Agrobacterium-mediated transformation. The constructs were then expressed in leaf cell of *Nicotiana benthaminana* under control of the cauliflower mosaic virus *CaMV 35S* promoter. Protoplasts were prepared from transformed tobacco leaves and analysed by fluorescence microscopy (Fig. 20) under conditions that allowed the monitoring of YFP as well as chlorophyll fluorescence.

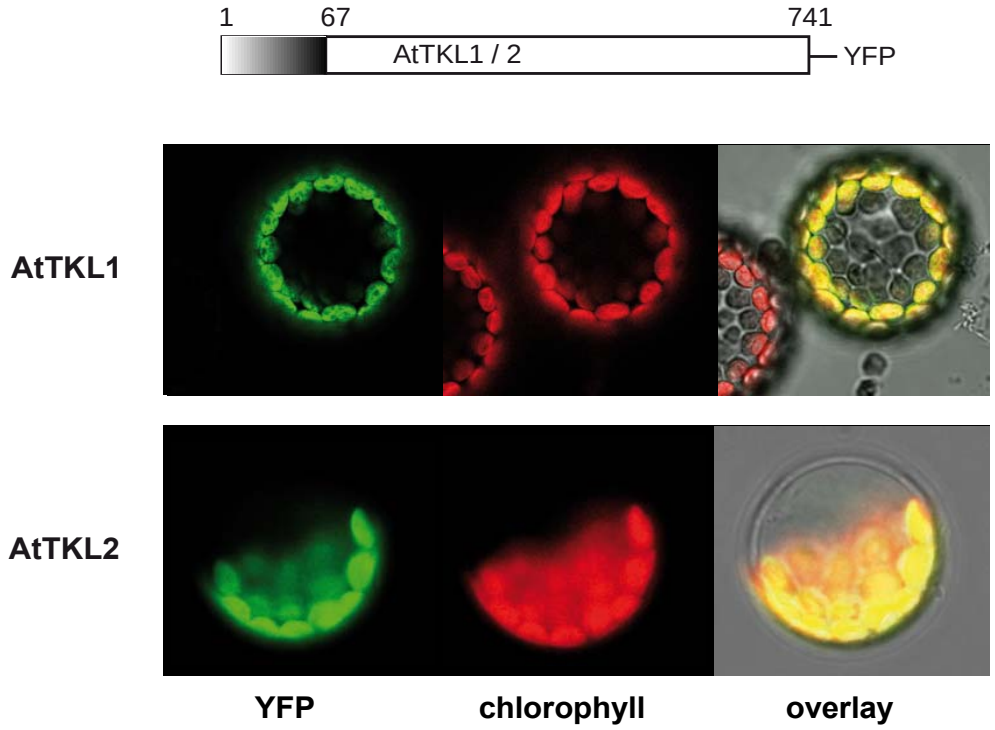

Fig. 20 - AtTKL1 and AtTKL2 are localized exclusively in chloroplasts - AtTKL1-YFP and AtTKL2-YFP were transiently expressed in tobacco leaf cells. Fluorescence of YFP (green) and chlorophyll (red) was analyzed by laser scanning fluorescence microscopy using protoplasts isolated from transformed leafs.

For both constructs the YFP signal clearly overlaps with the chlorophyll fluorescence (Fig. 20, chlorophyll) and is not visible anywhere else in the cell (Fig. 20, merged), thereby supporting an exclusive chloroplast localization of both AtTKL1 and 2.

4.6. Thylakoid targets of calcium-dependent protein phosphorylation

In collaboration with the group of Dr. Markus Teige at the Max F. Perutz Laboratories of the University of Vienna, potential target of calcium-dependent phosphorylation were also elucidated within the thylakoid proteome. In an approach similar to what is described in 4.1.3 for stromal proteins, Simon Stael identified potential thylakoid targets by LC-MS/MS and a list of candidates is represented on table 12.

Table 12 - Overview of potential thylakoid targets of calcium-dependent phosphorylation - As identified by LC-MS/MS within the thesis work of Simon Stael in the group of. Dr. Markus Teige at the Max F. Perutz Laboratories of the University of Vienna (Stael et al., 2012). In case of Var, peptide matched both known isoforms of the protein.

ID	AGI code	Description
PsaN	At5g64040	Photosystem I subunit N
CAS	At5g23060	'Calcium sensing' protein
VAR1/VAR2	At5g42270/At2g30950	Variegated 1 and 2, FtsH proteases
PsbP-1	At1g06680	Photosystem II subunit P-1
PsaH-2	At1g52230	Photosystem I subunit H-2

4.6.1. Validation of calcium-dependent phosphorylation

As with the TKL, these potential targets needed to be further validated by using recombinant proteins. To that end, the most likely targets PsaN, CAS, VAR1, and VAR2 were expressed and purified under native conditions from *E. coli*. In case of CAS and PsaN, the proteins were purified without a tag by using the pTwin system. By contrast, VAR1 and VAR2 were purified by a C-terminal gluthathione-*S*-transferase (GST) tag. PsaN is a small nuclear-encoded component of PSI that is only associated with the thylakoid membrane and was expressed in its mature form without its targeting sequence.

CAS, VAR1, and VAR2 are nuclear-encoded proteins that reside in the thylakoid membrane but all known phosphorylation sides were found in the C-terminal, stromal exposes part of the proteins (Vainonen et al. 2008; Reiland et al. 2009). Therefore, only the C-terminal part was cloned, resulting in soluble expression of the proteins.

All constructs were then used for *in vitro* phosphorylation assays using catalytical amounts of stromal extracts in the presence of either Ca^{2+} or EGTA. As before, control kinase assays were performed with recombinant protein or stromal extracts alone. Proteins were separated by SDS-PAGE, stained by coomassie brilliant blue and phosphorylation was detected by autoradiogram (Fig 21).

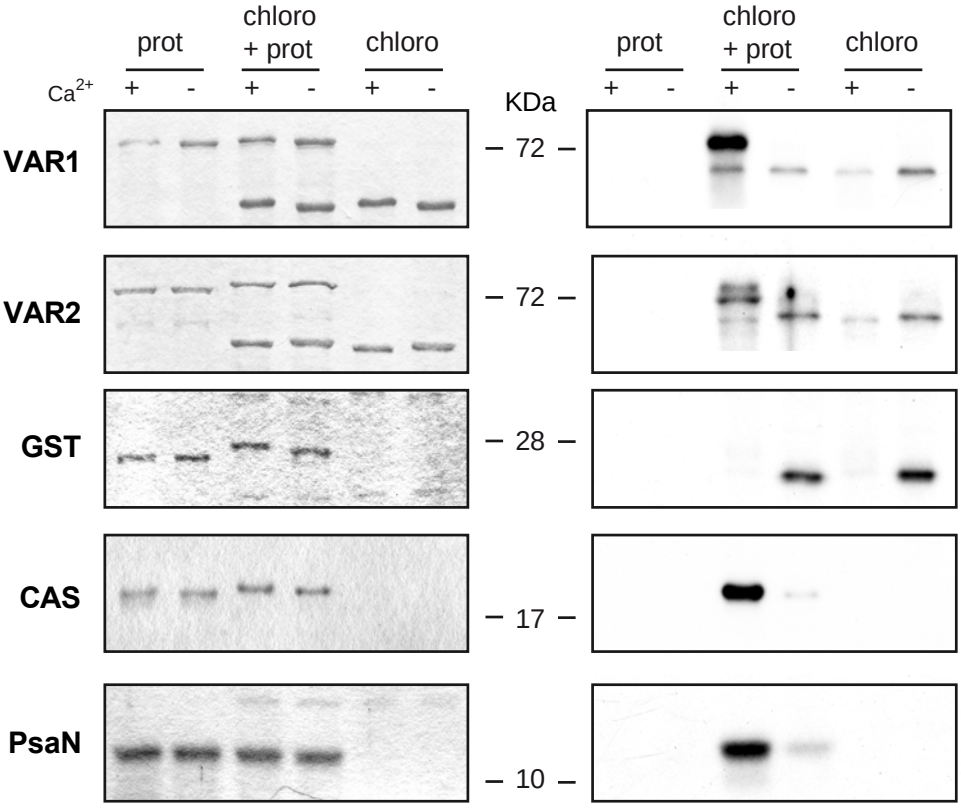

Fig. 21 - Validation of potential thylakoid targets of calcium-dependent phosphorylation - Purified recombinant PsaN, CAS, VAR1, VAR2, and GST were analysed using catalytically amounts of stromal extracts. All four proteins can be phosphorylated in a calcium-dependent manner. Recombinant proteins (two lanes on the right) and stromal extract (two lanes on the left) alone were used as controls. The left panel display the autoradiogram of ^{32}P-labelled proteins and the right panel is the protein loading control stained with coomassie brilliant blue.

No phosphorylation was detected when only recombinant proteins were included in the assay, showing that there is no contamination with an E. coli protein kinase able to phosphorylate these proteins (Fig 21, first two lanes). On the other hand, PsaN, CAS, VAR1 and VAR2 were all clearly phosphorylated in a calcium-dependent manner by stromal extracts. However, despite similar amounts of proteins in the assay, the intensity of VAR2 phosphorylation was significantly less compared to VAR1. While in the case of PsaN and CAS a slight reaction in the presence of EGTA can be observed, the signal is highly increased in the presence of calcium. Phosphorylation in the absence of calcium could be due to further phosphorylation sides that are targeted by another calcium-independent kinase.

4.7 Identification of chloroplast calcium-binding proteins

The overall aim of this thesis was to elucidate novel components of the calcium-regulation network in chloroplasts. In addition to calcium-dependent phosphorylation, stromal proteins were also analysed for the presence of calcium-binding proteins. To that end, stromal proteins were separated by 2D-PAGE using isoelectric focusing in the first and SDS-PAGE in the second dimension. The separated proteins were then transferred by Western blot onto a PVDF membrane and calcium-binding assay was executed by incubation of the membrane with the radioactive isotope ^{45}Ca after re-naturation of the proteins on the membrane. To avoid unspecific binding due to positive charge, the reaction was competed with an excess of the divalent cation Mg. As can be seen from the autoradiogram, a prominent protein of about ~12 kDa which resides on the acidic region of the membrane shows the only clear calcium-binding under these conditions.

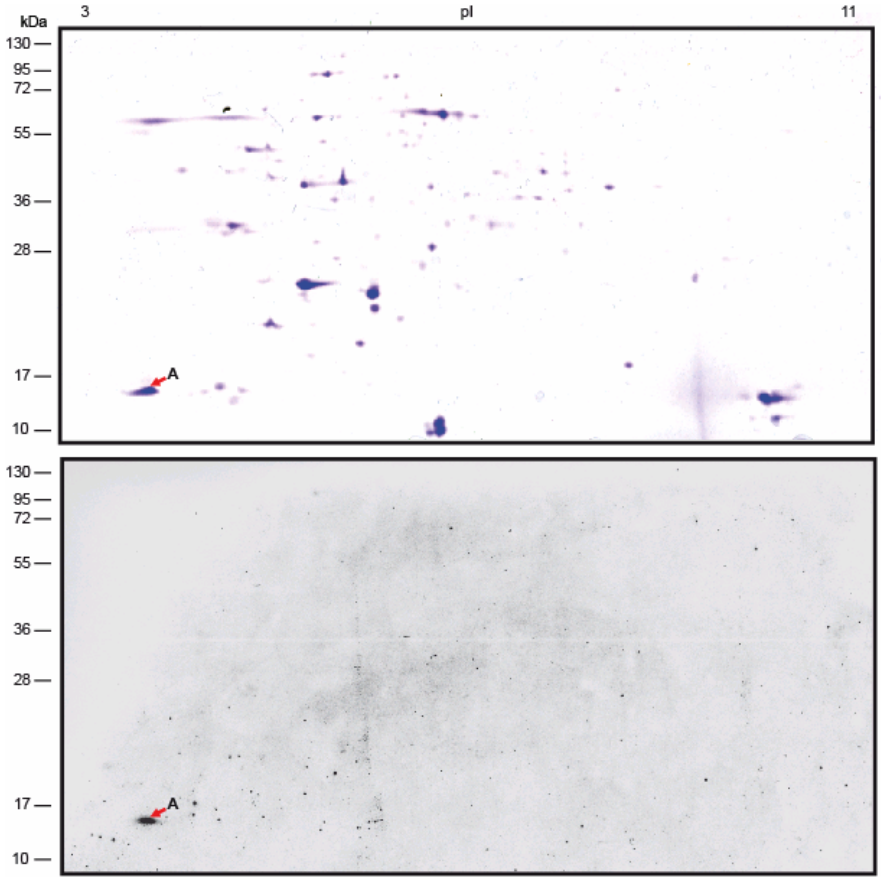

Fig. 22 – Calcium-binding assay of stromal proteins – Stromal proteins from Arabidopsis separated by 2D-PAGE (IEF followed by SDS-PAGE), after calcium-binding assays in the presence of ^{45}Ca. **C**oomassie brilliant blue stained gel (upper panel) and autoradiogram (lower panel). The protein indicated by an arrow was excised and analyzed by LC-MS/MS.

Due to its location and abundance, the protein spot was easily identified on a corresponding SDS-PAGE stained with coomassie brilliant blue. The spot of interest (Fig. 22, A) was excised out of the gel and analysed by LC-MS/MS. Two peptides matched the sequence of one isoform of the small chloroplast protein CP12-1 from Arabidopsis (AtCP12-1, At2g47400) as shown by the grey bars in figure 23. The predicted protein mass of AtCP12-1 is 13.5 kDa for the full length protein and 12 kDa for the mature protein after cleavage of the targeting peptide. Furthermore, the mature protein has a theoretical isoelectric point of 4.15 (Wilkins et al. 1999), which is in agreement with the position of the protein in the 2D PAGE analysis.

```
  1 MTTIAAAGLN VATPRVVVRP VARVLGPVRL NYPWKFGSMK RMVVVKATSE GEISEKVEKS
 61 IQEAKETCAD DPVSGECVAA WDEVEELSAA ASHARDKKKA GGSDPLEEYC NDNPETDECR
121 TYDN*
```

Fig. 23 - Deduced amino acid sequence of AtCP12-1 - Grey bars behind the sequence indicate peptides found by tandem mass spectroscopy that matched to this protein. A triangle indicates the potential cleavage site for the transit peptide (Emanuelsson et al. 1999) as well as the N-terminal of the protein used for the calcium-binding assays.

To validate if AtCP12-1 can indeed bind calcium, recombinant protein was produced in *E. coli*. For this propose, the coding region of AtCP12-1 without targeting peptide was cloned in the pTwin vector and recombinant protein was purified under native conditions without a tag. Calcium-binding assays with ^{45}Ca were performed by spotting of purified protein onto a PDVF membrane (Fig. 24, A). Equal amounts of Aequorin (Aeq) were spotted as positive control, since the protein contains three calcium-binding EF domains. Cytochrom C (CytC) was used as a negative control. Results were analyzed by autoradiogram and equal loading of the different proteins onto the PDVF membrane was assessed by coomassie brilliant blue staining of the membrane (Fig. 24, B).

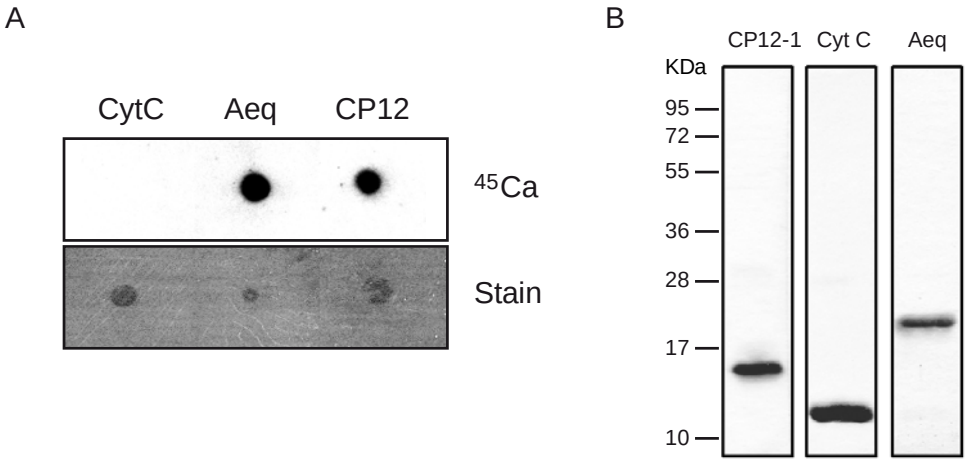

Fig. 24 – Calcium-binding capacity of AtCP12-1 - A. Autoradiograms of calcium-binding assay using recombinant AtCP12-1 (CP12), aequorin (Aeq) and Cytochrom C (CytC). Four µg of each protein were spotted onto a PVDF membrane. The calcium-binding protein aequorin and cytochrome C were used as positive and negative controls, respectively. **B.** Purity of recombinant proteins used for calcium-binding assays was assessed by SDS-PAGE.

It is clearly visible, that by using approximately equal amounts of protein, AtCP12-1 is able to bind calcium to a similar extent than Aeq and no binding was detected for the negative control CytC.

In addition to AtCP12-1, calcium-binding assays were also performed to validate the SAM transporter-like protein as a calcium-binding protein (SAMTL). Within frame of the collaboration with the Teige group, SAMTL, a calcium-dependent mitochondrial carrier was found to localize to inner envelope of chloroplasts (Stael et al. 2011). Furthermore, SAMTL contains a predicted and rather unusual single EF-hand.

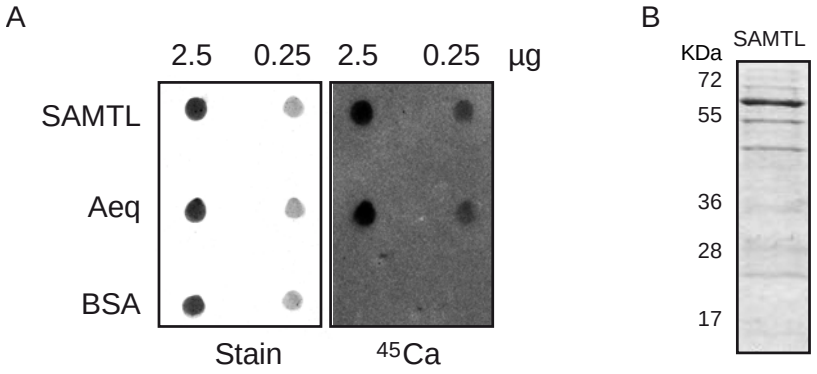

Fig. 25 - Calcium-binding capacity of SAMTL - A. Autoradiograms of calcium-binding assay (^{45}Ca) using recombinant SAM transporter-like protein (SAMTL), aequorin (Aeq) and bovine serum albumin (BSA). Proteins were spoted onto PVDF membrane (2.5 µg and 0.25 µg, respectively, Stain) **B.** Purity of recombinant SAMTL was assessed by SDS-PAGE.

In order to test the calcium-binding capacity of SAMTL, the N-terminal domain of the carrier, containing the predicted EF-hand, but excluding the carrier domain was recombinantly expressed and purified from *E. coli* under native conditions. A radiolabeled calcium (^{45}Ca) overlay assay was then performed by spotting two different amounts of SAMTL onto a PVDF membrane. Aeq was used as positive and BSA as negative control (Fig. 25). SAMTL is able to bind Ca^{2+} *in vitro* to a similar extent as Aeq and no binding to calcium was detected for BSA. Surprisingly, the intensity of the autoradiogram of SAMTL, with one single EF-hand, appeared to be comparable to that of Aeq even though this protein contains three EF-hands. Nonetheless, from this calcium binding assay, no quantitative conclusion can be drawn.

5 Discussion

Protein phosphorylation is one of the most important post-translational modifications and involved in the regulation of many cellular processes. In the cytosol calcium-dependent protein phosphorylation is a well-established process (Kudla et al. 2010; Harper et al. 2004) but so far very little was known about this kind of regulation in chloroplast. This study provides clear evidences for multiple targets of calcium-dependent phosphorylation in this organelle both in the stroma as well as in the thylakoid membrane.

5.1 Transketolase as a calcium-dependent phosphoprotein

The metabolic enzyme transketolase (TKL) was identified as one of the main targets undergoing calcium-dependent phosphorylation in the stroma. TKL is a ubiquitous enzyme present in every living organism and is involved in carbon metabolism. Several lines of evidence indicate that in all plant tissues TKL protein accumulates at higher levels than would be expected from transcript abundance (Baginsky et al. 2005; Teige et al. 1995). This way, a post-translational modification, such as calcium-dependent phosphorylation, might play a role in the regulation of this enzyme. The genome of Arabidopsis encodes two isoforms of this enzyme, both localized exclusively in chloroplasts. By using recombinant protein we can observe that both isoform undergo calcium-dependent phosphorylation in the same manner. Furthermore, the experiments presented here indicate that AtTKL1 and 2 are phosphorylated by a stroma localized kinase, since no membrane proteins are required in the assay. Very little is known about soluble kinases in chloroplasts (Bayer et al. 2012) but it was suggested, that casein kinase II (CKII) is mainly responsible for phosphorylation of stromal proteins (Baginsky and Gruissem 2009). However, CKII is not known to work in a calcium-dependent manner and till present, it was not possible to phosphorylate AtTKL with CKII *in vitro*. The only report of TKL *in vitro* phosphorylation comes from animal models. By using protein kinase C and to smaller extent cAMP-dependent protein kinase and CKII, the TKL from rat can be phosphorylated (Soh 1996). However, neither cAMP-dependent protein kinase nor protein kinase C have been identified in chloroplasts. Therefore, it will be eminent in the future to further elucidate the complete content of chloroplast kinases and their relation to the known substrates of protein phosphorylation.

Phosphoproteomic studies have revealed at least 39 different chloroplast proteins targets of phosphorylation involved in carbohydrate metabolism (Lohrig et al. 2009). In addition, serine is the most common phosphorylation site in chloroplast proteins (Baginsky and Gruissem 2009). The evidences presented in this work, indicate that AtTKL1 is exclusively phosphorylated on Ser_{428} since a single exchange of this amino acid to an alanine is sufficient to completely abolish AtTKL1 phosphorylation (Fig. 12). Thereby, results presented in this study corroborate earlier reports from large-scale proteomic studies that AtTKL1 is subject to phosphorylation (Reiland et al. 2009; Sugiyama et al. 2008; Nakagami et al. 2010). These studies use proteins isolated directly from biological material without any additional phosphorylation reaction thereby confirming that this phosphorylation indeed occurs *in vivo*. By multiple sequence alignment of TKLs from different photosynthetic organisms, we can observe the high homology in the sequence surrounding this potential phosphorylation site among vascular plants. In some cases, like Pisum, a threonine replaces the serine, but this residue is equally well phosphorylated by all known serine/threonine kinases (Edelman et al. 1987). Remarkable is the fact that orthologous proteins from cyanobacteria, algae and mosses contain a highly conserved asparate in the same position. Aspartate is not commonly phosphorylated in chloroplasts but is often employed to mimic serine phosphorylation in protein studies (Wittekind et al. 1989). Comparative genomic analysis has revealed that a replacement of acidic residues by a phosphorylatable serine or threonine has occurred frequently during evolution (Pearlman et al. 2011) and TKL seems to represent another example. Another interesting fact is that the TKL of Selaginella, also contains a serine in this position. Phylogenetically, lycophytes are the oldest extant vascular plants placed in the transition between the bryophytes and the euphyllophytes, which comprise ferns, gymnosperms and flowering plants. They have been suggested as key models for the understanding of major evolutionary adaptation to life on land, such as vascular tissue, leaves, stems, and lignification (Banks 2009). In fact, lignin is the hallmark of vascular land plants, and recent studies revealed that syringyl lignin accumulates in the plant cell wall in response to fungal penetration (Menden et al. 2007). Bringing together, these evidences indicate that calcium-dependent phosphorylation of TKLs is a later evolutionary acquisition that occurs from lycophytes onwards. Thus, TKL phosphorylation might present an environmental adaptation important for regulation of metabolic pathways involved in protection of terrestrial stresses such as pathogen attack (see below).

TKLs in general form functional homodimers with the active site located in a groove formed by the contact site of the two monomers (Gerhardt et al. 2003; Svergun et al. 2000). Based on the 3D crystal structure of the maize TKL (Gerhardt et al. 2003), the Ser_{428} is localized in a loop far removed from the substrate entrance channel and the enzyme active center. This way, phosphorylation of AtTKL1 is unlikely to influence dimerization and no evidence for such a function could be obtained in this study either by BN-PAGE or size exclusion chromatography (data not shown). While enzyme activity is a tempting target, there are also other features that might be influenced by this post-translational modification, such as the spatial distribution of the enzyme with chloroplasts. One of the greatest enigmas with regard to TKL is its functional distribution between different pathways that take place in the same compartment and that utilize the opposite direction of a readily reversible reaction. That both TKLs from Arabidopsis are indeed localized in the chloroplast could be confirmed by our YFP-fusion analysis. One way, to allocate TKL between different pathways would be the interaction of TKLs with other enzymes of the CBB or PPP but such interactions have so far not been demonstrated. Nevertheless, it has been suggested that TKLs undergoes spatial distribution within the chloroplasts (Teige et al. 1998). Based on immuno-gold labeling, using spinach chloroplasts, they proposed a strong association of TKL non-apressed thylakoids. Phosphorylation of TKL might therefore be a means to associate or dissociate the protein with the thylakoid membrane.

5.2 The role of phosphorylation in chloroplast carbon metabolism

Protein phosphorylation/dephosphorylation is one of the most important regulatory modifications on the post-translational level (Olsen et al. 2006; Hunter 2007). The speed in transfer a phosphoryl group catalysed by protein kinases and the conformational changes caused by adding negative charges, make this mechanism an effective way of controlling enzyme activity. For enzyme assays using recombinant proteins, an exchange of serine to aspartate is often employed since this amino acid residue mimics serine phosphorylation due to its shape and charge (Wittekind et al. 1989). In case of AtTKL1, the effect of the S/D exchange was measured for different substrates representing distinct reactions of TKL in both the PPP and CBB. The study was further extended by measuring kinetic parameters

of AtTKL1 at different pH values, representing the physiological range of the stroma under light (pH 8.0) or dark (pH 7.2) conditions (Heldt et al. 1973; Werdan et al. 1975).

The first reaction analysed was the conversion of X5P and R5P into S7P and G3P (Table 8 and 9). This reaction is part of the PPP, which is especially important in the night or in non-photosynthetic tissues. The PPP comprises an oxidative and a non-oxidative phase, the former of which generates NADPH independent from photosynthesis (Izawa et al. 1998) and produces X5P and R5P. The non-oxidative phase of PPP starts with these products of the oxidative phase, and it is important to point out that the kinetic constants calculated for the wild-type AtTKL1 upon X5P and R5P are in a range of those previously observed in other studies with TKLs from photosynthetic organisms (Bouvier et al. 1998; Gerhardt et al. 2003; Teige et al. 1998). More importantly, it is precisely the reaction with those two substrates where AtTKL1 phosphorylation seems to have a modulation effect in 'night' conditions, i.e. at pH 7.2. Glucose 6-phosphate dehydrogenase is the starting enzyme of the oxidative branch of PPP and it catalyzes the conversion of glucose 6-phosphate to 6-phosphogluconolactone in presence of $NADP^+$. This enzyme is inhibited by light (Scheibe et al. 1989) due to a redox regulation by thioredoxins (Udvardy et al. 1984). This way, the non-oxidative steps of PPP mediated by TKL are also inhibited due to a lack of substrate but can readily occur in dark conditions. This is reflected by an extreme increase in Km for R5P in the light. Based on these considerations, any change in enzyme performance due to a post-translation modification should have its biological relevance during the dark period. This fits very well with the observation, that changes in the kinetic parameters between AtTKL1 and $AtTKL1_{(S/D)}$ are indeed much more pronounced at a lower pH. The Km of the non-phosphorylated enzyme for X5P increased by about 50 %, suggesting that phosphorylation lowers affinity to this substrate under dark conditions. The serine to aspartate exchange also lowers the catalytic efficiency (Kcat/Km) for substrate utilization by about two fold. Depending on the metabolic demand of the organism, phosphorylation might thus play an important role in modulating carbon fluxes within the PPP. When AtTKL1 is phosphorylated, the affinity to X5P decreases and this way, pentose phosphates can be channeled out of the PPP into other metabolic reactions. One of the reasons might be a cellular need for the synthesis of nucleic acids and other derivatives of these. This way, the excess of X5P can be exported to the cytosol by the X5P/phosphate translocator (Eicks et al. 2002). It was reported that the desiccation-tolerant plant *C. plantagineum*, which contains three TKLs, has continuously high expression of one

TKL. The other two genes are only expressed during the process of rehydration (Bernacchia et al. 1995). Based on these observations, Schenk and coworkers proposed that increase in expression might be linked to the increased need for nucleotides and amino acids during the accelerated growth of rehydrating plants (Schenk et al. 1998). By contrast, if PPP runs its course, the pentose phosphates X5P and R5P are converted into G3P and F6P mediated by a higher affinity of the non-phosphorylated TKL for X5P. The non-oxidative branch of PPP also generates E4P, a precursor of the shikimate pathway that produces aromatic amino acids as well as precursors for secondary metabolites involved in plant defense and signalling (Jensen 1986; Dixon and Paiva 1995). E4P is a product of both the PPP and the CBB, however, Geiger and Servaites suggested that if E4P would be withdrawn from the CBB in large amounts, the cycle would be depleted (Geiger and Servaites 1994). Thus it is more likely that E4P is removed from the non-oxidative branch of the PPP rather than from the CBB. This would require the TKL reaction with X5P and R5P to take place and channel these pentose phosphates into the non-oxidative branch of the pathway. Activity studies with small changes in TKL content, showed reduced levels of E4P in tobacco plants. This led to photosynthesis inhibition and significantly decreased of aromatic amino acids and soluble phenylpropanoids content (Henkes et al. 2001). Thus it can be envisioned that even minor changes in affinity of AtTKL1 for one of the sugars also affect E4P levels. Therefore, calcium-dependent phosphorylation of TKL could be a mechanism to coordinate the different cellular requirements of intermediates of the PPP.

The second reaction analysed was the conversion of G3P and F6P into X5P and E4P (Table 10 and 11), which occurs in the CBB and represents an important decision point for the fate of the sugars. The affinity of AtTKL1 for G3P does not reflect any dependence on phosphorylation either in the dark or the light, since only minor changes were observed on the kinetic parameters at both pHs. Nevertheless, the analysis did detect an inhibitory effect of G3P on AtTKL1 activity (Fig. 19, C). This is consistent with previous studies, where a feedback inhibition of TKL by G3P was identified and proposed to restrict the regeneration of ribulose 1,5-bisphosphate under conditions where high steady-state concentrations of the intermediates of the CBB are maintained (Knowles 1985). In order to avoid inhibition of the cycle, the triose phosphate/phosphate translocator would than mediate the export of G3P to the cytosol for sucrose synthesis (Fliege et al. 1978; Flugge et al. 1989; Fischer et al. 1994; Flügge and Heldt 1984). However, phosphorylation has a significant impact on the biochemical properties of TKL for F6P. The Km_{F6P} calculated is

higher than those of all the other sugars analyzed. Indeed, it is in the mM range and thus about 10 times higher than the Km_{R5P}. Nevertheless, this is in agreement with previous *in vivo* measurements with spinach TKL that revealed a Km_{F6P} of 3.2 mM and Km_{R5P} of 0.4 mM (Schenk et al. 1998). Furthermore, the cellular content of F6P was estimated to be approximately 5 to 10 fold higher than R5P (Cruz et al. 2008; Sagisaka 1974). Considering that the one goal of CBB is to fix CO_2 to generate carbohydrates and F6P is an important intermediate, the results presented here are in agreement with previous observations. F6P is a precursor for starch synthesis, the major storage carbohydrate in plants. During photosynthesis, transient starches are accumulated during the day and degraded at night to provide carbons for non-photosynthetic metabolism (Geiger and Servaites 1994). Since F6P is also required for the regeneration of ribulose 1,5-bisphosphate by CBB, the cell has to drive F6P utilization preferentially in the direction of X5P and E4P production during the day. This could explain the relatively low Km_{F6P} observed at light-simulated conditions compared to the dark. Furthermore, diurnal analysis of metabolites has shown that F6P contents decreased after transition from dark to light (Kenyon et al. 1981). This way, the higher Km_{F6P} values observed at pH 7.2 might be correlated with the greater availability of this sugar in the dark. The data presented here furthermore indicate that phosphorylation influences the affinity of AtTKL1 to F6P independent of dark/light-simulated conditions. In both cases, $AtTKL1_{(S/D)}$ exhibits an approximately two fold higher affinity to F6P than the wild-type. The extremely low catalytic efficiency of AtTKL1 in catalysing this reaction can be related to a high activation energy of F6P or to the *in vitro* conditions under which this assay was carried. However, there is no available data showing the real efficiency of this reaction. Nevertheless, minor changes detected for the catalytic efficiency of AtTKL1 (~20 - 30%) upon phosphorylation are sufficient to enhance the protein performance towards the usage of F6P as a substrate. Based on the observations presented here, it could be suggested that AtTKL1 is mostly dephosphorylated during the normal flow of the CBB, thereby allowing 5 out of 6 fixated carbons to be used for regeneration of ribulose 1,5-bisphosphate. However, as a fast response to external stimuli, a higher demand on E4P would be required for secondary metabolism and this signal could be mediated by calcium-dependent processes. This would affect the CBB enzymes FBP and SBP that undergo an inhibition upon increase of calcium (Charles and Halliwell 1980; Portis and Heldt 1976; Wolosiuk et al. 1982), which would stop the CBB temporarily from running. This is important, since the removal of E4P out of the cycle would prevent regeneration of

ribulose 1,5-phosphate. Even though, the high amounts of F6P accumulated in the chloroplast should be enough to transiently produce enough E4P by TKL for such an immediate response. Consequently, the transient of calcium would also mediate the phosphorylation of TKL, which than would exhibit higher affinity to F6P. This is necessary since the F6P pool would rapidly be diminishing under these conditions.

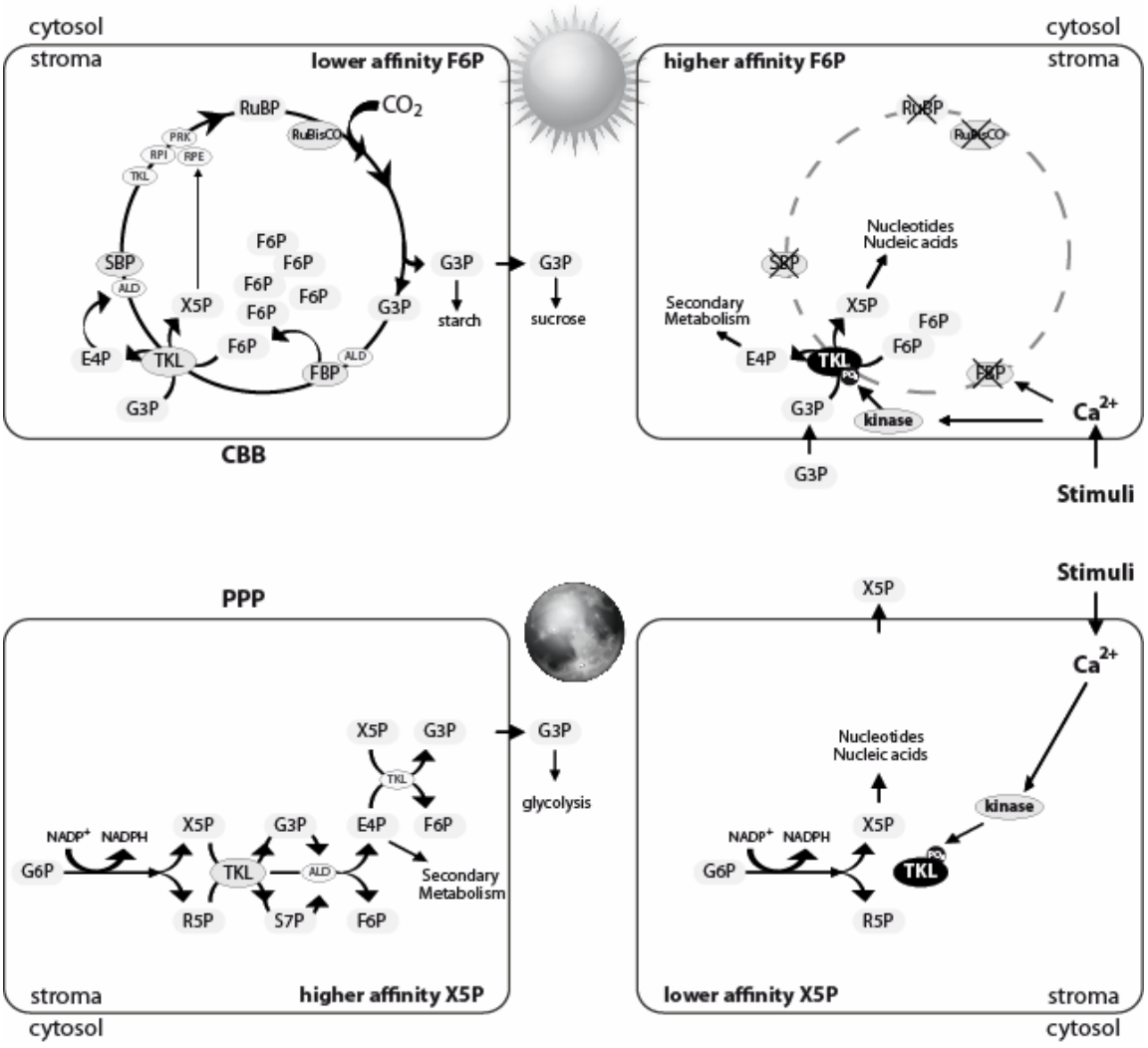

Fig. 26 – Proposed model for TKL regulation by calcium-dependent phosphorylation – The upper panels represent the regulation mechanism of transketolase (TKL) during light and the lower panels during dark conditions. Enzymes included in the scheme are: aldolase (ALD), phosphoribulokinase (PRK), fructose 1,6-bisphosphatase (FBP), sedoheptulose-bisphosphatase (SBP), ribose 5-phosphate isomerase (RPI), ribulose phosphate 3-epimerase (RPE) and ribulose 1,5-bisphosphate carboxylase/oxygenase (RuBisCO). Sugars included in the scheme are: glucose 6-phosphate (G6P), fructose 6-phosphate (F6P), glyceraldehyde 3-phosphate (G3P), ribulose 5-phosphate (R5P), xylulose 5-phosphate (X5P), sedoheptulose 7-phosphate (S7P) and erythrose 4-phosphate (E4P).

All in all, these results indicate that phosphorylation of AtTKL1 might be an important part of its regulation during a typical light-dark cycle of the plant and Figure 26 represents a proposed model for the TKL regulation mechanism in correlation to its function in carbon metabolism. Nevertheless, it remains unclear whether calcium-dependent phosphorylation of AtTKL1 is limited to a role on enzyme activity exclusively in the diurnal rhythm of the plant. For instance, studies on Populus revealed oscillations in phosphate sugars content throughout the year (Sagisaka 1974) without any evidence how this oscillation is regulated. To really understand the role of calcium-dependent phosphorylation of AtTKL1 for the plant it will be essential to elucidate the *in vivo* effect of this modification, e.g. by introducing non-phosphorylatable or phospho-mimicking variants of AtTKL1 into Arabidopsis plants.

5.3 Thylakoid targets of calcium-dependent protein phosphorylation

Our studies on calcium-dependent phosphorylation also identified potential targets in the thylakoid membrane (Stael et al. 2012) and *in vitro* phosphorylation assays confirmed PsaN, CAS, VAR1 and VAR 2 as calcium-dependent phosphoproteins.

The ATP-dependent peptidaseVAR1 and it's a close homologue VAR2 belong to the gene family of metalloproteases. Mutants lacking VAR1 or 2 exhibit leaf variegation and sensitivity to photoinhibition (Sakamoto et al. 2003). Together, they are responsible for the protein turnover of photo-damaged D1 subunits of photosystem II (PSII) (Lindahl et al. 2000; Aro et al. 2005; Kato et al. 2009). In order to prevent photo-inhibition of the PSII, the subunit D1 needs to be constantly recycled (Aro et al. 1993). Protein phosphorylation may control VAR1 and VAR2 activity in the same way it regulates other group of proteases (Kurokawa and Kornbluth 2009). This way, the transient increase on stromal free calcium concentration upon transition from light to dark (Sai and Johnson 2002) might be responsible for phosphorylation of VAR1 and 2. In the dark, the phosphorylated protease will switch off its activity, since it is longer needed to degrade photo-damaged D1 protein.

The calcium-sensing receptor (CAS) was previously reported to be phosphorylated in a light dependent manner (Vainonen et al. 2008). Contrary to current knowledge that have only shown a calcium spike after light-dark transition this would suggest calcium-dependent phosphorylation is mediated by an increase of the calcium concentration under light (Kreimer et al. 1985; Roh et al. 1998; Muto et al. 1982). This is another indication that indeed our current model on chloroplast calcium fluxes might be very incomplete. By instance, a transient increase in calcium concentration could mediate regulation of CAS upon stress. The region comprising the previously identified phosphorylation site of CAS (Thr_{380}) was used for the calcium-dependent phosphorylation assays (Vainonen et al. 2008; Reiland et al. 2009). Interestingly, this threonine is exposed to the stromal site but the calcium-binding site of CAS is part of the proteins transmembrane region (Han et al. 2003). This raises the question if binding of calcium to CAS is in any way related to its calcium-dependent phosphorylation.

PsaN, the extrinsic luminal PSI component, had been previously identified as a potential calmodulin binding protein (Reddy et al. 2002). The role of PsaN phosphorylation within the PSI is more difficult to explain, however, this is more an indication of a diferencial regulation of function.

The identity of the protein kinase(s) responsible for this calcium-dependent phosphorylation is still elusive. However, this data demonstrate that most likely it is a soluble kinase, for several reasons. First, the recombinant proteins were phosphorylated by a fraction containing salt-washed soluble proteins. Second, the phosphorylation site of CAS as well as the C-terminal part of VAR1 and 2 (Sakamoto et al. 2003) faces the stromal side of the thylakoid. This would exclude membrane-intrinsic thylakoid protein kinases such as the STN7 and STN8. Nevertheless, further studies must be conducted to elucidate the role of calcium-dependent phosphorylation on these targets and to identify both the kinase and phosphatase involved in this regulation.

5.4 Identification of novel calcium-binding proteins

Calcium-binding is known to play a role in the regulating enzyme activity (Cheung 1980) and therefore calcium-binding proteins might be part of the chloroplast calcium regulon. The results presented here demonstrate that the chloroplast protein AtCP12-1 is such a calcium-binding protein. CP12 has been identified in many photosynthetic organisms including plants, green algae, cyanobacteria and diatoms (Wedel et al. 1997; Wedel and Soll 1998; Lebreton et al. 2003; Scheibe et al. 2002; Nicholson et al. 1987; O'Brien et al. 1976; Boggetto et al. 2007; Erales et al. 2008). In higher plants, the CP12 family is comprised of three members, CP12-1, 2 and 3 (Singh et al. 2008). CP12 contains four conserved cysteine residues which form two disulfide bridges (Wedel and Soll 1998; Graciet et al. 2003; Marri et al. 2009) and it plays an important role in the regulation of the CBB serving as a linker for the assembly of a supramolecular complex between phosphoribulokinase (PRK) and glyceraldehyde 3-phosphate dehydrogenase (GAPDH). GAPDH was the first light-regulated chloroplast enzyme discovered in plants (Ziegler and Ziegler 1965). *In vivo*, GAPDH is dark-inactivated through the interaction with PRK and CP12 (Wedel and Soll 1998). This process, like several other CBB enzymes, is mediated by the ferredoxin-thioredoxin system upon light-dark transition (Buchanan and Balmer 2005; Wolosiuk et al. 1993). This way, only oxidized CP12, with two disulfide bonds, is active in complex formation (Wedel and Soll 1998). Other experiments demonstrated that the oxidized CP12 is able to bind other divalent cations such as Cu^{2+} and Zn^{2+} (Delobel et al. 2005). Furthermore, Cu^{2+} was found to be involved in modulation of CP12 transition from reduced to oxidized state by modulating the protein structure (Erales et al. 2009). In the same way, binding of calcium might as well represent a mechanism to regulate the CP12-1 by inducing conformational changes. The role of calcium in modulating enzyme activity is extended to other CBB enzymes (Charles and Halliwell 1980; Wolosiuk et al. 1982). Ettinger suggested that calcium is actively transported into the lumen during the day to prevent calcium-dependent inhibition of CO_2-fixation (Ettinger et al. 1999). Upon light-dark transition, the transient increase on stromal free calcium concentration (Sai and Johnson 2002) might be responsible for regulation of the CP12-1. However, additional experiments will be needed to investigate the role of calcium in CP12-1 mediated super-complex formation and its correlation to redox regulation.

6 List of references

A

Alefounder PR, Perham RN (1989) Identification, molecular cloning and sequence analysis of a gene cluster encoding the class II fructose 1,6-bisphosphate aldolase, 3-phosphoglycerate kinase and a putative second glyceraldehyde 3-phosphate dehydrogenase of Escherichia coli. Mol Microbiol 3 (6):723-732

Anderson JM, Charbonneau H, Jones HP, Mccann RO, Cormier MJ (1980) Characterization of the Plant Nicotinamide Adenine-Dinucleotide Kinase Activator Protein and Its Identification as Calmodulin. Biochemistry-Us 19 (13):3113-3120

Anderson LE (1973) Regulation of pea leaf ribulose-5-phosphate kinase activity. Biochimica et Biophysica Acta (BBA) - Enzymology 321 (2):484-488. doi:10.1016/0005-2744(73)90190-3

Anderson LE (1974) Activation of pea leaf chloroplast sedoheptulose 1,7-diphosphate phosphatase by light and dithiothreitol. Biochem Biophys Res Commun 59 (3):907-913

Arnon DI (1949) Copper Enzymes in Isolated Chloroplasts - Polyphenoloxidase in Beta-Vulgaris. Plant Physiol 24 (1):1-15

Aro EM, McCaffery S, Anderson JM (1993) Photoinhibition and D1 Protein Degradation in Peas Acclimated to Different Growth Irradiances. Plant Physiol 103 (3):835-843

Aro EM, Suorsa M, Rokka A, Allahverdiyeva Y, Paakkarinen V, Saleem A, Battchikova N, Rintamaki E (2005) Dynamics of photosystem II: a proteomic approach to thylakoid protein complexes. J Exp Bot 56 (411):347-356. doi:10.1093/jxb/eri041

B

Baginsky S (2009) Plant Proteomics: Concepts, Applications, and Novel Strategies for Data Interpretation. Mass Spectrom Rev 28 (1):93-120. doi:Doi 10.1002/Mas.20183

Baginsky S, Gruissem W (2009) The chloroplast kinase network: new insights from large-scale phosphoproteome profiling. Molecular plant 2 (6):1141-1153. doi:10.1093/mp/ssp058

Baginsky S, Kleffmann T, von Zychlinski A, Gruissem W (2005) Analysis of shotgun proteomics and RNA profiling data from Arabidopsis thaliana chloroplasts. J Proteome Res 4 (2):637-640. doi:10.1021/pr049764u

Banks JA (2009) Selaginella and 400 Million Years of Separation. Annu Rev Plant Biol 60 (1):223-238. doi:doi:10.1146/annurev.arplant.59.032607.092851

Bassham JA, Benson AA, Calvin M (1950) The path of carbon in photosynthesis. J Biol Chem 185 (2):781-787

Bayer RG, Stael S, Csaszar E, Teige M (2011) Mining the soluble chloroplast proteome by affinity chromatography. Proteomics 11 (7):1287-1299. doi:10.1002/pmic.201000495

Bayer RG, Stael S, Rocha AG, Mair A, Vothknecht UC, Teige M (2012) Chloroplast-localized protein kinases: a step forward towards a complete inventory. J Exp Bot 63 (4):1713-1723. doi:10.1093/jxb/err377

Bellafiore S, Barneche F, Peltier G, Rochaix JD (2005) State transitions and light adaptation require chloroplast thylakoid protein kinase STN7. Nature 433 (7028):892-895. doi:Doi 10.1038/Nature03286

Bennett J (1977) Phosphorylation of Chloroplast Membrane Polypeptides. Nature 269 (5626):344-346

Berg JM TJ, Stryer L. (2002) The Calvin Cycle and the Pentose Phosphate Pathway. Biochemistry. 5th edition. W H Freeman, New York

Bernacchia G, Schwall G, Lottspeich F, Salamini F, Bartels D (1995) The transketolase gene family of the resurrection plant Craterostigma plantagineum: differential expression during the rehydration phase. The EMBO journal 14 (3):610-618

Berridge MJ, Lipp P, Bootman MD (2000) The versatility and universality of calcium signalling. Nat Rev Mol Cell Bio 1 (1):11-21

Bevan M (1984) Binary Agrobacterium vectors for plant transformation. Nucleic acids research 12 (22):8711-8721

Boggetto N, Gontero B, Maberly SC (2007) Regulation of phosphoribulokinase and glyceraldehyde 3-phosphate dehydrogenase in a freshwater diatom, Asterionella formosa1. Journal of Phycology 43 (6):1227-1235. doi:10.1111/j.1529-8817.2007.00409.x

Bonardi V, Pesaresi P, Becker T, Schleiff E, Wagner R, Pfannschmidt T, Jahns P, Leister D (2005) Photosystem II core phosphorylation and photosynthetic acclimation require two different protein kinases. Nature 437 (7062):1179-1182. doi:Doi 10.1038/Nature04016

Boschi-Muller S, Azza S, Pollastro D, Corbier C, Branlant G (1997) Comparative enzymatic properties of GapB-encoded erythrose-4-phosphate dehydrogenase of Escherichia coli and phosphorylating glyceraldehyde-3-phosphate dehydrogenase. The Journal of biological chemistry 272 (24):15106-15112

Bouvier F, d'Harlingue A, Suire C, Backhaus RA, Camara B (1998) Dedicated roles of plastid transketolases during the early onset of isoprenoid biogenesis in pepper fruits1. Plant Physiol 117 (4):1423-1431

Brand JJ, Becker DW (1984) Evidence for direct roles of calcium in photosynthesis. Journal of bioenergetics and biomembranes 16 (4):239-249

Buaboocha T, Liao B, Zielinski RE (2001) Isolation of cDNA and genomic DNA clones encoding a calmodulin-binding protein related to a family of ATPases involved in cell division and vesicle fusion. Planta 212 (5-6):774-781

Buchanan BB, Balmer Y (2005) Redox regulation: a broadening horizon. Annu Rev Plant Biol 56:187-220. doi:10.1146/annurev.arplant.56.032604.144246

Bussemer J, Chigri F, Vothknecht UC (2009) Arabidopsis ATPase family gene 1-like protein 1 is a calmodulin-binding AAA+-ATPase with a dual localization in chloroplasts and mitochondria. Febs J 276 (14):3870-3880. doi:10.1111/j.1742-4658.2009.07102.x

C

Cadet F, Meunier JC (1988) Spinach (Spinacia-Oleracea) Chloroplast Sedoheptulose-1,7-Bisphosphatase - Activation and Deactivation, and Immunological Relationship to Fructose-1,6-Bisphosphatase. Biochem J 253 (1):243-248

Cavalier-Smith T (2000) Membrane heredity and early chloroplast evolution. Trends in plant science 5 (4):174-182

Chardot T, Meunier JC (1990) Fructose-1,6-Bisphosphate and Calcium Activate Oxidized Spinach (Spinacia Oleracea) Chloroplast Fructose-1,6-Bisphosphatase. Plant Sci 70 (1):1-9

Charles SA, Halliwell B (1980) Action of Calcium-Ions on Spinach (Spinacia-Oleracea) Chloroplast Fructose Bisphosphatase and Other Enzymes of the Calvin Cycle. Biochem J 188 (3):775-779

Chen CG, Kazimir J, Cheniae GM (1995) Calcium Modulates the Photoassembly of Photosystem-Ii (Mn)(4)-Clusters by Preventing Ligation of Nonfunctional High-Valency States of Manganese. Biochemistry-Us 34 (41):13511-13526

Cheng SH, Willmann MR, Chen HC, Sheen J (2002) Calcium signaling through protein kinases. The Arabidopsis calcium-dependent protein kinase gene family. Plant Physiol 129 (2):469-485. doi:10.1104/pp.005645

Cheung W (1980) Calmodulin plays a pivotal role in cellular regulation. Science 207 (4426):19-27. doi:10.1126/science.6243188

Chigri F, Hörmann F, Stamp A, Stammers DK, Bölter B, Soll J, Vothknecht UC (2006) Calcium regulation of chloroplast protein translocation is mediated by calmodulin binding to Tic32. Proceedings of the National Academy of Sciences 103 (43):16051-16056. doi:10.1073/pnas.0607150103

Clapham DE (2007) Calcium signaling. Cell 131 (6):1047-1058. doi:DOI 10.1016/j.cell.2007.11.028

Clough SJ, Bent AF (1998) Floral dip: a simplified method for Agrobacterium-mediated transformation of Arabidopsis thaliana. The Plant journal : for cell and molecular biology 16 (6):735-743

Cohen P (2000) The regulation of protein function by multisite phosphorylation – a 25 year update. Trends Biochem Sci 25 (12):596-601. doi:10.1016/s0968-0004(00)01712-6

Crooks GE, Hon G, Chandonia JM, Brenner SE (2004) WebLogo: a sequence logo generator. Genome research 14 (6):1188-1190. doi:10.1101/gr.849004

D

De La Haba G, Leder IG, Racker E (1955) Crystalline transketolase from bakers' yeast: isolation and properties. J Biol Chem 214 (1):409-426

DeFalco TA, Bender KW, Snedden WA (2010) Breaking the code: Ca(2+) sensors in plant signalling. Biochem J 425:27-40. doi:Doi 10.1042/Bj20091147

Delobel A, Graciet E, Andreescu S, Gontero B, Halgand F, Laprévote O (2005) Mass spectrometric analysis of the interactions between CP12, a chloroplast protein, and metal ions: a possible regulatory role within a PRK/GAPDH/CP12 complex. Rapid Communications in Mass Spectrometry 19 (22):3379-3388. doi:10.1002/rcm.2192

Dennis DT, Greyson MF (1987) Fructose 6-phosphate metabolism in plants. Physiologia Plantarum 69 (2):395-404. doi:10.1111/j.1399-3054.1987.tb04306.x

Dixon RA, Paiva NL (1995) Stress-Induced Phenylpropanoid Metabolism. Plant Cell 7 (7):1085-1097

Dodd AN, Kudla J, Sanders D (2010) The language of calcium signaling. Annu Rev Plant Biol 61:593-620. doi:10.1146/annurev-arplant-070109-104628

Dolmetsch RE, Xu K, Lewis RS (1998) Calcium oscillations increase the efficiency and specificity of gene expression. Nature 392 (6679):933-936. doi:10.1038/31960

Durek P, Schmidt R, Heazlewood JL, Jones A, MacLean D, Nagel A, Kersten B, Schulze WX (2010) PhosPhAt: the Arabidopsis thaliana phosphorylation site database. An update. Nucleic acids research 38 (Database issue):D828-834. doi:10.1093/nar/gkp810

E

Edelman AM, Blumenthal DK, Krebs EG (1987) Protein Serine/Threonine Kinases. Annual review of biochemistry 56 (1):567-613. doi:doi:10.1146/annurev.bi.56.070187.003031

Eicks M, Maurino V, Knappe S, Flügge U-I, Fischer K (2002) The Plastidic Pentose Phosphate Translocator Represents a Link between the Cytosolic and the Plastidic Pentose Phosphate Pathways in Plants. Plant Physiol 128 (2):512-522. doi:10.1104/pp.010576

Emanuelsson O, Nielsen H, von Heijne G (1999) ChloroP, a neural network-based method for predicting chloroplast transit peptides and their cleavage sites. Protein science : a publication of the Protein Society 8 (5):978-984. doi:10.1110/ps.8.5.978

Enz C, Steinkamp T, Wagner R (1993) Ion channels in the thylakoid membrane (a patch-clamp study). Biochimica et Biophysica Acta (BBA) - Bioenergetics 1143 (1):67-76. doi:10.1016/0005-2728(93)90217-4

Erales J, Gontero B, Maberly SC (2008) SPECIFICITY AND FUNCTION OF GLYCERALDEHYDE-3-PHOSPHATE DEHYDROGENASE IN A FRESHWATER DIATOM, ASTERIONELLA FORMOSA (BACILLARIOPHYCEAE)1. Journal of Phycology 44 (6):1455-1464. doi:10.1111/j.1529-8817.2008.00600.x

Erales J, Gontero B, Whitelegge J, Halgand F (2009) Mapping of a copper-binding site on the small CP12 chloroplastic protein of Chlamydomonas reinhardtii using top-down mass spectrometry and site-directed mutagenesis. Biochem J 419 (1):75-82, 74 p following 82. doi:10.1042/BJ20082004

Ettinger WF, Clear AM, Fanning KJ, Peck ML (1999) Identification of a Ca2+/H+ antiport in the plant chloroplast thylakoid membrane. Plant Physiol 119 (4):1379-1386

F

Ferro M, Salvi D, Brugiere S, Miras S, Kowalski S, Louwagie M, Garin J, Joyard J, Rolland N (2003) Proteomics of the chloroplast envelope membranes from Arabidopsis thaliana. Molecular & cellular proteomics : MCP 2 (5):325-345. doi:10.1074/mcp.M300005-MCP200

Fessner WD (1998) Enzyme mediated C-C bond formation. Curr Opin Chem Biol 2 (1):85-97

Fischer K, Arbinger B, Kammerer B, Busch C, Brink S, Wallmeier H, Sauer N, Eckerskorn C, Flügge U-I (1994) Cloning and in vivo expression of functional triose phosphate/phosphate translocators from C3- and C4-plants: evidence for the putative participation of specific amino acid residues in the recognition of phosphoenolpyruvate. The Plant Journal 5 (2):215-226. doi:10.1046/j.1365-313X.1994.05020215.x

Fliege R, Flugge UI, Werdan K, Heldt HW (1978) Specific transport of inorganic phosphate, 3-phosphoglycerate and triosephosphates across the inner membrane of the envelope in spinach chloroplasts. Biochim Biophys Acta 502 (2):232-247

Flugge UI, Fischer K, Gross A, Sebald W, Lottspeich F, Eckerskorn C (1989) The triose phosphate-3-phosphoglycerate-phosphate translocator from spinach chloroplasts: nucleotide sequence of a full-length cDNA clone and import of the in vitro synthesized precursor protein into chloroplasts. The EMBO journal 8 (1):39-46

Flügge UI, Heldt HW (1984) The phosphate-triose phosphate-phosphoglycerate translocator of the chloroplast. Trends Biochem Sci 9 (12):530-533. doi:10.1016/0968-0004(84)90283-4

G

Geiger DR, Servaites JC (1994) Diurnal Regulation of Photosynthetic Carbon Metabolism in C3 Plants. Annu Rev Plant Physiol Plant Mol Biol 45 (1):235-256. doi:doi:10.1146/annurev.pp.45.060194.001315

Gerhardt S, Echt S, Busch M, Freigang J, Auerbach G, Bader G, Martin WF, Bacher A, Huber R, Fischer M (2003) Structure and properties of an engineered transketolase from maize. Plant Physiol 132 (4):1941-1949

Goujon M, McWilliam H, Li W, Valentin F, Squizzato S, Paern J, Lopez R (2010) A new bioinformatics analysis tools framework at EMBL–EBI. Nucleic acids research 38 (suppl 2):W695-W699. doi:10.1093/nar/gkq313

Graciet E, Lebreton S, Camadro JM, Gontero B (2003) Characterization of native and recombinant A4 glyceraldehyde 3-phosphate dehydrogenase. Kinetic evidence for confromation changes upon association with the small protein CP12. Eur J Biochem 270 (1):129-136

H

Han S, Tang R, Anderson LK, Woerner TE, Pei Z-M (2003) A cell surface receptor mediates extracellular Ca2+ sensing in guard cells. Nature 425 (6954):196-200. doi:http://www.nature.com/nature/journal/v425/n6954/suppinfo/nature01932_S1.html

Hanahan D (1985) DNA Cloning: A Practical Approach, vol 1. Virginia

Harmon AC, Gribskov M, Harper JF (2000) CDPKs - a kinase for every Ca2+ signal? Trends Plant Sci 5 (4):154-159. doi:S1360-1385(00)01577-6 [pii]

Harper JF, Breton G, Harmon A (2004) DECODING Ca2+ SIGNALS THROUGH PLANT PROTEIN KINASES. Annu Rev Plant Biol 55 (1):263-288. doi:doi:10.1146/annurev.arplant.55.031903.141627

Harper JF, Harmon A (2005) Plants, symbiosis and parasites: a calcium signalling connection. Nat Rev Mol Cell Biol 6 (7):555-566. doi:10.1038/nrm1679

Heazlewood JL, Durek P, Hummel J, Selbig J, Weckwerth W, Walther D, Schulze WX (2008) PhosPhAt: a database of phosphorylation sites in Arabidopsis thaliana and a plant-specific phosphorylation site predictor. Nucleic acids research 36 (Database issue):D1015-1021. doi:10.1093/nar/gkm812

Heldt HW, Werdan K, Milovancev M, Geller G (1973) Alkalization of the chloroplast stroma caused by light-dependent proton flux into the thylakoid space. Biochimica et Biophysica Acta (BBA) - Bioenergetics 314 (2):224-241. doi:10.1016/0005-2728(73)90137-0

Henkes S, Sonnewald U, Badur R, Flachmann R, Stitt M (2001) A Small Decrease of Plastid Transketolase Activity in Antisense Tobacco Transformants Has Dramatic Effects on Photosynthesis and Phenylpropanoid Metabolism. The Plant Cell Online 13 (3):535-551. doi:10.1105/tpc.13.3.535

Heredia P, De Las Rivas J (2003) Calcium-dependent conformational change and thermal stability of the isolated PsbO protein detected by FTIR spectroscopy. Biochemistry 42 (40):11831-11838. doi:10.1021/bi034582j

Hers HG, Hue L (1983) Gluconeogenesis and related aspects of glycolysis. Annual review of biochemistry 52:617-653. doi:10.1146/annurev.bi.52.070183.003153

Hertig C, Wolosiuk RA (1980) A Dual Effect of Ca-2+ on Chloroplast Fructose-1,6-Bisphosphatase. Biochem Bioph Res Co 97 (1):325-333

Hertig CM, Wolosiuk RA (1983) Studies on the Hysteretic Properties of Chloroplast Fructose-1,6-Bisphosphatase. J Biol Chem 258 (2):984-989

Hunter T (2007) The age of crosstalk: phosphorylation, ubiquitination, and beyond. Molecular cell 28 (5):730-738. doi:10.1016/j.molcel.2007.11.019

I

Inoue H, Nojima H, Okayama H (1990) High efficiency transformation of Escherichia coli with plasmids. Gene 96 (1):23-28

Izawa S, Maeda K, Miki T, Mano J, Inoue Y, Kimura A (1998) Importance of glucose-6-phosphate dehydrogenase in the adaptive response to hydrogen peroxide in Saccharomyces cerevisiae. The Biochemical journal 330 (Pt 2):811-817

J

Jensen RA (1986) The shikimate/arogenate pathway: Link between carbohydrate metabolism and secondary metabolism. Physiologia Plantarum 66 (1):164-168. doi:10.1111/j.1399-3054.1986.tb01251.x

Johnson CH, Knight MR, Kondo T, Masson P, Sedbrook J, Haley A, Trewavas A (1995) Circadian oscillations of cytosolic and chloroplastic free calcium in plants. Science 269 (5232):1863-1865

Joyard J, Ferro M, Masselon C, Seigneurin-Berny D, Salvi D, Garin J, Rolland N (2010) Chloroplast proteomics highlights the subcellular compartmentation of lipid metabolism. Progress in lipid research 49 (2):128-158. doi:10.1016/j.plipres.2009.10.003

K

Kasai K, Kanno T, Endo Y, Wakasa K, Tozawa Y (2004) Guanosine tetra- and pentaphosphate synthase activity in chloroplasts of a higher plant: association with 70S ribosomes and inhibition by tetracycline. Nucleic acids research 32 (19):5732-5741. doi:10.1093/nar/gkh916

Kasai K, Usami S, Yamada T, Endo Y, Ochi K, Tozawa Y (2002) A RelA-SpoT homolog (Cr-RSH) identified in Chlamydomonas reinhardtii generates stringent factor in vivo and localizes to chloroplasts in vitro. Nucleic acids research 30 (22):4985-4992

Kato Y, Miura E, Ido K, Ifuku K, Sakamoto W (2009) The variegated mutants lacking chloroplastic FtsHs are defective in D1 degradation and accumulate reactive oxygen species. Plant Physiol 151 (4):1790-1801. doi:10.1104/pp.109.146589

Keller A, Nesvizhskii AI, Kolker E, Aebersold R (2002) Empirical Statistical Model To Estimate the Accuracy of Peptide Identifications Made by MS/MS and Database Search. Analytical Chemistry 74 (20):5383-5392. doi:10.1021/ac025747h

Kenyon WH, Holaday AS, Black CC (1981) Diurnal Changes in Metabolite Levels and Crassulacean Acid Metabolism in Kalanchoë daigremontiana Leaves. Plant Physiol 68 (5):1002-1007. doi:10.1104/pp.68.5.1002

Khyse-Andersen J (1984) Electroblotting of multiple gels: a simple apparatus without buffer tank for rapid transfer of proteins from polyacrylamide to nitrocellulose. Biochem Biophys Meth 10 (203)

Kleffmann T, Russenberger D, von Zychlinski A, Christopher W, Sjölander K, Gruissem W, Baginsky S (2004) The Arabidopsis thaliana Chloroplast Proteome Reveals Pathway Abundance and Novel Protein Functions. Current Biology 14 (5):354-362. doi:10.1016/j.cub.2004.02.039

Knowles FC (1985) Regulation of resynthesis of the CO2-acceptor in photosynthesis. Feedback inhibition of transketolase. Physiologia Plantarum 64 (2):247-252. doi:10.1111/j.1399-3054.1985.tb02344.x

Koop HU, Steinmuller K, Wagner H, Rossler C, Eibl C, Sacher L (1996) Integration of foreign sequences into the tobacco plastome via polyethylene glycol-mediated protoplast transformation. Planta 199 (2):193-201

Kreimer G, Melkonian M, Holtum JA, Latzko E (1988) Stromal free calcium concentration and light-mediated activation of chloroplast fructose-1,6-bisphosphatase. Plant Physiol 86 (2):423-428

Kreimer G, Melkonian M, Latzko E (1985) An electrogenic uniport mediates light-dependent Ca2+ influx into intact spinach chloroplasts. Febs Lett 180 (2):253-258. doi:10.1016/0014-5793(85)81081-4

Kruger NJ, von Schaewen A (2003) The oxidative pentose phosphate pathway: structure and organisation. Curr Opin Plant Biol 6 (3):236-246

Kruk J, Burda K, Jemiola-Rzeminska M, Strzalka K (2003) The 33 kDa protein of photosystem II is a low-affinity calcium- and lanthanide-binding protein. Biochemistry 42 (50):14862-14867. doi:Doi 10.1021/Bi0351413

Kudla J, Batistic O, Hashimoto K (2010) Calcium signals: the lead currency of plant information processing. The Plant cell 22 (3):541-563. doi:10.1105/tpc.109.072686

Kurokawa M, Kornbluth S (2009) Caspases and kinases in a death grip. Cell 138 (5):838-854. doi:10.1016/j.cell.2009.08.021

L

Laemmli UK (1970) Cleavage of Structural Proteins during Assembly of Head of Bacteriophage-T4. Nature 227 (5259):680-&

Larkin MA, Blackshields G, Brown NP, Chenna R, McGettigan PA, McWilliam H, Valentin F, Wallace IM, Wilm A, Lopez R, Thompson JD, Gibson TJ, Higgins DG (2007) Clustal W and Clustal X version 2.0. Bioinformatics 23 (21):2947-2948. doi:10.1093/bioinformatics/btm404

Larkum AWD (1968) Ionic Relations of Chloroplasts in vivo. Nature 218 (5140):447-449

Lazo GR, Stein PA, Ludwig RA (1991) A DNA transformation-competent Arabidopsis genomic library in Agrobacterium. Biotechnology (N Y) 9 (10):963-967

Lebreton S, Graciet E, Gontero B (2003) Modulation, via protein-protein interactions, of glyceraldehyde-3-phosphate dehydrogenase activity through redox phosphoribulokinase regulation. J Biol Chem 278 (14):12078-12084. doi:10.1074/jbc.M213096200

Li WH, Llopis J, Whitney M, Zlokarnik G, Tsien RY (1998) Cell-permeant caged InsP(3) ester shows that Ca2+ spike frequency can optimize gene expression. Nature 392 (6679):936-941

Lindahl M, Spetea C, Hundal T, Oppenheim AB, Adam Z, Andersson B (2000) The thylakoid FtsH protease plays a role in the light-induced turnover of the photosystem II D1 protein. Plant Cell 12 (3):419-431

Lohrig K, Muller B, Davydova J, Leister D, Wolters DA (2009) Phosphorylation site mapping of soluble proteins: bioinformatical filtering reveals potential plastidic phosphoproteins in Arabidopsis thaliana. Planta 229 (5):1123-1134. doi:10.1007/s00425-009-0901-y

Lopez-Juez E, Pyke KA (2005) Plastids unleashed: their development and their integration in plant development. Int J Dev Biol 49 (5-6):557-577. doi:DOI 10.1387/ijdb.051997el

Lowry OH, Rosebrough NJ, Farr AL, Randall RJ (1951) Protein Measurement with the Folin Phenol Reagent. J Biol Chem 193 (1):265-275

M

Margulis L (1970) Origin of eukaryotic cells; evidence and research implications for a theory of the origin and evolution of microbial, plant, and animal cells on the Precambrian earth. Yale University Press, New Haven,

Marri L, Zaffagnini M, Collin V, Issakidis-Bourguet E, Lemaire SD, Pupillo P, Sparla F, Miginiac-Maslow M, Trost P (2009) Prompt and easy activation by specific thioredoxins of calvin cycle enzymes of Arabidopsis thaliana associated in the GAPDH/CP12/PRK supramolecular complex. Molecular plant 2 (2):259-269. doi:10.1093/mp/ssn061

Martin W, Herrmann RG (1998) Gene transfer from organelles to the nucleus: how much, what happens, and Why? Plant Physiol 118 (1):9-17

Maruyama K, Mikawa T, Ebashi S (1984) Detection of calcium binding proteins by 45Ca autoradiography on nitrocellulose membrane after sodium dodecyl sulfate gel electrophoresis. Journal of biochemistry 95 (2):511-519

Mazanek M, Mituloviæ G, Herzog F, Stingl C, Hutchins JRA, Peters J-M, Mechtler K (2007) Titanium dioxide as a chemo-affinity solid phase in offline phosphopeptide chromatography prior to HPLC-MS/MS analysis. Nat Protocols 2 (5):1059-1069

Menden B, Kohlhoff M, Moerschbacher BM (2007) Wheat cells accumulate a syringyl-rich lignin during the hypersensitive resistance response. Phytochemistry 68 (4):513-520. doi:10.1016/j.phytochem.2006.11.011

Miqyass M, van Gorkom HJ, Yocum CF (2007) The PSII calcium site revisited. Photosynthesis research 92 (3):275-287. doi:10.1007/s11120-006-9124-2

Murphy DJ, Walker DA (1982) The Properties of Transketolase from Photosynthetic Tissue. Planta 155 (4):316-320

Muto S, Izawa S, Miyachi S (1982) Light-induced Ca2+ uptake by intact chloroplasts. Febs Lett 139 (2):250-254. doi:10.1016/0014-5793(82)80863-6

N

Nakagami H, Sugiyama N, Mochida K, Daudi A, Yoshida Y, Toyoda T, Tomita M, Ishihama Y, Shirasu K (2010) Large-scale comparative phosphoproteomics identifies conserved phosphorylation sites in plants. Plant Physiol 153 (3):1161-1174. doi:10.1104/pp.110.157347

Nakayama S, Kretsinger RH (1994) Evolution of the EF-Hand Family of Proteins. Annual Review of Biophysics and Biomolecular Structure 23 (1):473-507. doi:doi:10.1146/annurev.bb.23.060194.002353

Naula C, Alibu VP, Brock JM, Veitch NJ, Burchmore RJ, Barrett MP (2008) A new erythrose 4-phosphate dehydrogenase coupled assay for transketolase. J Biochem Biophys Methods 70 (6):1185-1187. doi:10.1016/j.jprot.2007.11.002

Neish AC (1939) Studies on chloroplasts: Their chemical composition and the distribution of certain metabolites between the chloroplasts and the remainder of the leaf. Biochem J 33 (3):300-308

Nelson N, Ben-Shem A (2004) The complex architecture of oxygenic photosynthesis. Nat Rev Mol Cell Bio 5 (12):971-982. doi:Doi 10.1038/Nrm1525

Nesvizhskii AI, Keller A, Kolker E, Aebersold R (2003) A Statistical Model for Identifying Proteins by Tandem Mass Spectrometry. Analytical Chemistry 75 (17):4646-4658. doi:10.1021/ac0341261

Neuhaus HE, Emes MJ (2000) Nonphotosynthetic Metabolism in Plastids. Annu Rev Plant Physiol Plant Mol Biol 51:111-140. doi:10.1146/annurev.arplant.51.1.111

Nicholson S, Easterby JS, Powls R (1987) Properties of a multimeric protein complex from chloroplasts possessing potential activities of NADPH-dependent glyceraldehyde-3-phosphate dehydrogenase and phosphoribulokinase. Eur J Biochem 162 (2):423-431. doi:10.1111/j.1432-1033.1987.tb10619.x

Nobel PS (1969) Light-induced changes in the ionic content of chloroplasts in Pisum sativum. Biochim Biophys Acta 172 (1):134-143

Nomura H, Komori T, Kobori M, Nakahira Y, Shiina T (2008) Evidence for chloroplast control of external Ca2+-induced cytosolic Ca2+ transients and stomatal closure. The Plant journal : for cell and molecular biology 53 (6):988-998. doi:10.1111/j.1365-313X.2007.03390.x

O

O'Brien MJ, Easterby JS, Powls R (1976) Algal glyceraldehyde-3-phosphate dehydrogenases conversion of the NADH-linked enzyme of Scenedesmus obliquus into a form which preferentially uses NADPH as coenzyme. Biochimica et Biophysica Acta (BBA) - Bioenergetics 449 (2):209-223. doi:10.1016/0005-2728(76)90134-1

O'Keefe DP, Dilley RA (1977) The effect of chloroplast coupling factor removal on thylakoid membrane ion permeability. Biochimica et Biophysica Acta (BBA) - Bioenergetics 461 (1):48-60. doi:10.1016/0005-2728(77)90068-8

Olsen JV, Blagoev B, Gnad F, Macek B, Kumar C, Mortensen P, Mann M (2006) Global, in vivo, and site-specific phosphorylation dynamics in signaling networks. Cell 127 (3):635-648. doi:10.1016/j.cell.2006.09.026

P

Pearlman SM, Serber Z, Ferrell JE, Jr. (2011) A mechanism for the evolution of phosphorylation sites. Cell 147 (4):934-946. doi:10.1016/j.cell.2011.08.052

Peltier JB, Cai Y, Sun Q, Zabrouskov V, Giacomelli L, Rudella A, Ytterberg AJ, Rutschow H, van Wijk KJ (2006) The oligomeric stromal proteome of Arabidopsis thaliana chloroplasts. Molecular & cellular proteomics : MCP 5 (1):114-133. doi:10.1074/mcp.M500180-MCP200

Pilz RB, Willis RC, Boss GR (1984) The influence of ribose 5-phosphate availability on purine synthesis of cultured human lymphoblasts and mitogen-stimulated lymphocytes. J Biol Chem 259 (5):2927-2935

Portis AR, Jr., Heldt HW (1976) Light-dependent changes of the Mg2+ concentration in the stroma in relation to the Mg2+ dependency of CO2 fixation in intact chloroplasts. Biochim Biophys Acta 449 (3):434-436

Preisinger C, von Kriegsheim A, Matallanas D, Kolch W (2008) Proteomics and phosphoproteomics for the mapping of cellular signalling networks. Proteomics 8 (21):4402-4415. doi:DOI 10.1002/pmic.200800136

R

Racker E, Delahaba G, Leder IG (1953) Thiamine Pyrophosphate, a Coenzyme of Transketolase. J Am Chem Soc 75 (4):1010-1011

Reddy VS, Ali GS, Reddy AS (2002) Genes encoding calmodulin-binding proteins in the Arabidopsis genome. J Biol Chem 277 (12):9840-9852. doi:10.1074/jbc.M111626200

Reiland S, Messerli G, Baerenfaller K, Gerrits B, Endler A, Grossmann J, Gruissem W, Baginsky S (2009) Large-Scale Arabidopsis Phosphoproteome Profiling Reveals Novel Chloroplast Kinase Substrates and Phosphorylation Networks. Plant Physiol 150 (2):889-903. doi:DOI 10.1104/pp.109.138677

Rocha AG, Vothknecht UC (2012) The role of calcium in chloroplasts-an intriguing and unresolved puzzle. Protoplasma. doi:10.1007/s00709-011-0373-3

Rochaix JD (2007) Role of thylakoid protein kinases in photosynthetic acclimation. Febs Lett 581 (15):2768-2775. doi:DOI 10.1016/j.febslet.2007.04.038

Rochaix JD, Mayfield, S. P., Goldschmidt-Clermont, M., and Erickson, J. (1988) Plant Molecular Biology: A Practical Approach. IRL, Oxford

Roh MH, Shingles R, Cleveland MJ, McCarty RE (1998) Direct measurement of calcium transport across chloroplast inner-envelope vesicles. Plant Physiol 118 (4):1447-1454

S

Sagisaka S (1974) Transition of metabolisms in living popular bark from growing to wintering stages and vice versa: changes in glucose 6-phosphate and 6-phosphogluconate dehydrogenase activities and in the levels of sugar phosphates. Plant Physiol 54 (4):544-549

Sai J, Johnson CH (2002) Dark-stimulated calcium ion fluxes in the chloroplast stroma and cytosol. Plant Cell 14 (6):1279-1291

Sakamoto W, Zaltsman A, Adam Z, Takahashi Y (2003) Coordinated regulation and complex formation of yellow variegated1 and yellow variegated2, chloroplastic FtsH metalloproteases involved in the repair cycle of photosystem II in Arabidopsis thylakoid membranes. Plant Cell 15 (12):2843-2855. doi:10.1105/tpc.017319

Sambrook J FE, Maniatis T. (1989) Molecular Cloning - A Laboratory Manual. Cold Spring Harbour Laboratory Press, New York

Scheibe R, Geissler A, Fickenscher K (1989) Chloroplast glucose-6-phosphate dehydrogenase: Km shift upon light modulation and reduction. Arch Biochem Biophys 274 (1):290-297

Scheibe R, Wedel N, Vetter S, Emmerlich V, Sauermann S-M (2002) Co-existence of two regulatory NADP-glyceraldehyde 3-P dehydrogenase complexes in higher plant chloroplasts. Eur J Biochem 269 (22):5617-5624. doi:10.1046/j.1432-1033.2002.03269.x

Schenk G, Duggleby RG, Nixon PF (1998) Properties and functions of the thiamin diphosphate dependent enzyme transketolase. Int J Biochem Cell B 30 (12):1297-1318

Schenk G, Layfield R, Candy JM, Duggleby RG, Nixon PF (1997) Molecular evolutionary analysis of the thiamine-diphosphate-dependent enzyme, transketolase. J Mol Evol 44 (5):552-572

Schmid M, Davison TS, Henz SR, Pape UJ, Demar M, Vingron M, Scholkopf B, Weigel D, Lohmann JU (2005) A gene expression map of Arabidopsis thaliana development. Nature genetics 37 (5):501-506. doi:10.1038/ng1543

Schnarrenberger C, Flechner A, Martin W (1995) Enzymatic Evidence for a Complete Oxidative Pentose Phosphate Pathway in Chloroplasts and an Incomplete Pathway in the Cytosol of Spinach Leaves. Plant Physiol 108 (2):609-614

Schwacke R, Schneider A, van der Graaff E, Fischer K, Catoni E, Desimone M, Frommer WB, Flugge UI, Kunze R (2003) ARAMEMNON, a novel database for Arabidopsis integral membrane proteins. Plant Physiol 131 (1):16-26. doi:10.1104/pp.011577

Seigneurin-Berny D, Salvi D, Dorne AJ, Joyard J, Rolland N (2008) Percoll-purified and photosynthetically active chloroplasts from Arabidopsis thaliana leaves. Plant physiology and biochemistry : PPB / Societe francaise de physiologie vegetale 46 (11):951-955. doi:10.1016/j.plaphy.2008.06.009

Shutova T, Nikitina J, Deikus G, Andersson B, Klimov V, Samuelsson G (2005) Structural dynamics of the manganese-stabilizing protein - Effect of pH, calcium, and manganese. Biochemistry-Us 44 (46):15182-15192. doi:Doi 10.1021/Bi0512750

Sillero A, Selivanov VA, Cascante M (2006) Pentose phosphate and calvin cycles: Similarities and three-dimensional views*. Biochemistry and Molecular Biology Education 34 (4):275-277. doi:10.1002/bmb.2006.494034042627

Singh P, Kaloudas D, Raines CA (2008) Expression analysis of the Arabidopsis CP12 gene family suggests novel roles for these proteins in roots and floral tissues. J Exp Bot 59 (14):3975-3985. doi:10.1093/jxb/ern236

Soh YJ, Jeong, K.S. (1996) In vitro phosphorylation of purified transketolase by protein kinase C. Molecules and Cells 6 (6):692-696

Spirek M, Estreicher A, Csaszar E, Wells J, McFarlane RJ, Watts FZ, Loidl J (2010) SUMOylation is required for normal development of linear elements and wild-type meiotic recombination in Schizosaccharomyces pombe. Chromosoma 119 (1):59-72. doi:10.1007/s00412-009-0241-5

Stael S, Rocha AG, Robinson AJ, Kmiecik P, Vothknecht UC, Teige M (2011) Arabidopsis calcium-binding mitochondrial carrier proteins as potential facilitators of mitochondrial ATP-import and plastid SAM-import. Febs Lett 585 (24):3935-3940. doi:10.1016/j.febslet.2011.10.039

Stael S, Rocha AG, Wimberger T, Anrather D, Vothknecht UC, Teige M (2012) Cross-talk between calcium signalling and protein phosphorylation at the thylakoid. J Exp Bot 63 (4):1725-1733. doi:10.1093/jxb/err403

Stefan MI, Edelstein SJ, Le Novere N (2008) An allosteric model of calmodulin explains differential activation of PP2B and CaMKII. Proceedings of the National Academy of Sciences of the United States of America 105 (31):10768-10773. doi:10.1073/pnas.0804672105

Stitt M, Aprees T (1979) Capacities of Pea-Chloroplasts to Catalyze the Oxidative Pentose-Phosphate Pathway and Glycolysis. Phytochemistry 18 (12):1905-1911

Sugiyama N, Nakagami H, Mochida K, Daudi A, Tomita M, Shirasu K, Ishihama Y (2008) Large-scale phosphorylation mapping reveals the extent of tyrosine phosphorylation in Arabidopsis. Mol Syst Biol 4:193. doi:10.1038/msb.2008.32

Surek B, Kreimer G, Melkonian M, Latzko E (1987) Spinach Ferredoxin Is a Calcium-Binding Protein. Planta 171 (4):565-568

Svergun DI, Petoukhov MV, Koch MH, Konig S (2000) Crystal versus solution structures of thiamine diphosphate-dependent enzymes. J Biol Chem 275 (1):297-302

T

Tang RH, Han S, Zheng H, Cook CW, Choi CS, Woerner TE, Jackson RB, Pei ZM (2007) Coupling diurnal cytosolic Ca2+ oscillations to the CAS-IP3 pathway in Arabidopsis. Science 315 (5817):1423-1426. doi:10.1126/science.1134457

Teige M, Kopriva S, Bauwe H, Suss KH (1995) Chloroplast pentose-5-phosphate 3-epimerase from potato: cloning, cDNA sequence, and tissue-specific enzyme accumulation. Febs Lett 377 (3):349-352. doi:10.1016/0014-5793(95)01373-3

Teige M, Kopriva S, Bauwe H, and Suess K (1996) Primary Structure of Chloroplast Transketolase from Potato. Plant Physiol 112:1735

Teige M, Melzer M, Suss KH (1998) Purification, properties and in situ localization of the amphibolic enzymes D-ribulose 5-phosphate 3-epimerase and transketolase from spinach chloroplasts. Eur J Biochem 252 (2):237-244

Tikkanen M, Aro EM (2012) Thylakoid protein phosphorylation in dynamic regulation of photosystem II in higher plants. Biochim Biophys Acta 1817 (1):232-238. doi:10.1016/j.bbabio.2011.05.005

Tozawa Y, Nozawa A, Kanno T, Narisawa T, Masuda S, Kasai K, Nanamiya H (2007) Calcium-activated (p)ppGpp synthetase in chloroplasts of land plants. J Biol Chem 282 (49):35536-35545. doi:10.1074/jbc.M703820200

Trewavas A (1999) Le calcium, C'est la vie: calcium makes waves. Plant Physiol 120 (1):1-6

Turner NJ (2000) Applications of transketolases in organic synthesis. Curr Opin Biotech 11 (6):527-531

U

Udvardy J, Borbely G, Juhasz A, Farkas GL (1984) Thioredoxins and the redox modulation of glucose-6-phosphate dehydrogenase in Anabaena sp. strain PCC 7120 vegetative cells and heterocysts. J Bacteriol 157 (2):681-683

V

Vainonen JP, Sakuragi Y, Stael S, Tikkanen M, Allahverdiyeva Y, Paakkarinen V, Aro E, Suorsa M, Scheller HV, Vener AV, Aro EM (2008) Light regulation of CaS, a novel phosphoprotein in the thylakoid membrane of Arabidopsis thaliana. Febs J 275 (8):1767-1777. doi:DOI 10.1111/j.1742-4658.2008.06335.x

Villafra.Jj, Axelrod B (1971) Heptulose Synthesis from Nonphosphorylated Aldoses and Ketoses by Spinach Transketolase. J Biol Chem 246 (10):3126-&

W

Waegemann K, Soil J (1991) Characterization of the protein import apparatus in isolated outer envelopes of chloroplasts. The Plant Journal 1 (2):149-158. doi:10.1111/j.1365-313X.1991.00149.x

Wedel N, Soll J (1998) Evolutionary conserved light regulation of Calvin cycle activity by NADPH-mediated reversible phosphoribulokinase/CP12/ glyceraldehyde-3-phosphate dehydrogenase complex dissociation. Proceedings of the National Academy of Sciences of the United States of America 95 (16):9699-9704

Wedel N, Soll J, Paap BK (1997) CP12 provides a new mode of light regulation of Calvin cycle activity in higher plants. Proceedings of the National Academy of Sciences of the United States of America 94 (19):10479-10484

Weinl S, Held K, Schlucking K, Steinhorst L, Kuhlgert S, Hippler M, Kudla J (2008) A plastid protein crucial for Ca^{2+}-regulated stomatal responses. The New phytologist 179 (3):675-686. doi:10.1111/j.1469-8137.2008.02492.x

Werdan K, Heldt HW, Milovancev M (1975) The role of pH in the regulation of carbon fixation in the chloroplast stroma. Studies on CO_2 fixation in the light and dark. Biochimica et Biophysica Acta (BBA) - Bioenergetics 396 (2):276-292. doi:10.1016/0005-2728(75)90041-9

Wilkins MR, Gasteiger E, Bairoch A, Sanchez JC, Williams KL, Appel RD, Hochstrasser DF (1999) Protein identification and analysis tools in the ExPASy server. Methods Mol Biol 112:531-552

Wittekind M, Reizer J, Deutscher J, Saier MH, Klevit RE (1989) Common structural changes accompany the functional inactivation of HPr by seryl phosphorylation or by serine to aspartate substitution. Biochemistry-Us 28 (26):9908-9912

Wolosiuk RA, Ballicora MA, Hagelin K (1993) The reductive pentose phosphate cycle for photosynthetic CO2 assimilation: enzyme modulation. Faseb J 7 (8):622-637

Wolosiuk RA, Hertig CM, Nishizawa AN, Buchanan BB (1982) Enzyme regulation in C4 photosynthesis. Role of Ca^{2+} in thioredoxin-linked activation of sedoheptulose bisphosphatase from corn leaves. Febs Lett 140 (1):31-35

Woodrow IE, Murphy DJ, Latzko E (1984) Regulation of stromal sedoheptulose 1,7-bisphosphatase activity by pH and Mg2+ concentration. J Biol Chem 259 (6):3791-3795

Y

Yamagishi A, Satoh K, Katoh S (1981) The concentrations and thermodynamic activities of cations in intact Bryopsis chloroplasts. Biochimica et Biophysica Acta (BBA) - Bioenergetics 637 (2):252-263. doi:10.1016/0005-2728(81)90164-x

Yang T, Poovaiah BW (2000) Arabidopsis Chloroplast Chaperonin 10 Is a Calmodulin-Binding Protein. Biochem Bioph Res Co 275 (2):601-607. doi:10.1006/bbrc.2000.3335

Yang T, Poovaiah BW (2003) Calcium/calmodulin-mediated signal network in plants. Trends in plant science 8 (10):505-512

Z

Zhao G, Pease AJ, Bharani N, Winkler ME (1995) Biochemical characterization of gapB-encoded erythrose 4-phosphate dehydrogenase of Escherichia coli K-12 and its possible role in pyridoxal 5'-phosphate biosynthesis. J Bacteriol 177 (10):2804-2812

Ziegler H, Ziegler I (1965) Der Einfluss der Belichtung auf Die $NADP^+$-Abhängige Glycerinaldehyd-3-Phosphat-Dehydrogenase. Planta 65 (4):369-380. doi:10.1007/bf00385415

Summary

Plants are sessile organisms that have to cope with many environmental adversities. In order to successfully respond to diverse biotic and abiotic stimuli, they created a number of different signalling networks. Calcium is one of the most important secondary messengers, mediating many environmental cues. As photosynthetic organisms, many important processes take place in chloroplasts. However, very little is known about calcium-regulation within this organelle. The aim of this work was to identify components of this calcium-regulation network in the chloroplast. This included the identification and partial characterization of the calcium-binding proteins CP12-1 and SAMTL. Based on a proteomic approach, calcium-dependent targets of phosphorylation were also identified in the thylakoids, such as CAS, VAR1, VAR2 and PsaN. In the same manner, the transketolase (TKL) was identified as the major target of calcium-dependent phosphorylation in the stroma. TKL plays an important role in carbon metabolism, by converting intermediates of the Calvin-Benson-Bassham cycle (CBB) and the pentose phosphate pathway (PPP). Calcium-dependent phosphorylation of Arabidopsis TKL by a stromal protein kinase could be confirmed *in vitro* using recombinant protein. Phosphorylation of TKL occurs at a single serine residue that is conserved in TKLs of vascular plants. By contrast, in cyanobacteria, algae and mosses, an aspartate is present in this position. No phosphorylation could be observed for the Chlamydomonas protein indicating that calcium-dependent phosphorylation of TKL evolved as a vascular plant specific trait. The influence of phosphorylation on enzyme activity was analysed using recombinant wild-type TKL and a variant where the phosphorylation site was exchanged to an aspartate residue, thereby mimicking phosphorylation. The study was extended by measuring the enzyme activity under two different pHs that would simulate the stromal conditions under light or dark. The effect of this serine exchange was measured for different substrates representing distinct reactions of TKL in both the CBB and the PPP. Indeed, depending on the substrate, differences could be observed between wild type and S/D variant as well as under different pH conditions. These differences indicate a distinct function of TKL phosphorylation within the CBB and the PPP. Together, these results not only present the first evidence for calcium-dependent phosphorylation of chloroplast proteins but also show that this regulation might play an important role in carbon metabolism..

Zusammenfassung

Da Pflanzen nicht in der Lage sind den Standort zu wechseln, entwickelten sie effektive Strategien, um auf biotische und abiotische Reize zu reagieren. Calcium ist einer der wichtigsten sekundären Botenstoffe, der Umweltreize in die Zelle vermittelt. In Pflanzen finden viele wichtige Prozesse in den Chloroplasten statt. Trotzdem ist nur sehr wenig über Calciumregulation in diesem Organell bekannt. Ziel dieser Arbeit war es Bestandteile des Calciumsignalnetzwerks in Chloroplasten zu finden und zu charakterisieren. Unter anderem wurden dabei die calciumbindenden Proteine CP12-1 und SAMTL identifiziert. In den Thylakoiden wurden Proteine wie CAS, VAR1, VAR2 und PsaN identifiziert, die Ziel einer calciumabhängigen Phosphorylierung sind. Auf die gleiche Weise wurde die stromale Transketolase (TKL) identifiziert, und es wurde gezeigt, dass diese einer calcium-abhängigen Phosphorylierung unterliegt. TKL spielt eine wichtige Rolle im Kohlenstoffmetabolismus, in dem sie Zwischenprodukte des Calvin-Benson-Bassham Zyklus (CBB) und des Pentosephosphatwegs (PPP) umsetzt. *In vitro* wurde bestätigt, dass TKL aus Arabidopsis durch eine stromale Proteinkinase calcium-abhängig phosphoryliert wird. Die Phosphorylierung der TKL findet sequenzspezifisch an einem Serin statt. Dieses befindet sich in einem in Gefäßpflanzen konserviertem Motiv, ist jedoch in Cyanobakterien, Algen und Moosen durch ein Aspartat ersetzt. In der TKL aus Chlamydomonas konnte entsprechend keine Phosphorylierung gezeigt werden, was darauf hinweist, dass sich diese calcium-abhängige Phosphorylierung erst in Gefäßpflanzen entwickelt hat. Der Einfluss der Phosphorylierung auf die Enzymaktivität wurde mit Hilfe von rekombinanter Wildtyp TKL und einer Variante, in der die Phosphorylierungsstelle durch ein Aspartat ausgetauscht wurde, was eine Phosphorylierung nachahmt, untersucht. Die Enzymaktivität der beiden TKL Varianten wurde unter zwei verschiedenen pH-Werten gemessen, welche den natürlichen stromalen Bedingungen unter Licht bzw. Dunkelheit entsprechen. Die Auswirkung des Aminosäurenaustauschs auf die Aktivität der TKL wurde für verschiedene Phosphozucker gemessen, die den Substraten des CBB und PPP entsprechen. In Abhängigkeit von den eingesetzten Substraten, konnten sowohl Unterschiede zwischen dem Wildtyp und der Aspartat-Mutante als auch unter verschiedenen pH-Bedingungen, festgestellt werden. Das weist auf eine Funktion der TKL Phosphorylierung für den Kohlenhydratfluss im CBB und PPP hin. Die Ergebnisse bestätigen die Präsenz calcium-abhängiger Phosphorylierung im Chloroplasten und zeigen, dass diese Regulation im Kohlenstoffmetabolismus eine wichtige Rolle spielt.

List of abbreviations

BSA	bovine serum albumin
CaM	calmodulin
CBB	Calvin-Benson-Bassham cycle
CDPK	calcium-dependent protein kinase
CP12	CP12 domain-containing protein
DTT	1,4-Dithiothreitol
E4P	erythrose 4-phosphate
E4PDH	erythrose 4-phosphate dehydrogenase
EDTA	ethylenediaminetetraacetic acid
EGTA	ethylene glycol tetraacetic acid
F6P	fructose 6-phosphate
FBP	fructose 1,6-bisphosphatase
G3P	glyceraldehydes 3-phosphate
G3PDH	α-glycerophosphate dehydrogenase-triosephosphate isomerise
GAPDH	glyceraldehydes 3-phosphate dehydrogenase
GDH	glycerol 3-phosphate dehydrogenase
IEF	isoelectric focusing
IEP	isoelectric point
Km	Michaelis constant
PSI	photosystem I
PSII	photosystem II
PPP	pentose phosphate pathway
PRK	phosphoribulokinase
PVDF	polyvinylidene difluoride
R5P	ribose 5-phosphate
RT	room temperature
S7P	sedoheptulose 7-phosphate
SBP	sedoheptulose-bisphosphatase
SDS-PAGE	sodium dodecyl sulfate polyacrylamide gel electrophoresis
TKL	transketolase
TPI	triose phosphate isomerase
Vmax	saturating velocity
X5P	xylulose 5-phosphate
YFP	yellow fluorescent protein
TPP	thiamine pyrophosphate

Acknowledgements

It is with immense gratitude that I acknowledge the support and help of Prof. Dr. Ute C. Vothknecht for giving me the opportunity to do my PhD in her group. Within this last four years she was not just a professor but a teacher in the true meaning of the word. I would also like to thank her for all the patience and for being open-minded to my ideas and research. You gave me freedom to select the directions of my work and for that I am most grateful.

A special thanks to Dr. Norbert Mehlmer and Dr. Fatima Chigri for constant supervision, discussion and help with the experiments.

I would also like to acknowledge the pleasant collaboration and fruitful discussions with Dr. Markus Teige and Dr. Simon Stael. With their enthusiasm and dedication it was easier to bring this thesis to its end.

I would like to say thanks to Prof. Dr. Jürgen Soll for helpful discussions and suggestions.

I would kindly like to thank Prof. Dr. Jörg Nickelsen for making part of this study possible by providing the Chlamy cell lines.

Many thanks to Claudia for technical assistance and my other lab colleagues Sandra, Monika, Geraldine, Nargis, Steffi and to all the students with whom I had the opportunity to work with: Adrian, Katarina, Sarah, Johanna and Paula. It was a great experience working with you!

I would like to thank Dorothea Anrather for all the help with the MS analysis and Alexandra Bohne for introducing me to the Chlamy world.

I want to express my gratitude to all my friends and colleagues especially Ana, Sabine and George for the valuable and sometimes long-discussions to remind that there is also life outside the lab.

A special Dankeschön to Gerd, Christine, Michaela and Oma. You are more than my German family!

Special thanks to the COSI network colleagues for the great moments we had together in our meetings and organizing the conference.

I am indebted to my parents (Dona Ilda and Senhor Agostinho) and my sister Alexandra for all their love and support.

This dissertation is dedicated to my wife Branimira for standing beside me throughout my career and writing this thesis. Thank you for agreeing to share your life with me.

Annexes

Annex Table 1 - Accession numbers used for sequence alignment and residue probability determination.

	Organism	EMBL / GenebankAccession Numbers
AtTKL1	*Arabidopsis thaliana*	NP_567103
AtTKL2	*Arabidopsis thaliana*	NP_566041.2
AlTKL	*Arabidopsis lyrata*	XP_002876580
ThTKL	*Thellungiella halophila*	BAJ33959
RcTKL	*Ricinus communis*	XP_002511690
StTKL	*Solanum tuberosum*	CAA90427
PtTKL	*Populus trichocarpa*	ABK92500
NtTKL	*Nicotiana tabacum*	ACF60500
SoTKL	*Spinacia oleracea*	O20250
CaTKL	*Capsicum annuum*	CAA75777
OsTKL	*Oryza sativa*	AAO033154
VvTKL	*Vitis vinifera*	XP_002280760
SbTKL	*Sorghum bicolor*	XP_002437762
ZmTKL	*Zea mays*	ACF88120
PsTKL	*Picea sitchensis*	ACN39962
PpTKL	*Physcomitrella patens*	XP_001769997
SmTKL	*Selaginella moellendorffii*	XP_002991185
OlTKL	*Ostreococcus lucimarinus*	XP_001418785
MpTKL	*Micromonas pusilla*	XP_003061196
VcTKL	*Volvox carteri*	XP_002953691
CrTKL	*Chlamydomonas reinhardtii*	XP_001701881
TeTKL	*Thermosynechococcus elongatus*	NP_682660
PmTKL	*Prochlorococcus marinus*	YP_292380

Annex Table 2 – Candidate targets of Ca^{2+}-dependent phosphorylation identified by LC-MS/MS - The list was filtered based on the estimated molecular weight (excluding cleaved targeting peptides), the theoretical isoelectric point of the mature protein (Wilkins et al. 1999) and predicted chloroplastidic localization according to the Aramemnon database (Schwacke et al. 2003).The phosphopeptides identified in previously phosphoproteomic approaches are also included (PhosPhAt database, (Durek et al. 2010; Heazlewood et al. 2008).

Spot	Accession Number	Aramenon Score	phosphopeptide identified	Theoretical pI / Mw (Da)
A	AT3G60750.1	28,20	ALPTYTPE(pS)PGDATR	5.33 / 73035.38
B	AT3G60750.1	28,20	ALPTYTPE(pS)PGDATR	5.33 / 73035.38
	AT5G36880.1	6,50	HVE(pS)MSQLPSGAGK	5.35 / 73223.11
C	ATCG00120.1	C	GKISA(pS)ESR	5.19 / 55328.27
	ATCG00480.1	C	TNPTTSNPEV(pS)IR	5.38 / 53933.84
	ATCG00490.1	C	LSGGDHIHAG(pT)VVGK K(pT)FQGPPHGIQVER	5.87 / 52955.06
D/E	AT1G06680.1	27,60	FEDNFDATSNLNVMV(pT)PTDK TNTDFLP(pY)NGDGFK	5.77 / 24797.62
	AT5G20720.1	23,40	(pY)AGTEVEFNDVK	5.23 / 21326.46
	AT4G05180.1	24,80	FYIQPL(pS)PTEAAAR	9.32 / 19506.14
	AT5G52960.1	19,30	SSDAEEV(pS)DTEDEWLK	6.17 / 14417.24
	AT4G21280.1	28,40	YDLN(pT)II(s)(s)KPK	9.14 / 19165.80
F	AT2G41220.1	28,50	NGSQVLVL(pS)DR MP(pT)V(pT)MEQAQK	6.07 / 170048.86
	AT1G10760.1	11,80	TPFVKSGGN(pS)HLK	5.35 / 148240.15
	AT5G13630.1	23,10	GSDKGIL(pS)DVELLK	5.33 / 143958.70
	AT1G29900.1	20,10	ELVDVEQYLMSGTLSEI(pT)K	5.27 / 123061.66
G	AT5G48960.1	17,30	LDDGFI(pS)ADLGTLDYKGLYK	5.26 / 64285.23
	AT5G51820.1	17,80	ANGGFI(oxM)SA(pS)HNPGGPEYDWGIK	5.27 / 62201.37
	AT1G70820.1	24,20	TA(pS)HLPYTR	5.27 / 62201.37
	AT1G55490.1	23,70	LA(pS)KVDAIKATLDNDEEK	5.26 / 58228.73
	AT2G28000.1	21,90	NVVLDEFG(pS)PK LADCVGL(pT)LGPR	4.80 / 57203.52
	ATCG00120.1	C	GKISA(pS)ESR	5.19 / 55328.27
H	AT5G48300.1	25,50	E(pT)DADITVAALPMDEQRATAFGL(oxM)K	5.33 / 49434.24
	AT1G48860.1	19,70	K(pT)FPD(pY)FQVLER	5.76 / 51760.43
	ATCG00120.1	C	GKISA(pS)ESR	5.19 / 55328.27
	ATCG00480.1	C	TNPTTSNPEV(pS)IR	5.38 / 53933.84
	ATCG00490.1	C	LSGGDHIHAG(pT)VVGK K(pT)FQGPPHGIQVER	5.87 / 52955.06
	AT1G32500.1	16,30	IRDSSAETLLSTPWP(pS)R	5.16 / 49001.06
	AT2G39730.1	22,80	GLAYD(pT)SDDQQDITR MGINPIMM(pS)AGELESGNAGEPAK	5.09 / 46260.61
	AT4G20360.1	22,70	V(pT)KIMNDK	5.31 / 44722.29
	AT3G12780.1	22,40	(pS)VGDLTSADLK	5.04 / 42638.25
	AT5G28500.1	19,80	(oxM)L(pS)LTATTLSSSIF(t)Q(s)K	4.73 / 42641.32
	AT1G42970.1	19,60	DSPLEVVVLND(pS)GGVK IVDNE(pT)ISVDGK	5.59 / 42795.92
	AT5G35630.1	25,00	TIEKPVEDP(pS)ELPK	5.28 / 42474.76
I	AT4G05180.1	24,80	FYIQPL(pS)PTEAAAR	9.32 / 19506.14
	AT4G21280.1	28,40	YDLN(pT)II(s)(s)KPK	9.14 / 19165.80

Annex Table 3 - Sequence coverage and total number of non-redundant peptides assigned to the 73 kDa protein identified as AtTKL1.

AT3G60750.1|Symbols:|transketolase, putative | chr3:22454004-22456824 FORWARD Protein identification probability (100%), Protein percentage of total spectra (0.76%) Total number of spectra (99), Number of unique peptides (20), Sequence coverage (26%)			
Peptide sequence	Previous aminoacid	Next aminoacid	Number of spectra
FAAYEK	K	K	3
AFGDFQK	K	A	4
TPSILALSR	K	Q	5
NPYWFNR	K	D	5
FLAIDAVEK	R	A	6
YPEEASELK	K	S	5
KTPSILALSR	R	Q	8
TVTDKPTLIK	K	V	4
NGNTGYDEIR	K	A	5
ESVLPSDVSAR	K	V	3
KYPEEASELK	K	S	9
VTTTIGYGSPNK	K	A	8
NLSQQCLNALAK	R	V	6
SIITGELPAGWEK	K	A	2
ANSYSVHGAALGEK	K	E	3
LPHLPGTSIEGVEK	K	G	4
ALPTYTPESPGDATR	K	N	10
HTPEGATLESDWSAK	R	F	3
QKLPHLPGTSIEGVEK	R	G	4
SIGINSFGASAPAPLLYK	K	E	2
			99

Annex Table 4 - TKL velocities calculated for the substrates X5P and R5P - The independent measurements were tested at pH 7.2 and 8.0, using purified recombinant AtTKL1 and AtTKL1$_{(S/D)}$.

X5P pH 7.2 - Velocity (µmol/min x mg TKL)										
n	**AtTKL1**					**AtTKL1 (S/D)**				
1	8.660	9.595	11.597	12.523	13.878	6.521	9.477	12.983	13.980	13.552
2	7.384	9.666	11.032	12.444	13.664	6.130	9.072	12.049	13.802	12.786
3	6.933	9.686	11.641	13.188	12.979	6.030	9.162	12.054	13.167	13.349
4	8.171	10.068	12.909	13.106	13.788	6.622	9.522	12.178	14.057	13.864
5	8.885									
[X5P] µM	200	400	1000	1500	3000	200	400	1000	1500	3000

X5P pH 8.0 - Velocity (µmol/min x mg TKL)										
n	**AtTKL1**					**AtTKL1 (S/D)**				
1	6.523	9.809	10.810	11.793	12.873	7.716	11.013	12.887	13.939	14.004
2	6.592	9.863	10.524	11.365	12.880	6.975	10.478	11.642	12.661	12.348
3	6.121	8.991	11.247	12.782	13.089	7.085	10.327	11.290	12.721	12.186
4	6.736	10.249	12.656	12.963	14.111	5.352	10.248	12.094	13.225	13.055
[X5P] µM	100	400	1000	1500	3000	100	400	1000	1500	3000

R5P pH 7.2 - Velocity (µmol/min x mg TKL)										
n	**AtTKL1**					**AtTKL1 (S/D)**				
1	4.578	6.817	8.488	14.019	15.992	4.677	6.087	8.288	13.179	15.849
2	4.510	6.324	8.053	13.721	15.522	4.843	5.927	7.886	12.257	15.719
3	4.128	6.413	7.940	13.414	14.953	4.980	6.168	7.929	12.001	15.701
4	5.555	6.161	8.447	13.919	16.557	5.118	6.663	7.419	12.010	16.605
5	5.226	6.319	8.890	14.255	17.268	5.112	6.197	7.852	12.919	16.675
[R5P] µM	125	250	500	1500	3000	125	250	500	1500	3000

R5P pH 8.0 - Velocity (µmol/min x mg TKL)										
n	**AtTKL1**					**AtTKL1 (S/D)**				
1	2.499	3.804	5.714	11.639	14.948	2.971	3.596	5.283	10.285	14.490
2	2.124	3.760	5.267	11.180	14.065	2.864	3.326	4.986	9.325	14.075
3	2.024	3.630	5.183	10.741	14.008	3.215	3.610	4.987	9.229	14.032
4	3.068	3.975	5.919	11.315	15.457	3.838	4.572	4.762	9.624	15.132
5	2.848	3.761	5.798	11.453	15.879	3.444	3.709	4.993	10.028	15.357
[R5P] µM	125	250	500	1500	3000	125	250	500	1500	3000

Annex Table 5 - TKL velocities calculated for the substrates F6P and G3P - The independent measurements were tested at pH 7.2 and 8.0, using purified recombinant AtTKL1 and AtTKL1$_{(S/D)}$.

F6P pH 7.2 - Velocity (µmol/min x mg TKL)

n	AtTKL1					AtTKL1 (S/D)				
1	0.252	0.902	2.201	3.078	4.143	0.229	0.996	2.194	2.943	3.434
2	0.238	0.877	2.147	2.994	4.096	0.216	0.928	2.056	2.837	3.387
3	0.265	0.847	2.165	3.029	4.090	0.205	0.873	2.037	2.866	3.347
4	0.236	0.876	2.248	3.143	4.208	0.208	0.891	2.123	2.915	3.444
[F6P] mM	0.1	1	5	10	20	0.1	1	5	10	20

F6P pH 8.0 - Velocity (µmol/min x mg TKL)

n	AtTKL1					AtTKL1 (S/D)				
1	0.193	0.372	0.722	1.181	1.873	0.213	0.384	0.747	1.105	1.587
2	0.188	0.361	0.687	1.136	1.799	0.214	0.377	0.704	1.074	1.494
3	0.183	0.360	0.673	1.153	1.837	0.214	0.381	0.693	1.083	1.497
4	0.190	0.371	0.696	1.194	1.889	0.206	0.384	0.734	1.123	1.564
[F6P] mM	1	2	5	10	20	1	2	5	10	20

G3P pH 7.2 - Velocity (µmol/min x mg TKL)

n	AtTKL1				AtTKL1 (S/D)			
1	0.4241	0.4587	0.6945	0.6583	0.3184	0.4821	0.6959	0.6677
2	0.3609	0.4527	0.6687	0.6389	0.3493	0.5185	0.6045	0.6510
3	0.3613	0.5025	0.6066	0.6385	0.3081	0.5036	0.6524	0.6623
4	0.3494		0.5697	0.6313	0.3559	0.4906	0.6506	0.7030
5			0.6100				0.6891	
[G3P] µM	125	250	500	1000	125	250	500	1000

G3P pH 8.0 - Velocity (µmol/min x mg TKL)

n	AtTKL1					AtTKL1 (S/D)				
1	0.309	0.549	0.760	1.119	1.164	0.244	0.425	0.799	1.090	1.344
2	0.365	0.515	0.699	0.863	1.036	0.221	0.452	0.571	0.986	1.215
3	0.249	0.401	0.512	0.860	1.063	0.190	0.402	0.555	0.973	1.268
4	0.275	0.298	0.516	0.805	1.347	0.259	0.349	0.683	0.996	1.242
5		0.403	0.678			0.227	0.489	0.743	1.051	
[G3P] µM	125	250	500	1000	2000	125	250	500	1000	2000

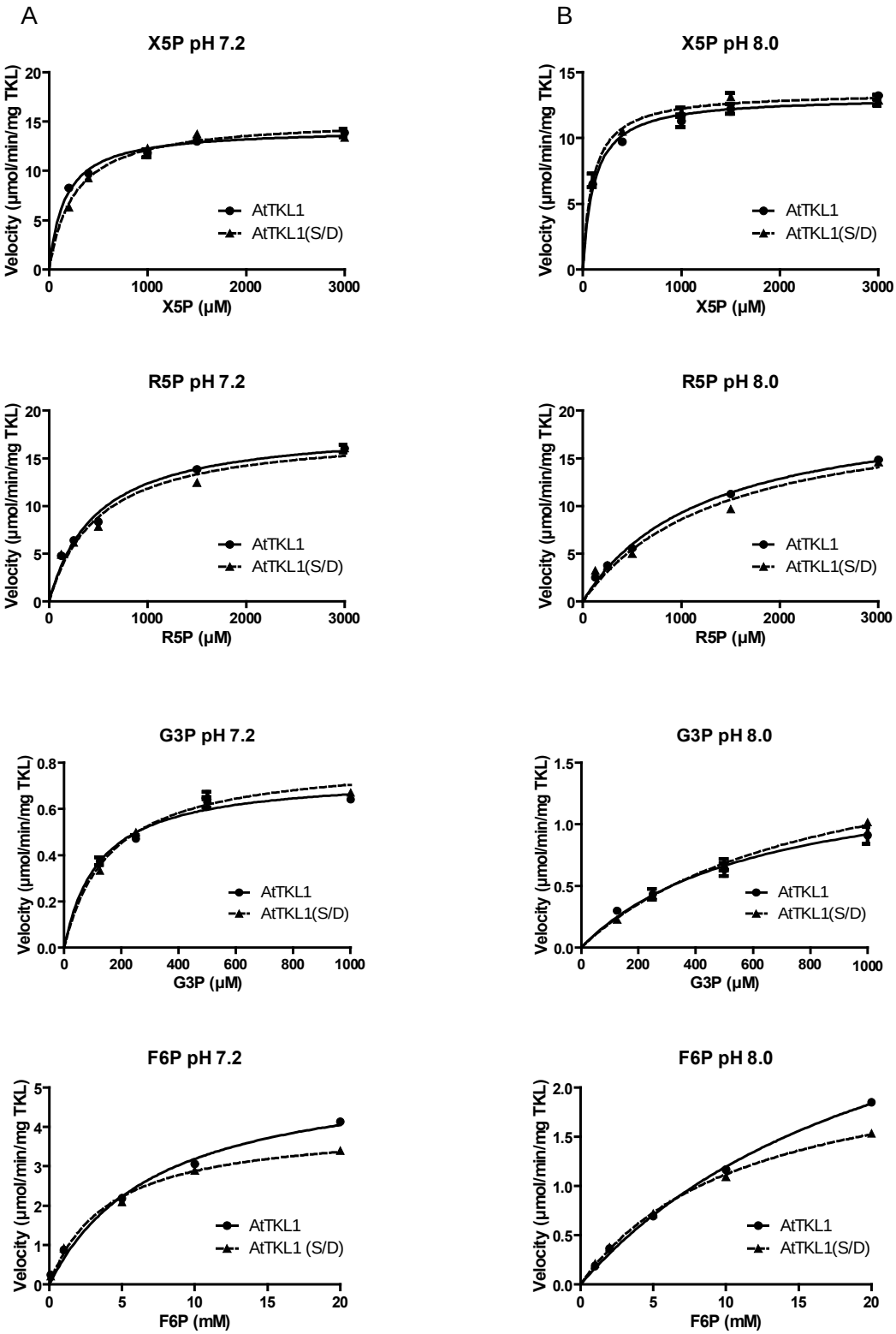

Annex Fig. 1 - Michaelis-Menten curves of TKL activity vs X5P, R5P, F6P and G3P concentration - Enzymatic reactions were performed pH 7.2 (A) and 8.0 (B). Enzyme parameters were calculated by nonlinear curve fitting using the software GraphPad Prism Version 5.01 for Windows.

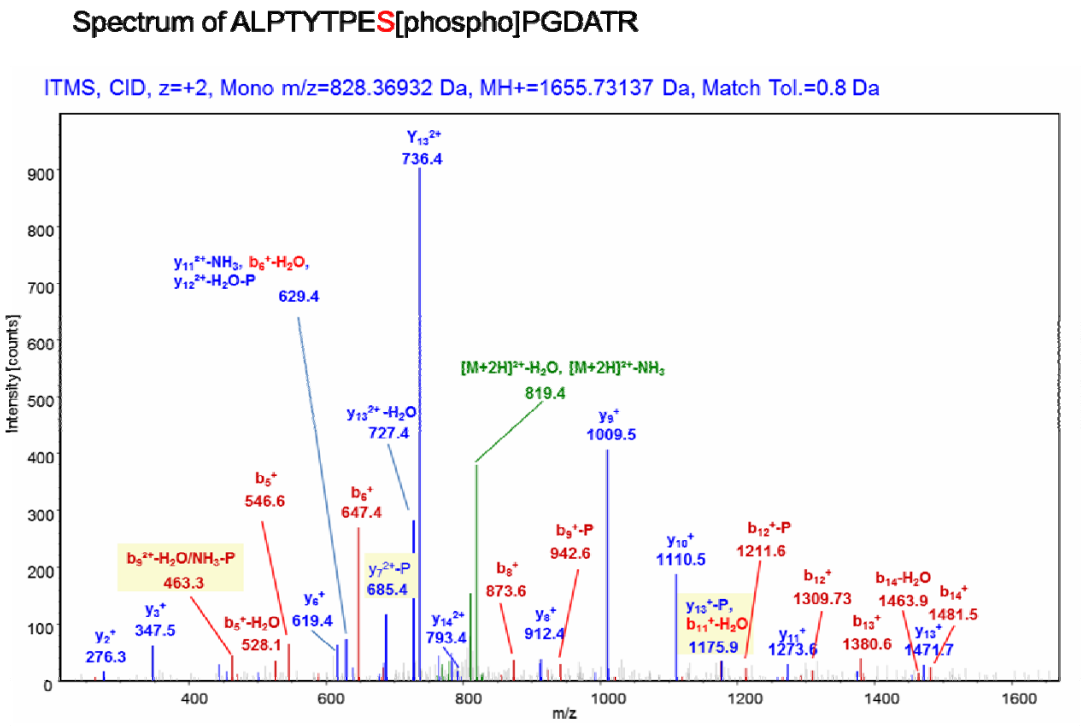

#1	b⁺	b²⁺	Seq.	y⁺	y²⁺	#2
1	72.04	36.52	A			15
2	185.13	93.07	L	1584.69	792.85	14
3	282.18	141.59	P	1471.61	736.31	13
4	383.23	192.12	T	1374.56	687.78	12
5	546.29	273.65	Y	1273.51	637.26	11
6	647.34	324.17	T	1110.45	555.73	10
7	744.39	372.70	P	1009.40	505.20	9
8	873.44	437.22	E	912.35	456.68	8
9	1040.43	520.72	S-Phospho	783.30	392.16	7
10	1137.49	569.25	P	616.30	308.66	6
11	1194.51	597.76	G	519.25	260.13	5
12	1309.53	655.27	D	462.23	231.62	4
13	1380.57	690.79	A	347.20	174.11	3
14	1481.62	741.31	T	276.17	138.59	2
15			R	175.11	88.06	1

Annex Fig. 2 - Annotated spectrum for the phosphopeptide identified in AtTKL1.


SbTKL_
ZmTKL_
OsTKL_
SoTKL_
NtTKL_
PsTKL_
CaTKL_
SsTKL_
AtTKL1_
AtTKL2_
AlTKL_
ThTKL_
RcTKL_
PtTKL_
VvTKL_
SeTKL_
PpTKL_
CrTKL_
VcTKL_
OlTKL_
MpTKL_
TeTKL_
PmTKL_

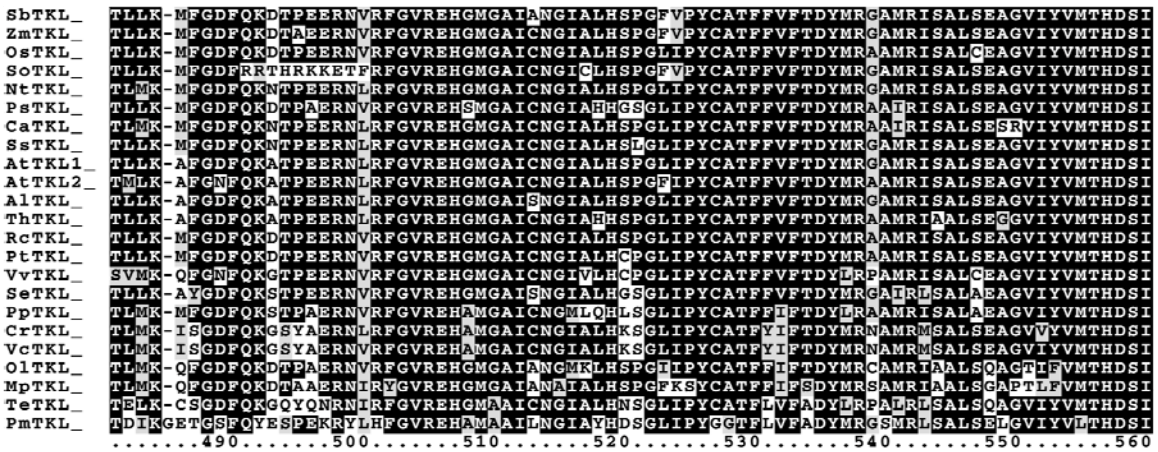
SbTKL_ TLLK-MFGDFQKDTPEERNVRFGVREHGMGAIANGIALHSPGFVPYCATFFVFTDYMRGAMRISALSEAGVIYVMTHDSI
ZmTKL_ TLLK-MFGDFQKDTAEERNVRFGVREHGMGAICNGIALHSPGFVPYCATFFVFTDYMRGAMRISALSEAGVIYVMTHDSI
OsTKL_ TLLK-MFGDFQKDTPEERNVRFGVREHGMGAICNGIALHSPGLIPYCATFFVFTDYMRAAMRISALCEAGVIYVMTHDSI
SoTKL_ TLLK-MFGDFRRTHRKKETFRFGVREHGMGAICNGICLHSPGFVPYCATFFVFTDYMRGAMRISALSEAGVIYVMTHDSI
NtTKL_ TLMK-MFGDFQKNTPEERNLRFGVREHGMGAICNGIALHSPGLIPYCATFFVFTDYMRGAMRISALSEAGVIYVMTHDSI
PsTKL_ TLLK-MFGDFQKDTPAERNVRFGVREHSMGAICNGIAHHGGSGLIPYCATFFVFTDYMRAAIRISALSEAGVIYVMTHDSI
CaTKL_ TLMK-MFGDFQKNTPEERNLRFGVREHGMGAICNGIALHSPGLIPYCATFFVFTDYMRAAIRISALSESRVIYVMTHDSI
SsTKL_ TLLK-MFGDFQKNTPEERNLRFGVREHGMGAICNGIALHSLGLIPYCATFFVFTDYMRGAMRISALSEAGVIYVMTHDSI
AtTKL1_ TLLK-AFGDFQKATPEERNLRFGVREHGMGAICNGIALHSPGLIPYCATFFVFTDYMRGAMRISALSEAGVIYVMTHDSI
AtTKL2_ TMLK-AFGNFQKATPEERNLRFGVREHGMGAICNGIALHSPGFIPYCATFFVFTDYMRAAMRISALSEAGVIYVMTHDSI
AlTKL_ TLLK-AFGDFQKATPEERNLRFGVREHGMGAISNGIALHSPGLIPYCATFFVFTDYMRGAMRISALSEAGVIYVMTHDSI
ThTKL_ TLLK-AFGDFQKATPEERNLRFGVREHGMGAICNGIAHHSPGLIPYCATFFVFTDYMRAAMRIAALSEGGVIYVMTHDSI
RcTKL_ TLLK-MFGDFQKDTPEERNVRFGVREHGMGAICNGIALHSPGLIPYCATFFVFTDYMRAAMRISALSEAGVIYVMTHDSI
PtTKL_ TLLK-MFGDFQKDTPEERNVRFGVREHGMGAICNGIALHCPGLIPYCATFFVFTDYMRAAMRISALSEAGVIYVMTHDSI
VvTKL_ SVMK-QFGNFQKGTPEERNVRFGVREHGMGAICNGIVLHCPGLIPYCATFFVFTDYLRPAMRISALCEAGVIYVMTHDSI
SeTKL_ TLLK-AYGDFQKSTPEERNVRFGVREHGMGAISNGIALHGSGLIPYCATFFVFTDYMRGAIRLSALAEAGVIYVMTHDSI
PpTKL_ TLMK-MFGDFQKSTPAERNVRFGVREHAMGAICNGMLQHLSGLIPYCATFFIFTDYLRAAMRISALAEAGVIYVMTHDSI
CrTKL_ TLMK-ISGDFQKGSYAERNLRFGVREHAMGAICNGIALHKSGLIPYCATFYIFTDYMRNAMRMSALSEAGVVYVMTHDSI
VcTKL_ TLMK-ISGDFQKGSYAERNVRFGVREHAMGAICNGIALHKSGLIPYCATFYIFTDYMRNAMRMSALSEAGVIYVMTHDSI
OlTKL_ TLMK-QFGDFQKDTPAERNVRFGVREHGMGAIANGMKLHSPGIIPYCATFFIFTDYMRCAMRIAALSQAGTIFVMTHDSI
MpTKL_ TLMK-QFGDFQKDTAAERNIRYGVREHGMGAIANAIALHSPGFKSYCATFFIFSDYMRSAMRIAALSGAPTLFVMTHDSI
TeTKL_ TELK-CSGDFQKGQYQNRNIRFGVREHGMAAICNGIALHNSGLIPYCATFLVFADYLRPALRLSALSQAGVIYVMTHDSI
PmTKL_ TDIKGETGSFQYESPEKRYLHFGVREHAMAAILNGIAYHDSGLIPYGGTFLVFADYMRGSMRLSALSELGVIYVLTHDSI
.....490.....500.....510.....520.....530.....540.....550.....560

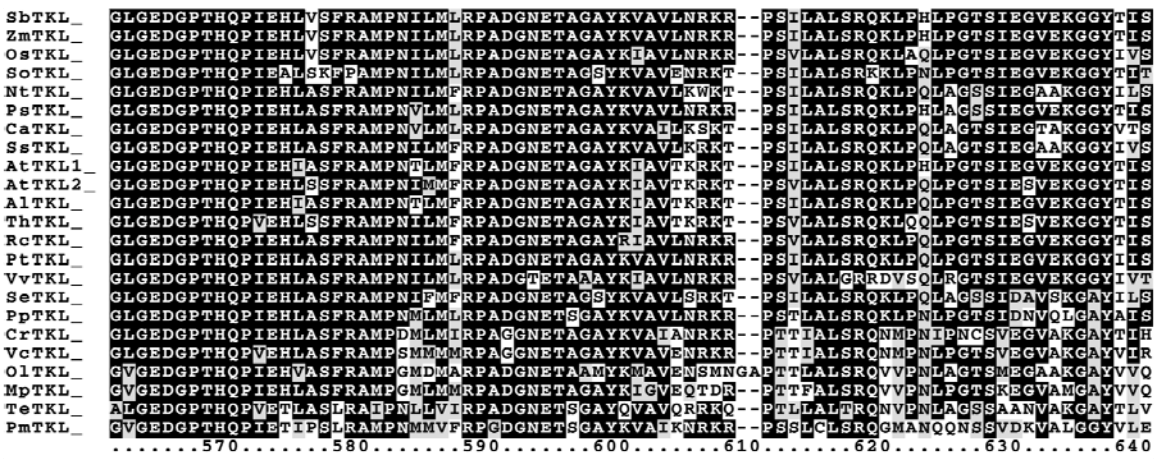
SbTKL_ GLGEDGPTHQPIEHLVSFRAMPNILMLRPADGNETAGAYKVAVLNRKR--PSILALSRQKLPHLPGTSIEGVEKGGYTIS
ZmTKL_ GLGEDGPTHQPIEHLVSFRAMPNILMLRPADGNETAGAYKVAVLNRKR--PSILALSRQKLPHLPGTSIEGVEKGGYTIS
OsTKL_ GLGEDGPTHQPIEHLVSFRAMPNILMLRPADGNETAGAYKIAVLNRKR--PSVLALSRQKLAQLPGTSIEGVEKGGYIVS
SoTKL_ GLGEDGPTHQPIEALSKFPAMPNILMLRPADGNETAGSYKVAVENRKT--PSILALSRKKLPNLPGTSIEGVEKGGYTIT
NtTKL_ GLGEDGPTHQPIEHLASFRAMPNILMFRPADGNETAGAYKVAVLKWKT--PSILALSRQKLPQLAGSSIEGAAKGGYILS
PsTKL_ GLGEDGPTHQPIEHLASFRAMPNVLMLRPADGNETAGAYKVAVLNRKR--PSILALSRQKLPHLAGSSIEGVEKGGYTIS
CaTKL_ GLGEDGPTHQPIEHLASFRAMPNVLMLRPADGNETAGAYKVAILKSKT--PSILALSRQKLPQLAGTSIEGTAKGGYVTS
SsTKL_ GLGEDGPTHQPIEHLASFRAMPNILMFRPADGNETAGAYKVAVLKRKT--PSILALSRQKLPQLAGTSIEGAAKGGYIVS
AtTKL1_ GLGEDGPTHQPIEHIASFRAMPNTLMFRPADGNETAGAYKIAVTKRKT--PSILALSRQKLPHLPGTSIEGVEKGGYTIS
AtTKL2_ GLGEDGPTHQPIEHLSSFRAMPNIMMFRPADGNETAGAYKIAVTKRKT--PSVLALSRQKLPQLPGTSIESVEKGGYTIS
AlTKL_ GLGEDGPTHQPIEHIASFRAMPNTLMFRPADGNETAGAYKIAVTKRKT--PSILALSRQKLPQLPGTSIEGVEKGGYTIS
ThTKL_ GLGEDGPTHQPVEHLSSFRAMPNILMFRPADGNETAGAYKIAVTKRKT--PSVLALSRQKLQQLPGTSIESVEKGGYTIS
RcTKL_ GLGEDGPTHQPIEHLASFRAMPNILMFRPADGNETAGAYRIAVLNRKR--PSVLALSRQKLPQLPGTSIEGVEKGGYTIS
PtTKL_ GLGEDGPTHQPIEHLASFRAMPNILMLRPADGNETAGAYKVAVLNRKR--PSILALSRQKLPQLPGTSIEGVEKGGYIIS
VvTKL_ GLGEDGPTHQPIEHLASFRAMPNILMLRPADGTETAAAYKIAVLNRKR--PSVLALGRRDVSQLRGTSIEGVEKGGYIVT
SeTKL_ GLGEDGPTHQPIEHLASFRAMPNIFMFRPADGNETAGSYKVAVLSRKT--PSILALSRQKLPQLAGSSIDAVSKGAYILS
PpTKL_ GLGEDGPTHQPIEHLASFRAMPNMLMLRPADGNETSGAYKVAVLNRKR--PSTLALSRQKLPNLPGTSIDNVQLGAYAIS
CrTKL_ GLGEDGPTHQPIEHLASFRAMPDMLMIRPAGGNETAGAYKVAIANRKR--PTTIALSRQNMPNIPNCSVEGVAKGAYTIH
VcTKL_ GLGEDGPTHQPVEHLASFRAMPSMMMMRPAGGNETAGAYKVAVENRKR--PTTIALSRQNMPNLPGTSVEGVAKGAYVIR
OlTKL_ GVGEDGPTHQPIEHVASFRAMPGMDMARPADGNETAAMYKMAVENSMNGAPTTLALSRQVVPNLAGTSMEGAAKGAYVVQ
MpTKL_ GVGEDGPTHQPIEHLASFRAMPGMLMMRPADGNETAGAYKIGVEQTDR--PTTFALSRQVVPNLPGTSKEGVAMGAYVVQ
TeTKL_ ALGEDGPTHQPVETLASLRAIPNLLVIRPADGNETSGAYQVAVQRRKQ--PTLLALTRQNVPNLAGSSAANVAKGAYTLV
PmTKL_ GVGEDGPTHQPIETIPSLRAMPNMMVFRPGDGNETSGAYKVAIKNRKR--PSSLCLSRQGMANQQNSSVDKVALGGYVLE
.....570.....580.....590.....600.....610.....620.....630.....640


SbTKL_ DNSTGNKPDLIVLSTGSELEIAAKAADELRKEGKTIRVVSFVSWELFEEQSDEYKESVLPEAVTA-RISIEAGSTLGWQK
ZmTKL_ DNSTGNKPDLIVMGTGSELEIAAKAADELRKEGKTVRVVSFVSWELFDEQSDEYKESVLPAAVTA-RISIEAGSTLGWQK
OsTKL_ DNSTGNKPDFIVMSTGSELEIVAKAADELRKEGKTVRVVSFVCWELFDEQSAEYKESVLPEAVTA-RVSLEAGSTLGWQK
SoTKL_ DNSSGNKPDVILIGTGSELEIAAKAGDELRKEGKAVRVVSFVSWELPEKQSDEYKESVLPSDVTA-RVSIEAGSTFGWHK
NtTKL_ DNSSGNKPDVILIGTGSELEIAVKAADELRKEGKAVRVVSFVCWELFEEQSADYKESVLPSSVTA-RVSIEAGSTFGWEK
PsTKL_ CNASNNKPDVILMGTGSELEIAEKAAVTLRNEGKAVRVVSFVCWELFEEQTPEYKESVLPAAVAA-RVSVEAGSTFGWER
CaTKL_ DNSSGNNPDVILIGTGSELEIAVKAADELRKEGKAVRVVSLVSWELFDEQSAEYKESVLPAAVTA-RVSIEAGSTFGWEK
SsTKL_ DNSSGNKPDVILIGTGSELEIAVKAAEELKKEGKTVRVVSFVCWELYDEQSAEYKESVLPSSVTA-RVSIEAGSTFGWQK
AtTKL1_ DDSSGNKPDVILIGTGSELEIAAQAAEVLRKDGKTVRVVSFVCWELFDEQSDEYKESVLPSDVSA-RVSIEAASTFGWGK
AtTKL2_ DNSTGNKPDVILIGTGSELEIAAQAAEKLREQGKSVRVVSFVCWELFDEQSDAYKESVLPSDVSA-RVSIEAGSTFGWGK
AlTKL_ DDSSGNKPDVILIGTGSELEIAAQAAEVLRKEGKTVRVVSFVCWELFDEQSDEYKESVLPSDVSA-RVSIEAASTFGWGK
ThTKL_ DNSTGNKPDVILIGTGSELEIAAQAAEELRKEGKTVRVVSFVCWELFDEQSDAYKESVLPSDVSA-RVSIEAGSTFGWEK
RcTKL_ DNSSGNKPDVILIGTGSELEIAAKAAEELRREGKAVRVVSFVSWELFDEQSDAYKESVLPAAVTA-RVSIEAGSTFGWQK
PtTKL_ DNSSSNKPDVILIGTGSELEIAAKAAEELRKEGKAVRVVSFVSWELFDEQSDAYKESVLPAAVEA-RVSIEAGSTFGWEK
VvTKL_ DNSSGNKPDIILIGTGSELEIAAKAADELRKEGKAVRVVSLVSWALFDEQSDAYKESVLPAAVSA-RVSVEAASTFGWEK
SeTKL_ DNSSGNKPDLILIGTGSEVEIAAKAADVIRKEGKSVRVVSFPCWELFEKQSDEYKESVFPSEVTA-RVSVEAGSTFGWGK
PpTKL_ DDSKDNKPDLLIMASGSELEIAAKAADVIRGEGKTVRVISFVCWELFEEQSAEYKESLLPSDVTA-RVSVEAGATFGWER
CrTKL_ DTKAGVKPDVILMGTGSELELATAAAGILEKEGKNVRVVSFPCWELFEEQSAEYKESVLP-SDVTARVSVEAATSFGWAK
VcTKL_ DAAG--TPDVILMGTGSELQLCAEAADILEKEGKKVRIVSFPCWELFEEQSAEYKESVLP-RSVEARVSVEAATSFGWAK
OlTKL_ GAAAGEACDVILIGTGTELELACQAGAELESKGKKVRVVSMPCWEAFERQPAAYQESVLPAAMRAKTVSIEAGTTFGWAK
MpTKL_ GPAAGEDCDCVLIGTGTELELACKAGAEL---GDKARVVSMPCWELFEEQSDEYKESIFPKDCKA-IVSIEAGSTFGWSK
TeTKL_ DCEG--TPDLILIGTGSEVALCVKAAETLTANGKKVRVVSMPSWELFEEQSPEYKASVLP-AGV-KRLAVEAAASFGWCR
PmTKL_ ECDG--TPELILIGTGTELDLCVQAAKKLTKEGRKVRVVSMPCVELFEEQSDSYKEEVLP-SNIRKRLVVEAAESFGWHK
.....650.....660.....670.....680.....690.....700.....710.....720

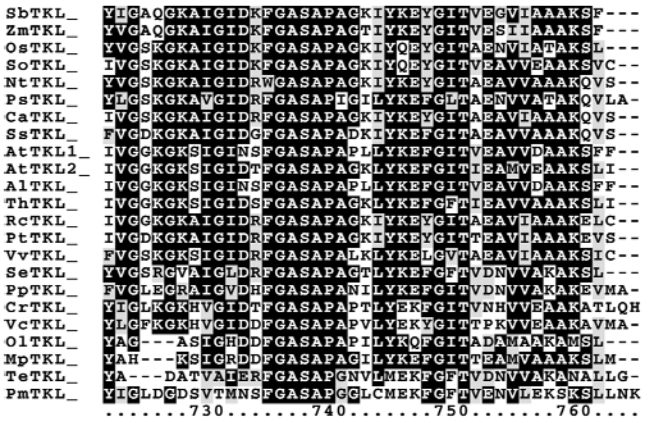

Annex Fig. 3 – Sequence alignment of TKLs from different photosynthetic organisms – The phosphor-peptide identified by LC-MS/MS is marked with red asterisks. The list of accession numbers is given by annex table 1.

Curriculum Vitae

Name: Agostinho Manuel Gomes Rocha

Date of Birth: April the 20th, 1979

Place of Birth: Ovar, Portugal

Education and Positions Held

Since 2008	PhD studies in the laboratory of Prof. Dr. Ute Vothknecht at the Biocenter, LMU Munich, Germany.
2005 - 2006	Research assistant in biochemistry at the University of Vigo, Spain.
2000 – 2005	Diploma degree in Applied Biology at the Department of Biology, University of Minho, Portugal. Diploma research in the laboratory of Prof. Dr. Ricardo Beiras García-Sabell at the University of Vigo, Spain.
1998 – 2000	Studies in Biological Engineering at the Department of Biological Engineering, University of Minho, Portugal.

Scientific Publications

Rocha AG, Stael S, Chigri F, Mehlmer N, Teige M and Vothknecht UC. (2012) Chloroplast transketolase is a target of calcium dependent phosphorylation by a stromal kinase (revision submitted JBC).

Rocha AG and Vothknecht UC (2012) The role of calcium in chloroplasts – an intriguing and unresolved puzzle. Protoplasma, DOI: 10.1007/s00709-011-0373-3.

Bayer RG, Stael S, **Rocha AG**, Mair A, Vothknecht UC, Teige M (2012) Chloroplast localised protein kinases – a step forward towards a complete inventory. J Exp Bot, 63(4):1713-23.

Stael S, **Rocha AG**, Wimberger T, Anrather D, Vothknecht UC, Teige M (2012) Crosstalk between calcium signalling and protein phosphorylation at the thylakoid. J Exp Bot, 63(4):1725-33.

Stael S, **Rocha AG**, Robinson AJ, Kmiecik P, Vothknecht UC, Teige M (2011) Arabidopsis calcium-binding mitochondrial carrier proteins as potential facilitators of mitochondrial ATP-import and plastid SAM-import. FEBS letters 585(24):3935-40.

Ehrenwörtliche Versicherung

Ich versichere hiermit ehrenwörtlich, dass die vorliegende Dissertation von mir selbstständig und ohne unerlaubte Hilfe angefertigt wurde.

Erklärung

Diese Dissertation wurde keiner weiteren Prüfungskommission weder in Teilen noch als Ganzes vorgelegt. Ich habe nicht versucht, anderweitig eine Dissertation einzureichen oder mich einer Doktorprüfung zu unterziehen.

München, den 26. Juni 2012

_____

Agostinho Manuel Gomes Rocha